STUDIES OF LABILE POLYELECTROLYTE AT SOLID-LIQUID INTERFACES

By

Liang Zhang, B.ENG

A Thesis

Submitted to the School of Graduate Studies

In Partial Fulfillment of the Requirements

For the Degree

Master of Applied Science

McMaster University

STUDIES OF LABILE POLYELECTROLYTE AT SOLID-LIQUID INTERFACES

Master of Applied Science (2010) Chemical Engineering

McMaster University Hamilton, Ontario

TITLE: Studies of Labile polyelectrolyte at solid-liquid interfaces

AUTHOR: Liang Zhang

B.Eng. (Beijing University of Chemical Technology, China)

SUPERVISOR: Professor Robert H. Pelton

NUMBER OF PAGERS: 77

Abstract

Guar is naturally occurring polysaccharide. This thesis presents studies on hydroxypropyl guar (HPG) - borate, a Labile polyelectrolyte, interacting with a number of model tear film (eye) components including sulfate-stabilized polystyrene latex, anionic lipid-stabilized emulsions and cationic 1,2-dioleoyl-3-trimethylammonium-propane (DOTAP) liposomes. The presence of borate ions converts nonionic HPG into an anionic polyelectrolyte. However, the borate ions on HPG chains do not inhibit HPG-borate adsorption onto anionic polystyrene latex. Both HPG and HPG-borate show the same adsorption isotherms. As a comparison, HPG slightly oxidized to give C6 carboxyl groups, with a degree of substitution close to HPG-borate, does not adsorb onto anionic polystyrene latex when the polymer is fully ionized.

Although HPG and HPG-borate do not adsorb onto anionic lipid-stabilized emulsions, the emulsions aggregate at high polymer concentration (> 0.1 g/L) because of depletion flocculation. Borate ions do not influence the depletion threshold polymer concentration. However, HPG provides gravitational stability for flocculated emulsions to against phase separation.

Our work has shown that cationic colloids in the presence of HPG-borate display bridging flocculation, depletion flocculation, steric stabilization, salt induced coagulation, or no change at all, depending upon the HPG and salt concentrations. Developed were novel stability maps showing these phenomena mapped onto a log salt concentration versus log HPG concentration plane. The maps were generated by a combination of published models and experimental results. This portrayal of complex behaviors will be valuable to formulators because it clearly shows the effects of changing HPG molecular weight, colloids size and colloid volume fraction.

Acknowledgement

In the first place, I would like to express my deep appreciation to my advisor, Professor Dr. Robert H. Pelton for his instruction and constant encouragement during the whole period of my research.

I would like to thank Mr. Doug Keller and Ms. Sally Watson for their assistance with my research. I would like to thank Dr. Steve Kornic to help me with Elemental Analysis measurements.

I am grateful to all my colleagues in Interfacial Science and Technologies Group at McMaster: Dr. Yuguo Cui, Dr. Anil Khanal, Roger Ren, Leo Hsu, Songtao Yang, Yaqin Xu, Quan Wen, Zuohe Wang, Ruilin Li, Jingyun Wang, Vincent Leung and Behnam Naderi Zand. Special thanks to Dr. Yuguo Cui for lots of fruitful discussion about Labile polyelectrolyte, Roger Ren for general protocols of TEMPO oxidation and Professor Dr. An-Chang Shi in Physics & Astronomy Department for many useful suggestions in polymer physics.

I would like to thank my father Mr. Yonghui Zhang (张甬惠 先生) and my mother Mrs. Qun Fan (范群 女士) for their understanding and supportive of my life in Canada.

Finally, I would like to thank Alcon Lab and NSERC for the financial support.

TABLE OF CONTENTS

Chapter 1

Introduction and Literature Review

Millions of people in the world suffer from dry eye symptoms. From the definition given by National Eye Institute, dry eye is "a disorder of the tear film due to tear deficiency or excessive evaporation that causes damage to the interpalpebral ocular surface and is associated with symptoms of discomfort"[2]. In the past 25 years, one of the most successful therapeutics method is using artificial tear, which is assembled from analogue ingredients like natural tear[3]. One of the commercialized products from Alcon Laboratories has been proven to be particularly successful. The goal of my work is to elucidate interfacial behavior of *hydroxypropyl guar*, a naturally occurring polysaccharide in Alcon's lubricant eye drops. In the following sections, background information about tear components, *hydroxypropyl guar* properties and interfacial behavior of polymers at interfaces will be introduced.

1.1 TEAR FILM

1.1.1 Natural Tears

To delineate the scope of my research, it is critical to introduce the structure and key components in natural tears, as well as their functionalities. Wolff's classic model divided the tear film into three zones, exterior lipid layer, a protein rich aqueous layer, and a mucin rich layer next to the cornea[4]. (see Figure 1. 1)

Thickness — Maurice was the first to measure human tear film thickness (6 μm) by immersing glass fibres with known diameter into liquid phase[5]. A similar value was obtained by Ehlers (7-9 μm)[6], who weighed the amount of tear liquids. However, Prydal and colleagues got a total depth of tear film up to approximately 40 μm using interferometry and confocal microscopy[7, 8]. Details of the debate on tear film thickness was summarized by Bron et al. [9] To sum up, the value is still uncertain.

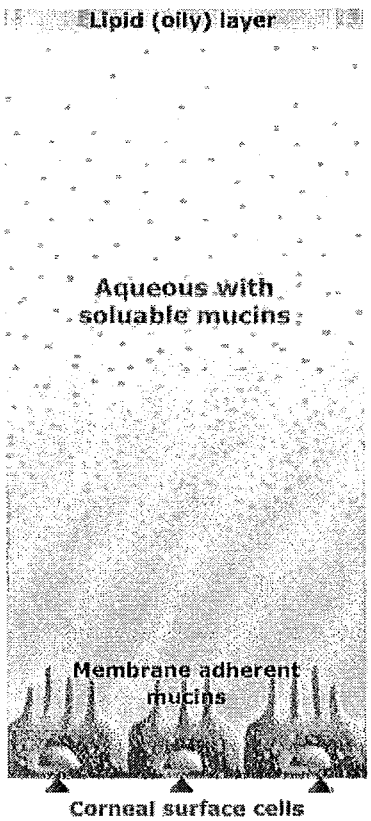

Figure 1. 1 Schematic illustration of natural tear film (a cross-sectional view) adapted from Alcon Laboratories website

Lipid layer — The lipid layer is the outermost layer (see Figure 1. 1) of tear film. The composition is a complicated mixture of non-polar lipids (wax esters, cholesterol esters and cholesterol) and polar lipids (phospholipids and glycolipids)[9]. From a physical chemistry perspective, the lipid layer plays an essential role in committing smooth optical surface, preventing evaporation and maintaining thick and stable sub-phase. For example, Mishima and Maurice found water loss speed of tear liquid increased from 6 to 100 micro liter per hour after lipid layer was stripped away[10]. Tiffany showed that the resistance to evaporation changed almost linearly with lipid film thickness in the range of 50 to 200 nm[11]. More recently, Goto and co-workers

confirmed evaporation retarding effects of the lipid film using microbalance sensor[12]. Interestingly, the spreading of lipid film over the below aqueous phase reduces the surface tension, which consequently forms a more stable and thicker tear film—an example of *Marangoni flow*[13, 14].

Aqueous layer — It is composed by 98.2% water and 1.8% solids[15]. Antibacterial such as lysozyme, immunoglobulin G (IgG), lactoferrin are key components in aqueous layer. Other than their biological functions, they also decrease the *surface tension* and maintain *viscosity* of the tear liquid[16, 17]. Also, they provide lubrication for the ocular surface. *Soluble mucin* is another key component whose role is rather controversial. Many studies has demonstrated soluble mucin is overestimated in generating low viscosity and high viscosity for tears[9]. In addition, oxygen, glucose and inorganic salts can also be found in aqueous layer.

Mucus layer — The mucus layer is a unique biological soft material, provides both biological functions and mechanical support for tear film. It is assembled from *goblet cell mucin*, immunoglobulin, glucose, leukocytes and cellular debris[16, 18]. Mucus layer is not immobilized tightly on the corneal epithelium; instead, it weakly attaches onto glycocalyx and moves freely across the corneal. Since the surface of the corneal epithelium is hydrophobic, tear liquid spreading is facilitated by the soft hydrophilic mucus layer, both vertically and horizontally. At the same time, mucus layer may also prevent the invasion of bacteria onto the corneal surface[19, 20].

Glycocalyx — It is on the bottom of the eyes, made up by glycoproteins and glycolipids[18, 21]. It stretches out for about 300 nm from microvili and microplicae, which covers corneal epithelium. The bottom of the mucus layer is associated with glycocalyx, which allows above layers homing on the corneal epithelium.

1.1.2 Artificial Tears

As a substitute of natural tear, artificial tear should mimic the optical, physical and chemical properties. Further more, it may also deliver therapeutic agents to eyes for eye disease treatments. Compositional categories of artificial tear will be illustrated in the context of a review by Murube et al. [22]

- ***Water*** — Natural tears have 98-98.5% water. In dry-eye drops, water is 97-99%
- ***Saline solutions*** — Natural tears are electrolyte solutions. In artificial tear formulation, salt is required not only for maintaining osmotic pressure, but also for its biological function in corneal epithelium metabolism (i.e., K^+, HCO_3^-)
- ***Glycerol, monosaccharides and Disaccharides*** — Take glycerol as an example, it is used as *emollient* and *humectant* for dry eyes.
- ***Polysaccharides*** — Mucilage (i.e., cellulose, guar gums), dextran and mucopolysaccharides (i.e., hyaluronate) are applicable candidates. Polysaccharide is essentially thickening agents to increase viscosity of the artificial tears for

longer residence time.

- ***Synthetic Polymers*** — Development of polymer synthetic method makes us possible to synthesis well-defined polymer for ocular application. Two major groups are vinyl derivatives and ethylene glycol derivatives. Vinyl derivative such as polyvinyl alcohol is used as contact lens lubricants and dry eye disorders.
- ***Gelatins*** — Extracted from animal collagen, gelatins are considered to be good surfactant for artificial tears.
- ***Biological Fluids*** — For example, mucins are high molecular weight glycoprotiens.
- ***Lipids*** — As one of the key component in natural tear, foremost lipid layer delivery of lipid into eyes can either act as lubricant or supply additional lipid for evaporation retention.

Hydroxypropyl guar and borate ions are adopted by Alcon Laboratories to produce artificial tear solution for dry eye application. Their behaviors in the context of artificial tear solution properties are of interest in my current work.

1.2 GUAR, HYDROXYPROPYL GUAR AND GUAR-BORATE

1.2.1 Guar & Hydroxypropyl Guar

Guar galactomannan is extracted from the seeds of *Cyamopsis teragonoloba.* The chemical structure of guar galactomannan is composed by a linear backbone of β-1, 4 linked mannose units and randomly distributed α-1, 6 linked galactose units as side chains[23] (see Figure 1. 2). One of the fascinating properties of guar is that high solution viscosity can be obtained even at very low concentration. A number of treatments can be applied to native guar galactomannan, leading to a series of guar derivates such as hydroxyethyl guar, hydroxypropyl guar and carboxymethyl guar. Hydroxypropyl guar is the most widely available guar derivates, which is substituted by hydroxypropyl groups along the chains through its reaction with propylene oxide in alkaline medium[23]. The presence of hydroxypropyl groups along guar chains leads to a number of different solution properties compared with native guar galactomannan. Some key results will be presented.

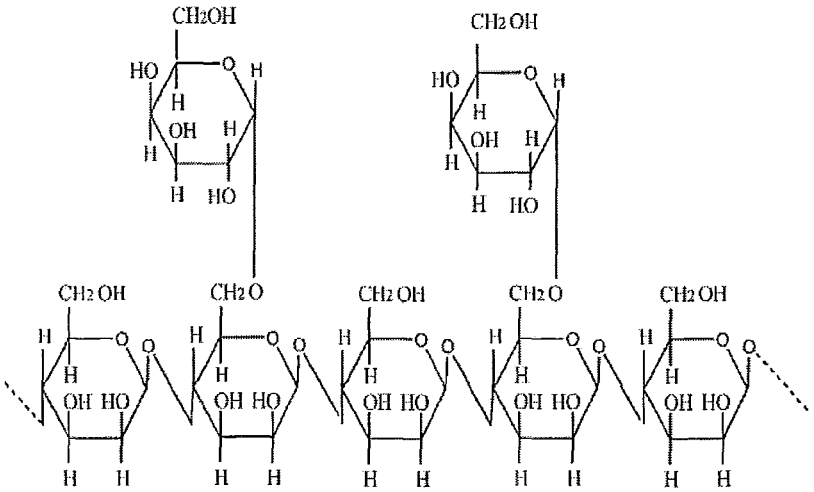

Figure 1. 2 The structure of guar galactomannan (adapted from reference 22)[23]

Compared with other water soluble natural polymers, guar has non-uniform molecular architecture along the chains. Mannose backbone and galactose branch have different solubility in water, thus, less soluble mannose un-substituted regions may associate each other to form partially crystalline structures[24], which leads to very different viscoelastic properties[25-28]. i.e., relationship between intrinsic viscosity ([η]) and molecular weight is departure from random coils when polymer concentration is above overlap concentration (c*). Gittings and Weitz suggested loosely interconnected aggregates might exist near Θ solvent conditions using light scattering techniques[24, 29].

Prud'homme and colleagues uncovered a number of factors influencing native guar and HPG solution network properties. For instance, they firmly demonstrated a transition from liquid crystalline form to crystalline structure of native guar solution—an intermolecular hydrogen bonding effect[30]. The modification of native guar into hydroxypropyl guar (HPG) blocks hydrogen bonding sites and increases hydrophobicity of guar molecules. For example, temperature dependence of the Huggins coefficient was observed only at high hydroxypropyl substitution. At the same time, the characteristic ratio (C_∞), an indicator of polymers intrinsic stiffness, was 13.02 at molecular substitution (MS) 0.6 compared with C_∞ =12.6 for native guar reported by Robinson et al. [28] The characteristic ratio difference was interpreted as steric hindrance provided by substituted hydroxypropyl groups, resulting greater chain stiffness[23].

1.2.2 Guar-borate

Borate anion ($B(OH)^{4-}$) is able to react with polymers carrying *cis*-diol groups via genetic borate-*cis*-diol reaction (see Figure 1. 3), which condenses borate ions onto polymer chains and converts nonionic polymers into polyelectrolytes[31]. In particular, the bond is sensitive to temperature, pH and salt concentration. As it has been shown in Figure 1. 3, borate-*cis*-diol reaction may lead to inter- or intra- molecular crosslink.

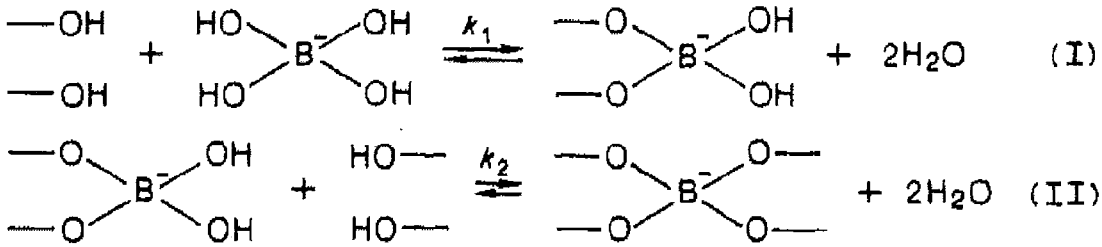

Figure 1. 3 Two steps reaction between borate and polyhydroxy (adapted from reference 30)[31]

The main features of these systems, compared with conventional polyelectrolyte with fixed charge, have been summarized by Audebert[31]. 1) The number of charges on the chain is determined by chemical equilibria. Free counterions (in the case of borax, Na^+ is the counterion) always exist even in the absence of passive salt, which may partially screen out electrostatic interactions. In addition, new complex formation may be suppressed by complexes already formed. 2) In dilute solutions, ions complexation only occurs internally (intra-chains complexation only); inter-chains complexation only takes place at semi-dilute concentration.

Interaction between guar and borate ions was extensively studied since the 1980s. Audebert, Prud'homme and Leibler contributed both experimental data and theoretical frameworks on guar-borate systems. Using ^{11}B NMR spectra and equilibrium dialysis techniques, Audebert was the first to explore guar-borate interaction systematically. The French group studied guar-borate complex formation in terms of phase behavior[32], complex formation constant[33], polymer concentration effect[31] and polyelectrolyte effect[34]. Their experimental data, coupled with Leibler's self-consistent argument[34, 35], firmly demonstrated the guar-borate solution properties listed above. In addition, Prud'homme and co-workers studied rheology of guar-borate and HPG-borate gel. They found rheology was strongly dependent on the number of effective cross-links[36]. One of the most cited theories for reversible network, which resembles guar-borate system, was proposed by Leibler and Rubinstein[37], who predicted two maxima might exist in loss modulus function (can be measured by oscillatory shear techniques[38]).

1.3 POLYMERS AT INTERFACES

Mixing guar-borate with tear film species may result a number of interesting phenomenon. For example, it may bind with protein via electrostatic interaction or hydrogen bonding, leading to liquid-liquid phase separation (often referred as coacervation, first described by Bungenberg de Jong[1]). It may also be adsorbed or depleted by lipid surfaces or corneal epithelium, depending on particular chemical, physical or even dynamic features of the interfaces[39]. In addition, the physiological environment should be seriously taken into account, i.e., salt concentration, which may have dramatic influence.

Some background knowledge of polymers at interfaces will be described in this section. Properties of polymer solution near interfaces are very different from bulk solution. The behaviors of polymers at interfaces are dominated by the difference between free energy of polymer segments/surface and solvent/surface. If free energy of polymer segments/surface is larger than that of solvent/surface, polymers will be adsorbed by the surface, leading to an increase of polymer concentration near the surface. This is called polymer *adsorption*. By contrast, polymer will be depleted from the surface—*depletion* effect, coined by Joanny, Leibler and De Gennes[40] in 1979, leading to polymer concentration reduction near the surface. Here, a number of fundamental aspects of polymers at interfaces will be presented. In addition, polymer effects on colloid stability will be described.

1.3.1 General Features

Adsorption Isotherms — One of the key parameter of polymer adsorption is the adsorbed amount. Adsorbed amount can be displayed on adsorption isotherms, which are plotted as adsorbed amount versus equilibrium bulk polymer concentration at fixed temperature[39]. In practical, units of adsorbed amount are milligrams per square meters (mg/m^2) or milligrams per substrate mass (i.e., mg/g).

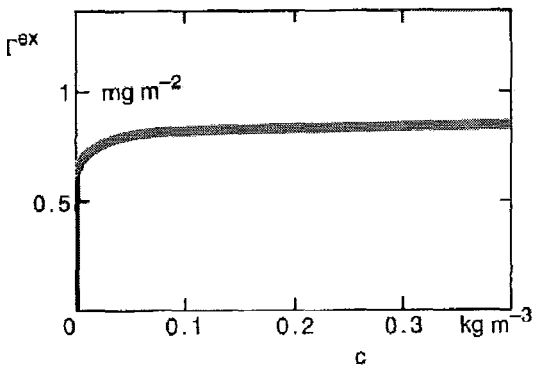

Figure 1. 4 Typical high-affinity adsorption isotherm (adsorbed amount (mg/m^2) against equilibrium bulk concentration (kg/m^3))

Typical polymer adsorption isotherm is *high-affinity* type. As is shown in Figure 1. 4, adsorption reaches a maximum adsorbed amount at very low bulk concentration and maintains a plateau value horizontally, indicating the surface is saturated. The adsorbed amount is a function of molecular weight; higher molecular weight normally generates higher saturated adsorbed amount under same solvent conditions. At the same time, the molecular weight distribution of the polymer affects the shapes of adsorption isotherms—polydisperse polymers give round isotherms than that of monodisperse polymers. However, hydrogen bonding, covalent bonding and even biological complexation may play roles in particular situations, which may influence shape of isotherms.

Structural Aspects — It was Jenkel and Rumbach, who first proposed conformation structure of adsorbed polymer layer[39]. The chain was divided into three sub-types: trains, loops and tails (as it is shown in Figure 1. 5). Trains are all contacted with

substrate. Loops do not contact with substrate but connect with two trains. Tails are non-adsorbing chain ends.

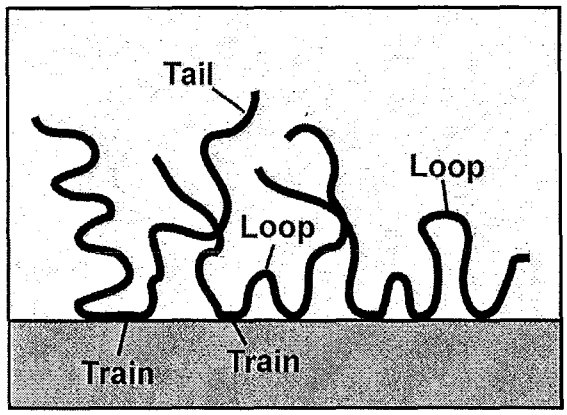

Figure 1. 5 Schematic illustration of adsorbed polymer layer

The development of experimental techniques (i.e., neutron scattering and reflectivity) at the end of last century brought significant changes in polymer science[41]. In polymer adsorption for example, it made us possible to obtain polymer chain density profile near the surface. When surface is far from full coverage, one found chains profile decayed steeper than that of saturation condition. Well-accepted explanation is that polymer has a tendency to be more "flatten down" under low coverage and gradually "stand up" by increasing the length of loops and tails[39].

Polydispersity Effects — Guar is natural occurring polymers and widely distributed in molecular weight. Adsorption of polydisperse polymer gives rounded isotherms. A number of experimental works and thermodynamic analysis provided insight of this interesting behavior[42-44]. It was found that high molecular weight polymers are more likely to be adsorbed than low molecular weight fractions. Fleer and co-workers argued that high molecular weight polymers have a lower mixing entropy, which might subsequently leads to preferential [44].

Take a mixture of two monodispersed polymers samples with different molecular weight as a model system[39]. Three distinct regions can be identified; first region, when bulk polymer concentration is very low (i.e., lower than saturation level), overall adsorption isotherm behaves the same as monodispersed polymer. Both fractions have chance to attach onto the surface. Second region, around saturation point, due to multi-point attachment on the surface, higher molecular weight polymer get less chance to desorb compared with low molecular weight polymer. Thus, high molecular weight polymer gradually "replaces" low molecular weight polymer on the surface. In this region, adsorbed amount linearly increases. Third region, most of low molecular weight polymer is replaced by high molecular weight polymer, plateau value is finally obtained. This process can be verified by desorption experiments (see reference 39, p 34)—it follows the track of high molecular weight polymer adsorption isotherm[44]. In the case of multi-component mixtures, rounded adsorption isotherm should be anticipated.

Electrostatic Effects — Condensation of borate ions onto guar molecule converts the nonionic polysaccharide into anionic polyelectrolyte. The key features of polyelectrolyte adsorption are discussed in this section. Besides regular rules presented above, adsorption of polyelectrolyte is also strongly dependent on charge densities (both polyelectrolyte and surface) and salt concentration. If polymer is charged, electrostatic repulsion between segments will impair polymer assembly on the surface. In addition, if surface is charged, it will either promote or even inhibit adsorption, depending on the charge sign. Salt, on the other hand, is able to screen out the electrostatic interactions. In this part, polyelectrolyte adsorption will be discussed in context of charge sign, salt concentration and pH effect (weak polyelectrolyte). Both theoretical and experimental results will be presented.

We first consider polyelectrolyte and surface have fixed opposite charge sign. This recalled a series of experimental and theoretical studies for last four decades [39, 45-48]. It is worth to mention that the formation of *polyelectrolyte multilayer* structures from aqueous solution by Decher[49] in 1997 heated up investigation of fundamental question behind the multilayer formation—charge inversion effect. A more elaborated mechanism was proposed by Rubinstein and colleagues[50] using scaling theory. Two regions, distinguished by relative charge density between polyelectrolyte and surface, are presented in Figure 1. 6.

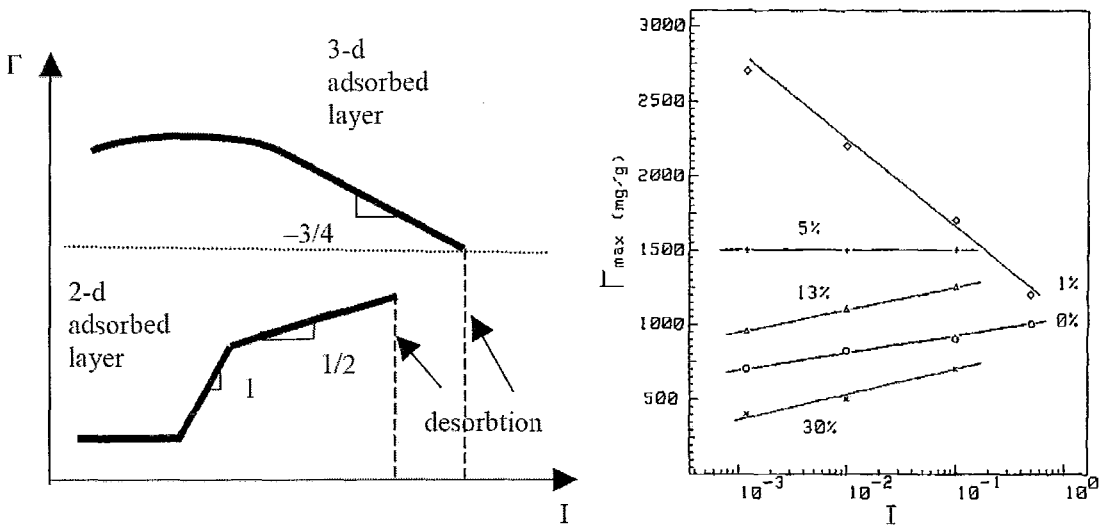

Figure 1. 6 Theoretical (left) and experimental (right) results of polymer adsorbed amount dependence on ionic strength. Specifically, upper curve in left figure represents *low* charge density polyelectrolyte, while lower curve represent *high* charge density polyelectrolyte. Labels on right figure indicate different charge density. Figure on the left is adapted from reference 42, figure on the right is adapted from reference 51. [51]

When surface charge density is low, polyelectrolyte forms 2-D adsorbed layer. In this case, electrostatic repulsion between segments is relatively strong, leads to more "swelling" polymer chains, and also dominates intra-molecular configuration as well

as inter-molecular spacing on the surface. Subsequently, two dimensional "flatten" polyelectrolyte layer is formed. Salt addition screens out electrostatic repulsion between segments while it does not affect surface charge. Using scaling argument, Dobrynin et al. [50] concluded the adsorbed amount grows proportional to square root of ionic strength (*screening-enhanced adsorption*[45]).

When surface charge density is relatively high, 3-D adsorbed layer is formed. Here, polyelectrolyte accumulates onto surface through electrostatic attraction, which is dominated by the surface charge. The layer is further stabilized by short-range electrostatic repulsion between the segments. It was found adsorbed amount first increased (*screening-enhanced adsorption*) and then decreased along with salt addition (*screening-reduced adsorption*[45]).

The theory shows agreement with experiments. Durand and Audebert studied cationic polyacrylamides adsorption onto anionic montmorillonite surface[51] (see Figure 1. 6 on the right side). They found adsorbed amount of polyacrylamides with low charge fraction (i.e., 0.01) decreased with increasing ionic strength (*screening-reduced adsorption*). Adsorbed amount with higher charge fraction (i.e., 0.13, 0.3) increased with increasing ionic strength (*screening-enhanced adsorption*). Charge density in the middle (i.e., 0.05), however, showed to be independent of ionic strength. According to scaling theory, linear charge density lower than 0.05 may form 3-D adsorption layer, while 2-D formation was favored when linear charge density is higher than 0.05. Examples of Screening-reduced adsorption in other systems were also reported by Pelton[52], Audebert[53, 54] and other researchers[55, 56]. Screening-enhanced adsorption was reported by Kawaguchi[57], who studied highly ionized poly (4-vinyl-N-n-propylpyridinium bromide) adsorption onto silica. Marra et al. [58] found adsorbed amount of poly (styrene sulfonate) (PSS) increased linearly against square root of ionic strength, which is qualitatively in agreement with theoretical prediction

Adsorption of weak polyelectrolyte onto opposite charged surface was studied by Fleer and colleagues[59, 60]. As a comparison, two patterns of adsorbed amount versus pH are shown in Figure 1. 7. The one on the left side is adapted from Fleer's work[59]. The one on the right side is experimental adsorption data of hydrolysed polyacrylamide onto negatively charged siliceous minerals[61]. When polyelectrolyte and surface have opposite charge sign, a maximum adsorption plateau value was found; experiments showed excellent agreement with theoretical calculation[59]. While in the case of hydrolysed polyacrylamide (with 30% hydrolysis), adsorption was almost inhibited when carboxyl groups are ionized[61].

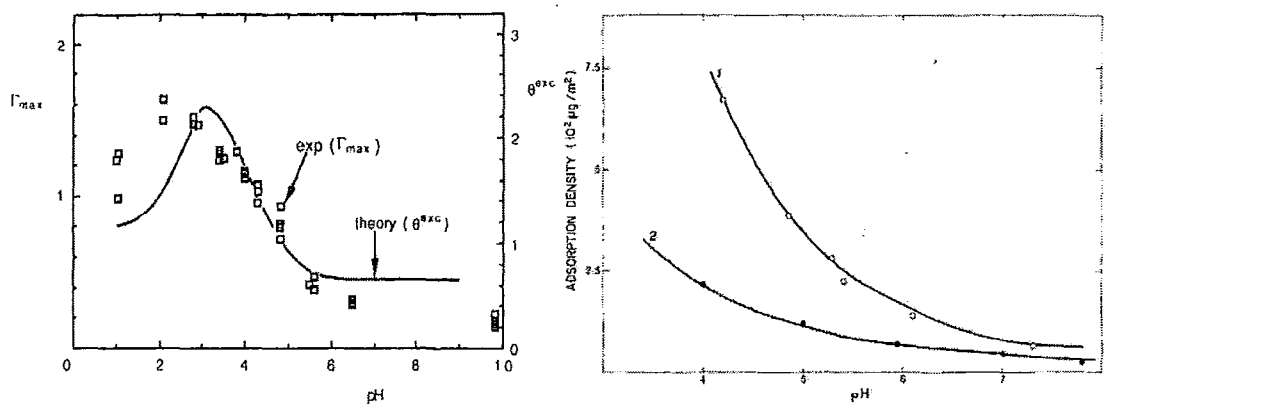

Figure 1. 7 Weak polyelectrolyte adsorption onto surface with different[59] (left) and same[61] (right) charge signs under different pH values

Depletion — Concept of polymers depletion at interfaces has been briefly introduced. Depletion induced by uncharged polymer and polyelectrolyte will be discussed in this section, respectively. Phase behavior of Colloid/non-adsorbing polymer mixtures will be presented in section 1.3.2.

Uncharged polymer depletion has been extensively studied since 1980s. The depletion energy may be a product of polymer osmotic pressure and depletion overlap volume[62, 63]. However, depletion by polyelectrolyte is much more complicated, the influencing factors, so far as we know including polyelectrolyte concentration, pH and ionic strength[64]. While in both instances, solvent molecules near the surface (in the region generally referred as depletion layer) have lower chemical potential than that of bulk liquid, hence, overlap of two depletion layer is energetically favored, and attractive force between the surfaces is subsequently generated.

Neutral polymer depletion has been described in some key theoretical papers by Asakura and Oosawa[63, 65] (often referred as AO theory), Vrij[66], Sperry[67] and Fleer et al. [62] Depletion layer thickness, for example, has been even analytically derived. Equation 1 shows so-called "pragmatic" analytical relationship between depletion layer thickness (δ) and bulk volume fraction for non-adsorbing polymer (φ^b), developed by Vincent[68].

$$\delta / R_g - R_g / \delta = \frac{R_g}{l}\left(\frac{r}{\varphi^b}\right)^{2/3}\left\{\ln(1-\varphi^b)+\varphi^b(1-1/r)+\chi(\varphi^b)^2\right\} \quad (1)$$

Where: R_g is radius of gyration of non-adsorbing polymer, l is length of one segment, r is polymer chain length.

Overlap volume between two surfaces may be calculated by adding geometry factors. Then, pair depletion energy may be calculated using appropriate osmotic pressure expression. See equation 2 below for spherical colloids in the presence of

non-adsorbing polymer, proposed by Fleer et al. [62] (Note that an analytical expression considering *many-body correlation* effects is not available at present)

$$V_{dep} = -\frac{2}{3}\pi \Pi (\delta - \frac{h}{2})^2 (3a + 2\delta + \frac{h}{2}) \frac{1}{k_b T} \quad (2)$$

Where: h is distance between two colloids, a is radius of one colloid

A large body of experimental literature on depletion effect was focused on colloid phase behavior[69, 70]. In the case of neutral non-adsorbing polymer, hard spherical colloids (i.e., hydrophobic silica particles) phase separation experiments demonstrated the correctness of the theories[71]. On the other hand, direct force measurement, an alternative way to understand colloid/colloid and colloid/surface interaction, was also applied[72]. For example Luckham et al. used surface force apparatus (SFA) to measure depletion force between two mica surfaces induced by polystyrene in toluene[73]. Milling and Biggs[74] used atomic force microscopy (AFM) to study poly(dimethylsiloxane) (PDMS) induced depletion force between a silica sphere with planar silica surface in cyclohexane. They estimated the depletion layer of about 10 nm, which is very close to radius of gyration (R_g) of their PDMS sample. These direct (force measurement) and indirect (phase separation) results all confirmed the trends predicted by the theories.

Depletion of polyelectrolyte is poorly understood. However, some experimental and a few theoretical frameworks may somehow lead to general features. In the light of neutral polymer depletion, discussion will also be presented in the context of depletion layer thickness and osmotic pressure. In the first place, I will discuss Böhmer's work, who used self-consistent method to estimate depletion layer thickness[60]. See Figure 1. 8,

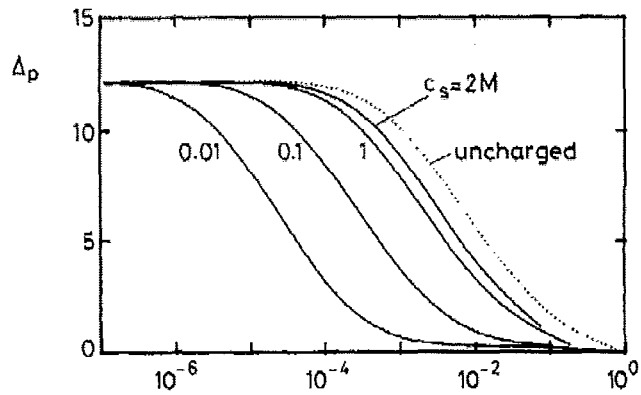

Figure 1. 8 depletion layer thickness as a function of bulk polyelectrolyte concentration at four salt concentrations, dotted line is the case of uncharged polymer.

In their mean-field approximation, depletion layer thickness in both charged and uncharged polymer was found to be the same at low polymer concentration, even under different ionic strength. At high salt concentration (>1 M) salt screened out

electrostatic interaction, polyelectrolyte resembled the behavior of uncharged polymer. Depletion layer thickness decreased above overlap concentration (c^*). At low salt concentration, increasing segment-segment repulsion lead to polyelectrolyte swelling and overlap concentration decreasing. Hence, depletion layer thickness decreased earlier than uncharged polymer in low salt regions.

Because of the complexity of polyelectrolyte solution[75], most of experimental estimation of depletion layer thickness was interpreted using scaling arguments. For example, Ausserré et al. measured depletion layer thickness of xanthan at quartz wall in aqueous solution using the evanescent wave techniques. It was found, above overlap concentration, depletion layer thickness equated to $c^{-0.8}$, while it equated to R_g below overlap concentration[76]. Their results were in accordance with de Gennes' work[77], in which exponent was predicted as -0.75 for good solvency conditions. Milling measured depletion layer thickness of poly(styrenesulfonate) (PSS)[78], poly(acrylate)[79] and poly(acrylic acid) (PAA)[64] at silica-water interface using AFM. Through scaling analysis, the exponents were estimated as -0.71, -0.62 and -0.33, respectively. These data includes "strong" polyelectrolyte and "weak" polyelectrolyte, indicating a very different scaling behavior.

Osmotic pressure of polyelectrolyte is also very different from uncharged polymer. According to Donnan equilibrium[80], electroneutrality dominates counterions distribution across the "membrane" between polyelectrolyte solution and bulk. In dilute polymeric solution with high salt, osmotic pressure may be calculated from below equation[81],

$$\frac{\Pi}{kT} = (c_p + \frac{z^2 c_p^2}{4 c_s}) \quad (3)$$

Where z is charge number of the polyelectrolyte, k is Boltzmann constant, c_p is the polyelectrolyte concentration. It is valid when $c_s >> z \times c_p$.

In *semi-dilute* condition, polymeric contribution is approximately kT per correlation volume ξ^{-3} (ξ is the correlation length). A better approximation for *low salt, semidilute* polyelectrolyte solution is[45],

$$\frac{\Pi}{kT} = \sqrt{(z\, c_p)^2 + 4\, c_s^2} - 2\, c_s + \xi^{-3} \quad (4)$$

Force measurement (i.e., AFM and SFA) and total internal reflection microscopy (TIRM) may be the most widely used apparatus for polyelectrolyte depletion. For example Biggs et al. [82] used AFM to study interaction between two silica surfaces in sodium polystyrene sulfonate (PSS) solution. A *secondary minimum* was found on the force-distance profiles. The minimum became deeper and moved to larger surface

separation as molecular weight increased. This observation has not been solved at present. Prieve and colleagues[83] studied polylysine depletion effects between glass sphere and glass plate using TIRM. In both salt and salt-free system, depletion energy profile shifted to smaller separation and the energy minimum increased with increasing polylysine concentration. On the other hand, the depletion energy was weakened with increasing ionic strength. Interestingly, they illustrated correlation between depletion interaction and bulk polylysine concentration at fixed distance. Ideally, depletion energy would be solely function of osmotic pressure. However, no linear relation between polymer molar concentration and depletion energy was found, indicating polymer concentration was *not* the only variable which affected depletion (as it is shown in equation 3 and 4). In addition, osmotic pressure versus depletion energy plots also scattered around a single straight line. (Osmotic pressure was calculated according to equation 3.) To sum up, many factors influencing polyelectrolyte depletion needed to be identified.

1.3.2 Stability of Colloidal Dispersion

The interaction between polymers and colloids has been extensively studied for decades due to its wide application including food colloid, paper making, pharmaceutical preparation and mineral processing[84]. Factors influencing colloids stability in the presence of polymers, such as colloids surface properties, polymers chemical structures, solvent quality of the medium are argued under particular situations. Thus, a big picture of is needed for the well-accepted conclusions. We present a schematic illustration below to show how polymers affect colloids stability. (Note the illustration is re-plotted according to Napper's text[85])

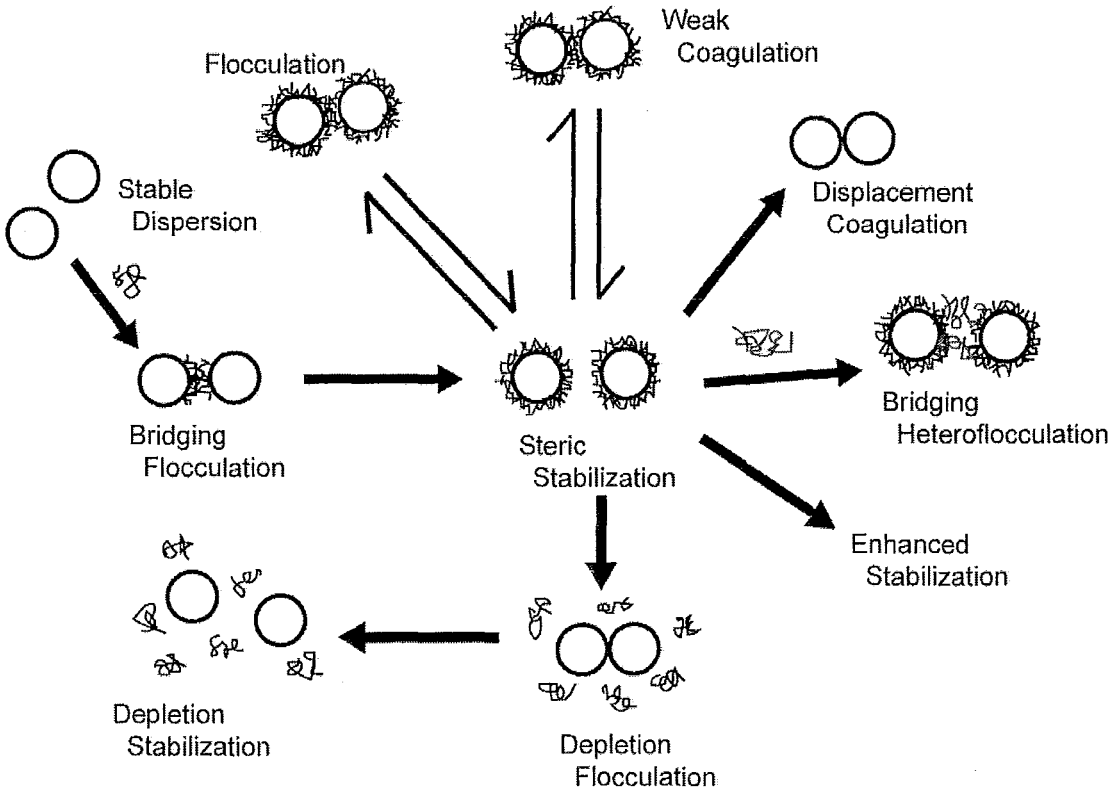

Figure 1. 9 Schematic illustration of colloids stability influenced by polymer addition (based on reference 85)

Bridging Flocculation — When adsorbing polymer is added into bare colloids suspension (see Figure 1. 9, bare dispersion), small amount of polymer (say several ppm, below giving saturation coverage) will induce bridging flocculation (see Figure 1. 10, bridging flocculation). Bridging flocculation usually requires long polymers to form long loops and tails, which are able to attach bare surfaces on a second particle surface during a collision. The bridging flocculation is sensitive to flocculant amount. In practical situations, the flocculation rate is low with small doses of flocculant and reaches maximum when particles are half covered and then the rate is decreased by increasing steric repulsion by covered polymers (see steric stabilization in the middle of Figure 1. 10). However, bridging flocculation is rather a dynamic process which involves several kinetic features. Studies on nonionic polymer induced charged colloids flocculation gave out a number of interesting results[86, 87]. For example flocculation can be induced either by high molecular weight polymer (1 million Dalton) or by low molecular weight polymer in the presence of salt. Colloids concentration also plays a role – low colloids concentration gives weaker flocculation. In the light of these results, Fleer and colleagues[86, 87] proposed a mechanism considering "equilibrium" and "non-equilibrium" flocculation (see Figure 1. 10). They summarized the results in the context of three characteristic time-scales: polymer adsorption, adsorbed polymer rearrangement (spreading on colloid surface) and colloids collision. If adsorbing polymers have sufficient time to flat down on the colloid surfaces, no flocculation will occur (i.e., low colloids or polymers concentration). However, flocculation may also happen if electrostatic barrier (κ^{-1}) is

lowered by salt addition. On the other hand, flocculation may happen if colloid-colloid collision is faster than polymer rearrangement (i.e., high colloids concentration). The latter case is named non-equilibrium flocculation[88, 89].

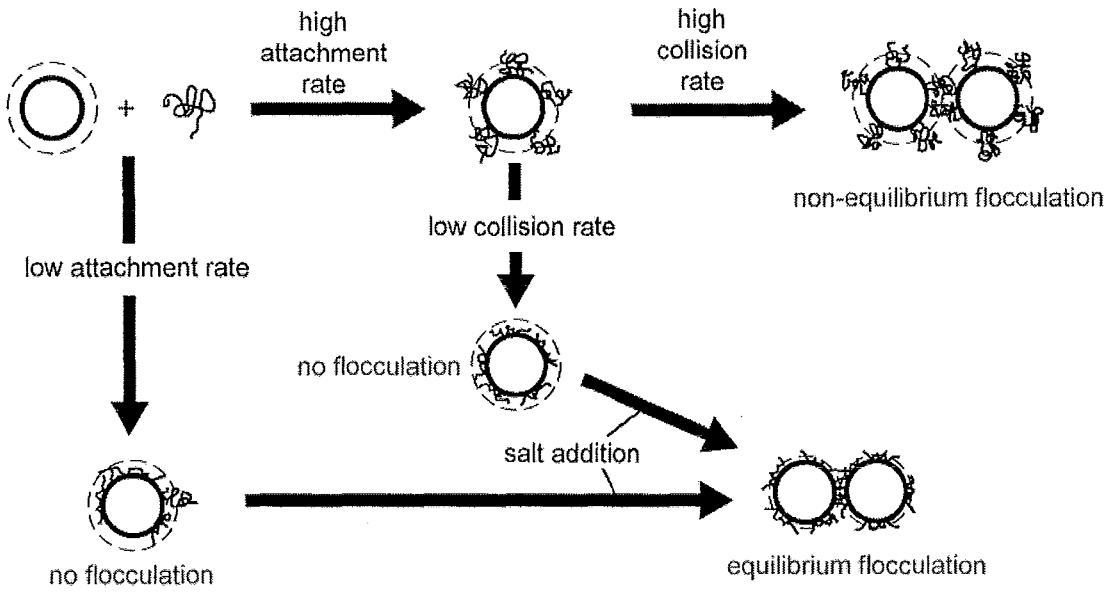

Figure 1. 10 schematic illustration of equilibrium and non-equilibrium flocculation of charged colloids by nonionic polymers (adapted from reference 77)

Depletion Flocculation — Considerable interest has focused on understanding the entropy driven colloidal phase separation induced by non-adsorbing polymer. As it has been discussed above, polymers are depleted from the colloid surfaces, leads to osmotic pressure Π near the surfaces lower than that of in the bulk. The depletion layers on each colloid surface, generated by excluded polymer segments, create overlap volume $V_{overlap}$ when colloids approach each other through Brownian motion (see Figure 1. 11, illustrate depletion mechanism of colloids in the presence of non-adsorbing polymer[90]). The generation of overlap volume $V_{overlap}$ lowers free energy of the system through $\Delta G = -\Pi \times V_{overlap}$, which forces the colloids aggregate into one separate phase.

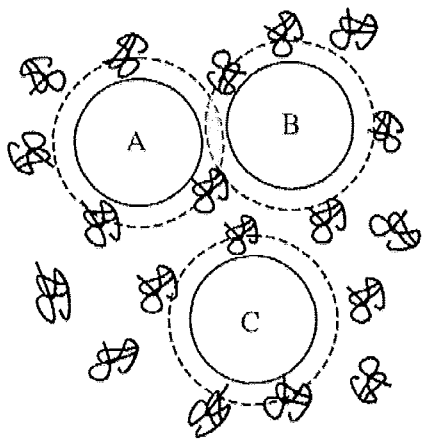

Figure 1. 11 Schematic illustration of colloids in non-adsorbing polymer solution, the depletion layer is indicated by dashed lines. (adapted from figure 1 in reference 90)[90]

A number of studies have used well-defined depletion systems to link experimental and theoretical works. De Hek and Vrij estimated phase separation threshold by mixing silica dispersion with polystyrene in cyclohexane[91]. Their results can semi-quantitatively fit Vrij's penetrable hard sphere model (PHS)[92]. The limiting polymer concentration, from which phase separation starts, decreases with increasing molecular weight at fixed silica volume fraction. At the same time, increasing silica volume fraction lowers the limiting polymer concentration value (Figure 1. 11 shows typical phase diagram of colloid/non-adsorbing polymer). Sperry and co-workers[67, 93] studied charge-stabilized latex depleted by hydroxyethylcellulose (HEC). They found polymer/colloid size ratio regulates phase behavior. If polymer is relatively small, solid/liquid equilibrium was observed. If polymer is large, they found gas-liquid equilibrium. Polymer/non-adsorbing polymer binary phase separation is one of key topics in soft condensed matter; a detailed discussion can be referred to a number of review articles[69, 70, 90, 94, 95]. Finally, depletion flocculation is non-equilibrium process; different systems[69, 90, 96] have been observed distinguished time scale for macroscopic phase separation. Hence, operation time inevitably becomes another variable.

THESIS OBJECTIVES

The aim of this work is to understand interfacial behavior of HPG in the presence of borate ions using model systems. Particular interest is focused on interaction between HPG-borate and colloidal suspensions, such as hydrophobic polystyrene latex and hydrophilic lipid-stabilized emulsions.

The hydrophobic polystyrene latex surface represents hydrophobic lipid layer and exposed corneal epithelium surface. Adsorption of HPG-borate onto hydrophobic surface may provide a key to understand curing efficiency of HPG-borate in dry eye. The results will be presented in chapter 2. This work confirms that HPG and HPG-borate readily adsorbs onto cationic and anionic hydrophobic surfaces."

Lipid in eyes is a complex mixture. It composed by polar and non-polar molecules. Interaction between HPG-borate and hydrophilic lipid mixture is quite universal in artificial tear. In chapter 3, interaction between HPG-borate and lipid-stabilized emulsions will be studied. This work showed HPG-borate is not adsorbed by the emulsions. High HPG-borate concentration leads to depletion flocculation of the emulsions. The presence of borate ions does not affect threshold depletion concentration of HPG.

Chapter 4 is a theoretical study on interaction between oppositely anionic HPG-borate, a Labile polyelectrolyte, and 1,2-dioleoyl-3-trimethylammonium-propane (DOTAP) liposomes. This system was chosen because it displays extreme salt concentration sensitivity, which may be operative in the tear film. The results are expressed as novel stability domain diagrams where properties are mapped upon a surface where the y-axis is salt concentration and the x-axis is the log polymer concentration. This gives

formulators designing artificial tear products a tool for understanding their systems.

REFERENCE

1. Bungenberg De Jong, H. G., Reversal of charge phenomena, equivalent weight and specific properties of the ionised groups. In *Colloid science*, Kruyt, H. R., Ed. Elsevier: Amsterdam, 1949; Vol. 2, p 259.
2. Lemp, M. A., Report of the national eye institute/industry workshop on clinical trials in dry eyes. *CLAO J* **1995,** 21, (4), 221-32.
3. Pflugfelder, S. C.; Solomon, A.; Stern, M. E., The diagnosis and management of dry eye - a twenty-five-year review. *Cornea* **2000,** 19, (5), 644-649.
4. Wolff, E., The muco-cutaneous junction of the lid-margin and the distribution of the tear fluid. *Trans. Ophthalmol. Soc. U.K.* **1946,** 66, 291-308.
5. Maurice, D. M., The dynamics and drainage of tears. *Int Ophthalmol Clin* **1973,** 13, (1), 103-16.
6. Ehlers, N., The precorneal film. Biomicroscopical, histological and chemical investigations. *Acta Ophthalmol Suppl* **1965**, SUPPL 81:1-134.
7. Prydal, J. I.; Artal, P.; Woon, H.; Campbell, F. W., Study of human precorneal tear film thickness and structure using laser interferometry. *Invest Ophthalmol Vis Sci* **1992,** 33, (6), 2006-11.
8. Prydal, J. I.; Campbell, F. W., Study of precorneal tear film thickness and structure by interferometry and confocal microscopy. *Invest Ophthalmol Vis Sci* **1992,** 33, (6), 1996-2005.
9. Bron, A. J.; Tiffany, J. M.; Gouveia, S. M.; Yokoi, N.; Voon, L. W., Functional aspects of the tear film lipid layer. *Exp Eye Res* **2004,** 78, (3), 347-60.
10. Mishima, S.; Maurice, D. M., The oily layer of the tear film and evaporation from the corneal surface. *Exp Eye Res* **1961,** 1, 39-45.
11. Tiffany, J. M., The lipid secretion of the meibomian glands. *Adv. Lipid Res.* **1987,** 22, 1-62.
12. Goto, E.; Endo, K.; Suzuki, A.; Fujikura, Y.; Matsumoto, Y.; Tsubota, K., Tear evaporation dynamics in normal subjects and subjects with obstructive meibomian gland dysfunction. *Invest. Ophthalmol. Vis. Sci.* **2003,** 44, (2), 533-539.
13. Holly, F., Formation and rupture of the tear film. *Experimental Eye Research* **1973,** 15, (5), 515-525.
14. Scriven, L.; Sternling, C., The marangoni effects. *Nature* **1960,** 187, 186-188.
15. Iwata, S., Chemical composition of the aqueous phase. *Int Ophthalmol Clin* **1973,** 13, (1), 29-46.
16. Davidson, H. J.; Kuonen, V. J., The tear film and ocular mucins. *Vet. Ophthalmol.* **2004,** 7, (2), 71-77.
17. Kaura, R.; Tiffany, J., The role of mucous glycoproteins in the tear film. *The Preocular Tear Film in Health, Disease and Contact Lens Wear. Lubbock, TX: Dry Eye Institute Inc* **1986,** 728–732.
18. Nichols, B. A.; Chiappino, M. L.; Dawson, C. R., Demonstration of the mucous layer of the tear film by electron-microscopy. *Invest. Ophthalmol. Vis. Sci.* **1985,** 26, (4), 464-473.
19. Adams, A., Conjunctival surface mucus. In Dry Eye Institute, Inc: 1986; pp 304-311.
20. Lemp, M. A.; Blackman, H. J., Ocular surface defense-mechanisms. *Ann. Ophthalmol.* **1981,** 13, (1), 61-63.
21. Chen, M. L.; Wang, Y.; Begley, C. G.; Wolosin, J. M., Synthesis of rabbit corneal epithelial glycocalyx in-vitro. *Experimental Eye Research* **1994,** 58, (3), 267-276.
22. Murube, J.; Paterson, A.; Murube, E., Classification of artificial tears i: Composition and properties. In *Lacrimal gland, tear film, and dry eye syndromes 2 - basic science and clinical relevance*, Sullivan, D. A.; Dartt, D. A.; Meneray, M. A., Eds. Plenum Press Div Plenum Publishing Corp: New

York, 1998; Vol. 438, pp 693-704.

23. Cheng, Y.; Brown, K. M.; Prud'homme, R. K., Characterization and intermolecular interactions of hydroxypropyl guar solutions. *Biomacromolecules* **2002,** 3, (3), 456-461.

24. Gittings, M. R.; Cipelletti, L.; Trappe, V.; Weitz, D. A.; In, M.; Marques, C., Structure of guar in solutions of h2o and d2o: An ultra-small-angle light-scattering study. *Journal of Physical Chemistry B* **2000,** 104, (18), 4381-4386.

25. Goycoolea, F. M.; Morris, E. R.; Gidley, M. J., Viscosity of galactomannans at alkaline and neutral ph - evidence of hyperentanglement in solution. *Carbohydrate Polymers* **1995,** 27, (1), 69-71.

26. Launay, B.; Cuvelier, G.; Martinez-Reyes, S., Viscosity of locust bean, guar and xanthan gum solutions in the newtonian domain: A critical examination of the log(eta(sp))(o)-logc[eta](o) master curves. *Carbohydrate Polymers* **1997,** 34, (4), 385-395.

27. Morris, E. R.; Cutler, A. N.; Ross-Murphy, S. B.; Rees, D. A.; Price, J., Concentration and shear rate dependence of viscosity in random coil polysaccharide solutions. *Carbohydrate Polymers* **1981,** 1, (1), 5-21.

28. Robinson, G.; Rossmurphy, S. B.; Morris, E. R., Viscosity molecular-weight relationships, intrinsic chain flexibility, and dynamic solution properties of guar galactomannan. *Carbohydrate Research* **1982,** 107, (1), 17-32.

29. Gittings, M. R.; Cipelletti, L.; Trappe, V.; Weitz, D. A.; In, M.; Lal, J., The effect of solvent and ions on the structure and rheological properties of guar solutions. *J. Phys. Chem. A* **2001,** 105, (40), 9310-9315.

30. Cheng, Y.; Prud'homme, R. K.; Chik, J.; Rau, D. C., Measurement of forces between galactomannan polymer chains: Effect of hydrogen bonding. *Macromolecules* **2002,** 35, (27), 10155-10161.

31. Pezron, E.; Leibler, L.; Ricard, A.; Lafuma, F.; Audebert, R., Complex-formation in polymer ion solutions .1. Polymer concentration effects. *Macromolecules* **1989,** 22, (3), 1169-1174.

32. Pezron, E.; Leibler, L.; Ricard, A.; Audebert, R., Reversible gel formation induced by ion complexation .2. Phase-diagrams. *Macromolecules* **1988,** 21, (4), 1126-1131.

33. Pezron, E.; Ricard, A.; Lafuma, F.; Audebert, R., Reversible gel formation induced by ion complexation .1. Borax galactomannan interactions. *Macromolecules* **1988,** 21, (4), 1121-1125.

34. Pezron, E.; Leibler, L.; Lafuma, F., Complex-formation in polymer-ion solutions .2. Poly-electrolyte effects. *Macromolecules* **1989,** 22, (6), 2656-2662.

35. Leibler, L.; Pezron, E.; Pincus, P. A., Viscosity behavior of polymer-solutions in the presence of complexing ions. *Polymer* **1988,** 29, (6), 1105-1109.

36. Kesavan, S.; Prudhomme, R. K., Rheology of guar and hpg cross-linked by borate. *Macromolecules* **1992,** 25, (7), 2026-2032.

37. Leibler, L.; Rubinstein, M.; Colby, R. H., Dynamics of reversible networks. *Macromolecules* **1991,** 24, (16), 4701-4707.

38. Ferry, J. D., *Viscoelastic properties of polymers*. 3rd Edition ed.; Wiley: New York: 1980.

39. Fleer, G. J.; Cohen Stuart, M. A.; Scheutjens, J. M. H. M.; Cosgrove, T.; Vincent, B., *Polymers at interfaces*. Springer: 1993.

40. Joanny, J. F.; Leibler, L.; Degennes, P. G., Effects of polymer-solutions on colloid stability. *Journal of Polymer Science Part B-Polymer Physics* **1979,** 17, (6), 1073-1084.

41. de Gennes, P., *Scaling concepts in polymer physics*. Cornell University Press: 1979.

42. Felter, R. E.; Ray, L. N., Polymer adsorption studies at the solid-liquid interface using gel

permeation chromatography : I. Molecular weight distribution along the adsorption isotherm. *Journal of Colloid and Interface Science* **1970,** 32, (2), 349-360.

43. Linden, C. V.; Leemput, R. V., Adsorption studies of polystyrene on silica i. Polydisperse adsorbate. *Journal of Colloid and Interface Science* **1978,** 67, (1), 63-69.

44. Stuart, M. A. C.; Scheutjens, J.; Fleer, G. J., Polydispersity effects and the interpretation of polymer adsorption-isotherms. *Journal of Polymer Science Part B-Polymer Physics* **1980,** 18, (3), 559-573.

45. Dobrynin, A. V.; Rubinstein, M., Theory of polyelectrolytes in solutions and at surfaces. *Prog. Polym. Sci.* **2005,** 30, (11), 1049-1118.

46. Grosberg, A. Y.; Nguyen, T. T.; Shklovskii, B. I., Colloquium: The physics of charge inversion in chemical and biological systems. *Rev. Mod. Phys.* **2002,** 74, (2), 329-345.

47. Kawaguchi, M.; Takahashi, A., Polymer adsorption at solid liquid interfaces. *Advances in Colloid and Interface Science* **1992,** 37, (3-4), 219-317.

48. Netz, R. R.; Andelman, D., Neutral and charged polymers at interfaces. *Phys. Rep.-Rev. Sec. Phys. Lett.* **2003,** 380, (1-2), 1-95.

49. Decher, G., Fuzzy nanoassemblies: Toward layered polymeric multicomposites. *Science* **1997,** 277, (5330), 1232-1237.

50. Dobrynin, A. V.; Deshkovski, A.; Rubinstein, M., Adsorption of polyelectrolytes at oppositely charged surfaces. *Macromolecules* **2001,** 34, (10), 3421-3436.

51. Durand, G.; Lafuma, F.; Audebert, R., Adsorption of cationic polyelectrolytes at clay-colloid interface in dilute aqueous suspensions — effect of the ionic strength of the medium *Progress in Colloid and Polymer Science* **1988,** 76, 278-282.

52. Pelton, R. H., Electrolyte effects in the adsorption and desorption of a cationic polyacrylamide on cellulose fibers. *Journal of Colloid and Interface Science* **1986,** 111, (2), 475-485.

53. Durandpiana, G.; Lafuma, F.; Audebert, R., Flocculation and adsorption properties of cationic polyelectrolytes toward na-montmorillonite dilute suspensions. *Journal of Colloid and Interface Science* **1987,** 119, (2), 474-480.

54. Wang, T. K.; Audebert, R., Adsorption of cationic copolymers of acrylamide at the silica--water interface: Hydrodynamic layer thickness measurements. *Journal of Colloid and Interface Science* **1988,** 121, (1), 32-41.

55. Davies, R. J.; Dix, L. R.; Toprakcioglu, C., Adsorption of poly-l-lysine to mica powder. *Journal of Colloid and Interface Science* **1989,** 129, (1), 145-152.

56. Shubin, V.; Linse, P., Effect of electrolytes on adsorption of cationic polyacrylamide on silica - ellipsometric study and theoretical modeling. *Journal of Physical Chemistry* **1995,** 99, (4), 1285-1291.

57. Kawaguchi, M.; Kawaguchi, H.; Takahashi, A., Competitive and displacement adsorption of poly-electrolyte and water-soluble nonionic polymer at the silica surface. *Journal of Colloid and Interface Science* **1988,** 124, (1), 57-62.

58. Marra, J.; van der Schee, H. A.; Fleer, G. J.; Lyklema, J., In *Adsorption in solutions*, Ottiwel, R.; Rochester, C. H.; Smith, A. L., Eds. Academic Press: London, 1983; p 245.

59. Blaakmeer, J.; Bohmer, M. R.; Stuart, M. A. C.; Fleer, G. J., Adsorption of weak polyelectrolytes on highly charged surfaces - poly(acrylic acid) on polystyrene latex with strong cationic groups. *Macromolecules* **1990,** 23, (8), 2301-2309.

60. Bohmer, M. R.; Evers, O. A.; Scheutjens, J. M. H. M., Weak polyelectrolytes between 2 surfaces - adsorption and stabilization. *Macromolecules* **1990,** 23, (8), 2288-2301.

61. Lecourtier, J.; Lee, L. T.; Chauveteau, G., Adsorption of polyacrylamides on siliceous minerals. *Colloids and Surfaces* **1990,** 47, 219-231.

62. Fleer G, J.; Scheutjens J. H. M, H.; Vincent, B., The stability of dispersions of hard spherical particles in the presence of nonadsorbing polymer. In *Polymer adsorption and dispersion stability*, American Chemical Society: Washington, D.C., 1984; pp 245-263.

63. Oosawa, F.; Asakura, S., Surface tension of high-polymer solutions. *The Journal of Chemical Physics* **1954,** 22, (7), 1255.

64. Milling, A. J.; Vincent, B., Depletion forces between silica surfaces in solutions of poly(acrylic acid). *J. Chem. Soc.-Faraday Trans.* **1997,** 93, (17), 3179-3183.

65. Asakura, S.; Oosawa, F., Interaction between particles suspended in solutions of macromolecules. *Journal of Polymer Science* **1958,** 33, (126), 183-192.

66. De Hek, H.; Vrij, A., Phase separation in non-aqueous dispersions containing polymer molecules and colloidal spheres. *Journal of Colloid and Interface Science* **1979,** 70, (3), 592-594.

67. Sperry, P. R., A simple quantitative model for the volume restriction flocculation of latex by water-soluble polymers. *Journal of Colloid and Interface Science* **1982,** 87, (2), 375-384.

68. Vincent, B., The calculation of depletion layer thickness as a function of bulk polymer concentration. *Colloids and Surfaces* **1990,** 50, 241-249.

69. Poon, W. C. K.; Haw, M. D., Mesoscopic structure formation in colloidal aggregation and gelation. *Advances in Colloid and Interface Science* **1997,** 73, 71-126.

70. Tuinier, R.; Rieger, J.; De Kruif, C., Depletion-induced phase separation in colloid–polymer mixtures. *Advances in Colloid and Interface Science* **2003,** 103, (1), 1-31.

71. Vincent, B.; Edwards, J.; Emmett, S.; Croot, R., Phase-separation in dispersions of weakly-interacting particles in solutions of non-adsorbing polymer. *Colloids and Surfaces* **1988,** 31, 267-298.

72. Israelachvili, J., *Intermolecular and surface forces*. Academic press London: 1991.

73. Luckham, P. F.; Klein, J., Interactions between smooth solid-surfaces in solutions of adsorbing and nonadsorbing polymers in good solvent conditions. *Macromolecules* **1985,** 18, (4), 721-728.

74. Milling, A.; Biggs, S., Direct measurement of the depletion force using an atomic-force microscope. *Journal of Colloid and Interface Science* **1995,** 170, (2), 604-606.

75. Dobrynin, A. V.; Colby, R. H.; Rubinstein, M., Scaling theory of polyelectrolyte solutions. *Macromolecules* **1995,** 28, (6), 1859-1871.

76. Ausserre, D.; Hervet, H.; Rondelez, F., Concentration-dependence of the interfacial depletion layer thickness for polymer-solutions in contact with nonadsorbing walls. *Macromolecules* **1986,** 19, (1), 85-88.

77. Degennes, P. G., Colloid suspensions in a polymer-solution. *Comptes Rendus Hebdomadaires Des Seances De L Academie Des Sciences Serie B* **1979,** 288, (21), 359-361.

78. Milling, A. J., Depletion and structuring of sodium poly(styrenesulfonate) at the silica-water interface. *Journal of Physical Chemistry* **1996,** 100, (21), 8986-8993.

79. Milling, A. J.; Kendall, K., Depletion, adsorption, and structuring of sodium poly(acrylate) at the water-silica interface. 1. An atomic force microscopy force study. *Langmuir* **2000,** 16, (11), 5106-5115.

80. Oosawa, F., *Polyelectrolytes*. New York: Marcel Dekker: 1971.

81. Hiemenz, P., *Principles of colloid and surface chemistry*. Marcel Dekker: New York: 1977.

82. Biggs, S.; Burns, J. L.; Yan, Y. D.; Jameson, G. J.; Jenkins, P., Molecular weight dependence of the depletion interaction between silica surfaces in solutions of sodium poly(styrene sulfonate).

Langmuir **2000,** 16, (24), 9242-9248.

83. Pagac, E. S.; Tilton, R. D.; Prieve, D. C., Depletion attraction caused by unadsorbed polyelectrolytes. *Langmuir* **1998,** 14, (18), 5106-5112.

84. Dickinson, E.; Eriksson, L., Particle flocculation by adsorbing polymers. *Advances in Colloid and Interface Science* **1991,** 34, 1-29.

85. Napper, D. H., *Polymeric stabilization of colloidal dispersions*. Academic Press: 1983; p 428.

86. Pelssers, E. G. M.; Stuart, M. A. C.; Fleer, G. J., Kinetics of bridging flocculation - role of relaxations in the polymer layer. *J. Chem. Soc.-Faraday Trans.* **1990,** 86, (9), 1355-1361.

87. Pelssers, E. G. M.; Stuart, M. A. C.; Fleer, G. J., Kinetic aspects of polymer bridging - equilibrium flocculation and nonequilibrium flocculation. *Colloids and Surfaces* **1989,** 38, (1-3), 15-25.

88. Gregory, J., Polymer adsorption and flocculation in sheared suspensions. *Colloids and Surfaces* **1988,** 31, 231-253.

89. Gregory, J., Rates of flocculation of latex particles by cationic polymers. *Journal of Colloid and Interface Science* **1973,** 42, (2), 448-456.

90. Poon, W. C. K., The physics of a model colloid-polymer mixture. *Journal of Physics-Condensed Matter* **2002,** 14, (33), R859-R880.

91. De Hek, H.; Vrij, A., Interactions in mixtures of colloidal silica spheres and polystyrene molecules in cyclohexane : I. Phase separations. *Journal of Colloid and Interface Science* **1981,** 84, (2), 409-422.

92. Vrij, A., Polymers at interfaces and interactions in colloidal dispersions. *Pure and Applied Chemistry* **1976,** 48, (4), 471-483.

93. Sperry, P. R., Morphology and mechanism in latex flocculated by volume restriction. *Journal of Colloid and Interface Science* **1984,** 99, (1), 97-108.

94. Likos, C. N., Effective interactions in soft condensed matter physics. *Phys. Rep.-Rev. Sec. Phys. Lett.* **2001,** 348, (4-5), 267-439.

95. Poon, W. C. K.; Pirie, A. D.; Pusey, P. N., Gelation in colloid-polymer mixtures. *Faraday Discuss.* **1995,** 101, 65-76.

96. Bibette, J.; Roux, D.; Nallet, F., Depletion interactions and fluid-solid equilibrium in emulsions. *Physical Review Letters* **1990,** 65, (19), 2470-2473.

Chapter 2

Charge Regulation Controls Anionic Hydroxypropyl Guar - Borate Adsorption onto Anionic and Cationic Polystyrene Latex

2.1 ABSTRACT

Reported are adsorption isotherms for guar and hydroxypropyl guar (HPG), with and without the presence of borate ions, onto surfactant free anionic polystyrene latex. Guar and HPG formed adsorbed monolayers on the hydrophobic latex. The maximum mass of adsorbed polymer increased with molecular weight – classical behavior. The presence of borate ions converted the nonionic guar and HPG into anionic polyelectrolyte. However, there was no measurable influence of bound borate ions on the adsorption of guar or HPG onto anionic, hydrophobic latex. By contrast, the adsorption of oxidized HPG was inhibited by the ionization of the carboxyl groups on the HPG. We propose that as HPG-borate segments approach the latex surface, the anionic charges bound to the latex surface induces the detachment of the labile borate groups from HPG.

2.2 INTRODUCTION

Hydroxypropyl guar (HPG), a derivatized natural polymer, has demonstrated efficacy as an additive with boric acid in artificial tear formulations. [1, 2] As part of larger study of HPG behavior in the tear film[3], we have systematically investigated HPG mixtures with boric acid in simple in vitro model systems with a view to understanding the potential range of behaviors under ophthalmic conditions. This chapter describes the adsorption behaviors of HPG-borate onto anionic, surfactant free polystyrene surfaces that serve as model hydrophobic interfaces that may be present in unhealthy eyes. [4]

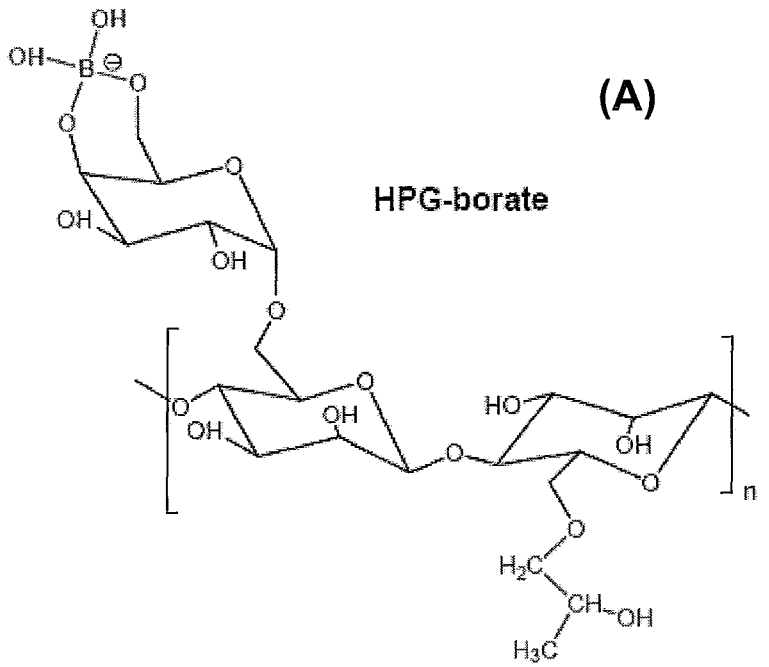

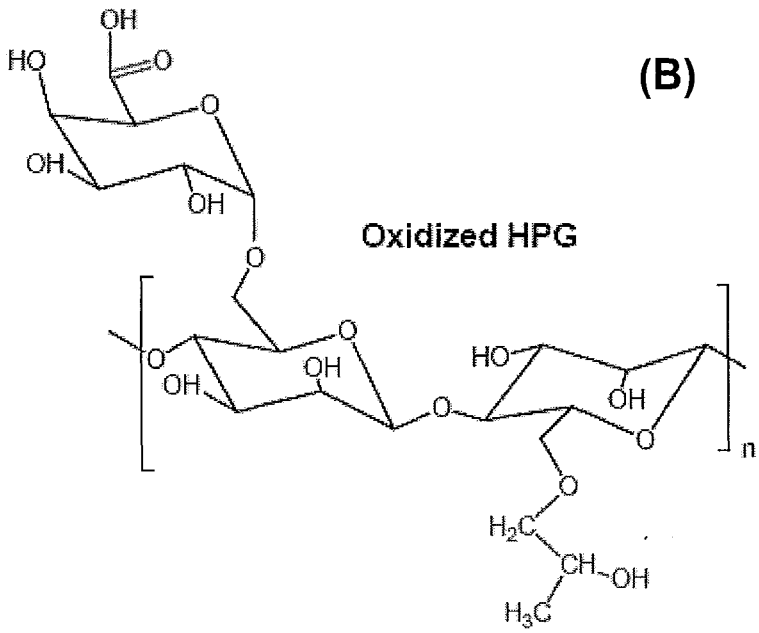

Figure 2. 1. The structure of HPG-borate (A) and oxidized HPG (B). Note the extent of borate substitution is very sensitive to pH and borate ion concentration.

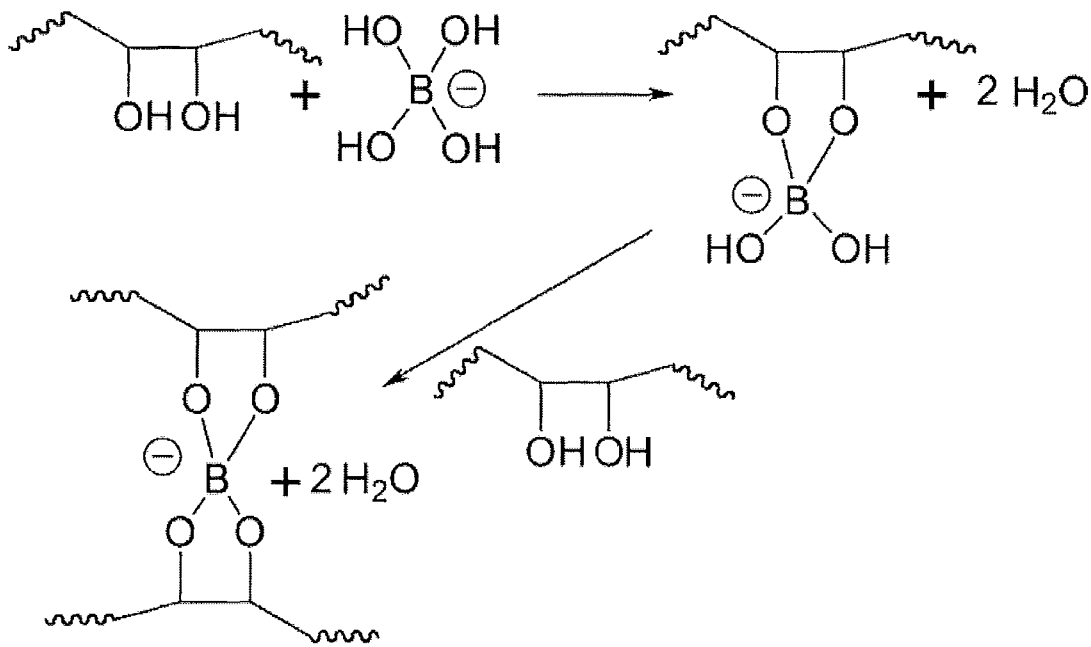

Figure 2. 2. Borate ions can condense with two pairs of cis-diols introducing an anionic charge and a crosslink.

HPG is a fascinating polymer, particularly in the presence of borate ions. It has been

long known that borate will condense onto and crosslink guar and other polyols – see Figure 2. 2. Audebert's group was the first to emphasize that borate binding converted nonionic guar, or HPG, into an anionic polyelectrolyte.[5] More importantly the French group emphasized that borate linkage was very weak, akin to hydrogen bonding. [5, 6] Thus the charge density on HPG-borate is very sensitive to the local environment, leading to unusual properties; we coined the term "labile polyelectrolyte" for such systems. [7] Examples of unusual behaviors include the following.

Conventional anionic polyelectrolytes irreversibly and stoichiometrically form complexes with cationic polyelectrolytes. This behavior forms the basis of the polyelectrolyte titration, a technique that is routinely used to measure polyelectrolyte concentration, or the charge density on a polyelectrolyte. When we attempted to measure the fraction of occupied borate binding sites on HPG by titration with polyDADMAC, a quaternary ammonium cationic polymer, we found that the endpoint of the titration corresponded to the HPG chain being saturated with borate. [7] Thus, the act of forming the polyelectrolyte complex changed the local electrostatic environment inducing more borates to bind to guar. Titration of traditional weak polyelectrolytes, such as polyethylene imine, does not show this behavior.[8] Another example of non-classical behavior involves the interaction with cationic surfactants. All traditional anionic polyelectrolytes interact strongly with cationic surfactants, usually resulting in precipitation.[9] By contrast, we have recently shown that HPG-borate does not interact with DTAB monomers and shows only a subtle tendency to flocculate DTAB micelles.[10]

On the other hand, HPG-borate induced strong bridging flocculation of cationic polystyrene latex, much like any other anionic polyelectrolyte. [11] An interesting distinction, however, is that the flocculation could be reversed by adding a sugar that had a higher borate binding constant than guar. Finally, another manifestation of labile borate binding is the observation the extent of guar crosslinking with borate is pressure sensitive. [12]

The current work is a classical adsorption study of HPG-borate onto anionic polystyrene latex, a negatively charged hydrophobic surface. There have been a number of reports of guar and HPG adsorption, without borate, onto a number of mineral surfaces because guar and HPG are used as additives (suppressants) in mineral processing. [13] Guar forms an adsorbed monolayer on a number of mineral surfaces. [13-15] Although, there has been some discussion of hydrogen bonding and acid-base interactions,[13] the currently accepted mechanism seems to involve hydrophobic interactions.[14, 15] There have been no reports in the literature on the adsorption behavior of HPG-borate, a labile anionic polyelectrolyte, onto any surface. Herein we report HPG-borate adsorption onto surfactant-free polystyrene latexes. We compare cationic and anionic latex substrates as well as types of guar. Particularly interesting are the differences between the adsorption behaviors of oxidized HPG, a conventional weak polyelectrolyte and HPG-borate, a labile polyelectrolyte. Specifically, we provide evidence that the latex surface charge regulates the borate binding density on HPG.

2.3 EXPERIMENTAL

2.3.1 Materials. Native guar ($Mw=3.0\times10^6$), partially hydrolyzed native guar ($Mw=1.5\times10^4$) and hydroxypropyl guar (HPG, $Mw=1.5\times10^6$) with a degree of substitution of 0.36 were gifts from Alcon Laboratories (Fort Worth, TX). 500 nm diameter polystyrene latex, bearing surface sulfate groups was purchased from Invitrogen Corporation (San Diego, CA). Sodium chloride, 2,2,6,6-tetramethyl-1-piperidinyoxyradical (TEMPO) NaBr, NaClO and borax (Na2B4O7 • 10H2O) were purchased from Sigma-Aldrich. The parameters of the samples are summarized in table 1.

Table 1. Parameters of the Samples

Name	*Designation*	*Degree of Substitution*	*Molecular Weight*
Hydroxypropyl guar	HPG	0.36 hydroxypropyl	1.5×10^6
Guar	Guar	0	3×10^6
Partially Hydrolyzed Guar	PH Guar	0	1.5×10^4
Oxidized HPG[a]	OX HPG	0.36 hydroxypropyl 0.2 carboxyl	1.5×10^6

a — Use typical TEMPO oxidation procedure, method can be found below.

2.3.2 HPG Oxidation.[16] HPG 0.5 g was dissolved in 0.5 L distilled water. TEMPO 0.01 g and NaBr 0.05 g were added. The solution was stirred and cooled in an ice bath (3±1℃). 15% sodium hypochlorite (3 ml) was cooled (3±1℃) and pH was adjusted to 9.4 with 2 M HCl. The solutions were mixed and pH was maintained at 9.4 by 0.5 M NaOH. The reaction was quenched by adding 3 ml methanol and neutralized to pH 6 by adding 4 M HCl. Then excess sodium borohydride (0.25 g) was added and the solution was stirred over night. The product was purified by exhaustive dialysis against deionized water and the product was freeze-dried. The carboxyl content was measured by conductometric titration.

2.3.3 Adsorption isotherms. 2 ml of polystyrene latex (0.1 wt%) were sonicated for about 20 min to ensure good dispersion and then placed in Beckman 26.3 ml polycarbonate centrifuge bottles (Beckman Coulter, Inc. USA). The solutions were made up to 25 mL with buffer, electrolyte and polymer solution. Finally, the centrifuge bottles were capped and slowly rotated end-over-end for 24 hours at room temperature.

The latex dispersions were centrifuged for 30 minutes at 8000 RPM (4710 g) in an

Optima L-XP Ultracentrifuge (Beckman Coulter, Inc. USA). The sediment was washed by three cycles of dispersion in the corresponding solvent (i.e., salt solutions with same ionic strength and pH used in adsorption experiments), centrifugation, and decantation to remove all unadsorbed polymer. The washed latex was vacuum dried over phosphoric anhydride and the atomic composition was measured with an elemental analyzer (FlashEA 1112, Thermo Fisher Scientific Inc, USA). The content of guar was calculated from the oxygen content of the precipitated latex. The analysis of known guar/latex mixtures indicated that the measurements were accurate within ± 3%.

2.3.4 Electrophoresis. Electrophoretic mobilities were measured at 25°C with a Brookhaven Zetapals Microelectrophoresis apparatus in the phase analysis light scattering mode using BIC Pals Zeta Potential Analyzer software version 2.5. Measurements were repeated 3 times.

2.4 RESULTS AND DISCUSSION

In earlier work we reported the flocculation of cationic, surfactant-free polystyrene latex with HPG-borate (structure in Figure 2. 1). [11] Some of the electrophoresis results from that work are reproduced in Figure 2. 3. The key observations were that nonionic HPG adsorbed onto the cationic latex, shifting the shear plane out from the charged surface, lowering the cationic mobility. By contrast, the anionic HPG-borate also adsorbed onto the cationic however the sign of the electrophoretic mobility was reversed due to bound borate ions on adsorbed guar. In this case, electrostatic and non-electrostatic interactions contributed to HPG-borate adsorption. In the new work, we consider the interaction of HPG-borate with negatively charged latex, a case in which electrostatics oppose adsorption.

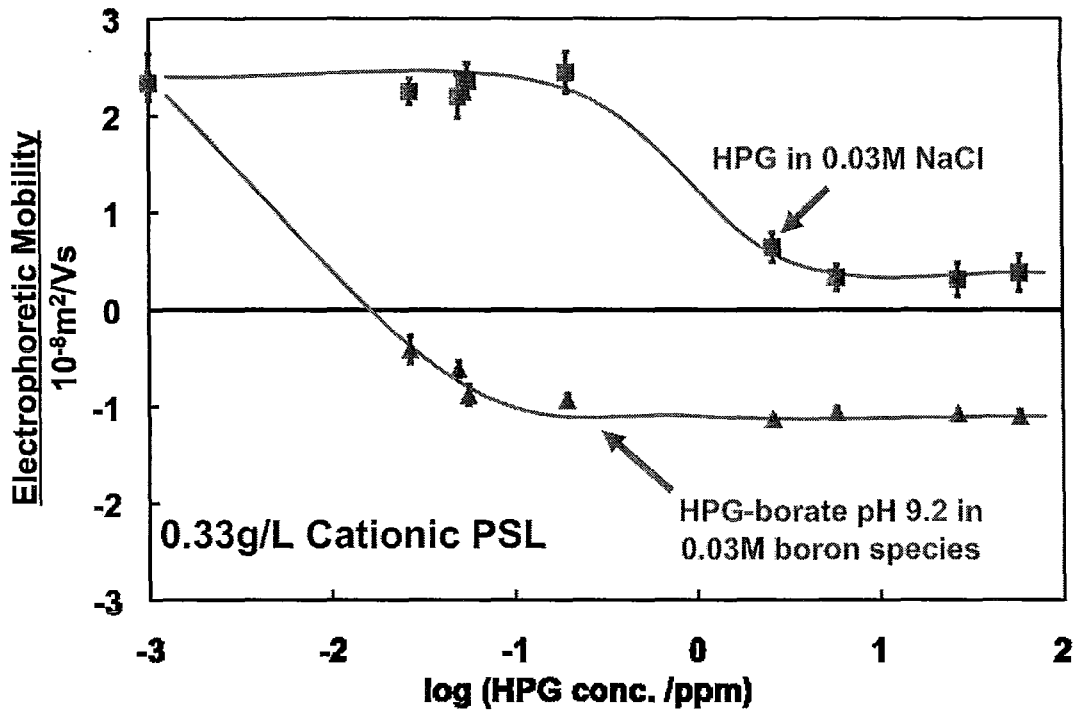

Figure 2. 3. The electrophoretic mobility of surfactant-free, cationic polystyrene latex as functions of the concentrations of HPG and HPG-borate. Results adapted from [11].

Figure 2. 4 shows the adsorption isotherms for HPG, with and without borax, onto anionic, surfactant-free polystyrene latex. The isotherms display typical high affinity behavior where essentially all the added polymer is adsorbed until the surfaces are saturated around 1.5 mg/m^2. However, the adsorption isotherms are not as sharp as those from theory. The usual explanation from Fleer et al. involves higher molecular weight displacing lower molecular weight polymer chains from the surface - a polydispersity effect. [17]

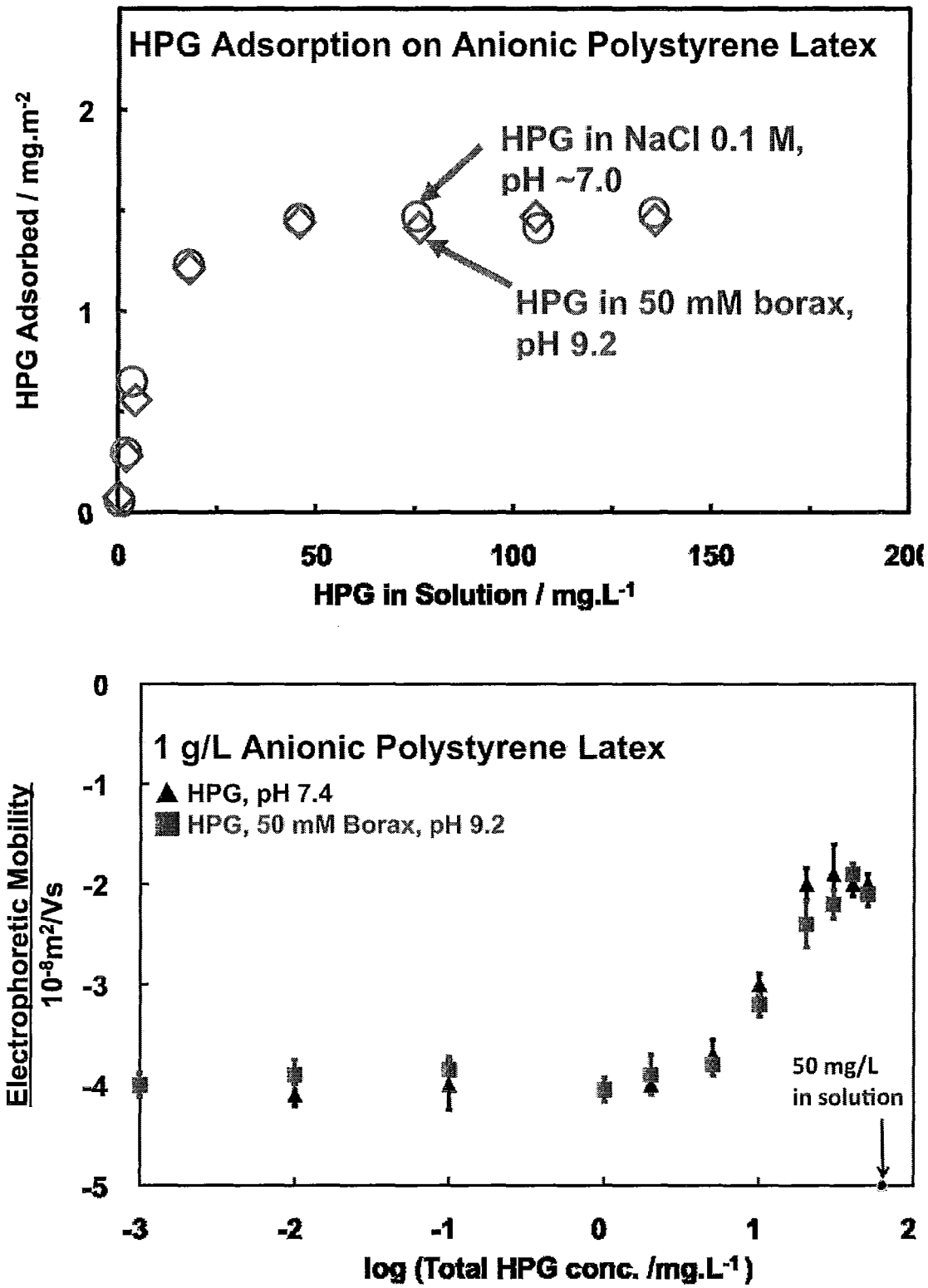

Figure 2. 4. Top -adsorption isotherms of HPG on polystyrene latex at 25℃, one with borax concentration 50mM (red square, pH 9.2), the other has 0.1M sodium chloride (blue circle, pH ~7). Bottom – influence of HPG and HPG-borate on electrophoretic mobility.

Guar adsorption on mineral surfaces has been explained by both acid-base and hydrophobic interactions – see summary in introduction. It is difficult to envision acid base interactions between HPG and polystyrene decorated with sulfate (negative latex) groups. We presume that hydrophobic interactions dominate.

Within experimental error, borax addition had no effect on HPG adsorption onto anionic latex – see Figure 2. 4. Top -adsorption isotherms of HPG on polystyrene latex at 25℃, one with borax concentration 50mM (red square, pH 9.2), the other has 0.1M sodium chloride (blue circle, pH ~7). Bottom – influence of HPG and HPG-borate on electrophoretic mobility.. This was surprising to us as we anticipated that the anionic charges on the HPG chain from borate binding (see Figure 2. 1), would influence adsorption. We envisioned two effects with borate. First, the negative charges on HPG-borate could interfere with adsorption onto a negatively charged latex surface. Second, the ability of borate to crosslink or couple guar chains (see Figure 2. 2) could lead to multilayer adsorption. Neither of these effects seemed to have occurred.

In previous work we have argued that borate binds predominately to the galactose moieties. [7] Under the conditions of our experiments we estimate that the average number of bound borate groups per sugar ring is 0.34, assuming Jasinski's binding constant of 100 L/mol, and only binding to galactose. [18] Nevertheless, the results in Figure 2. 4 suggest that borate does not influence HPG adsorption.

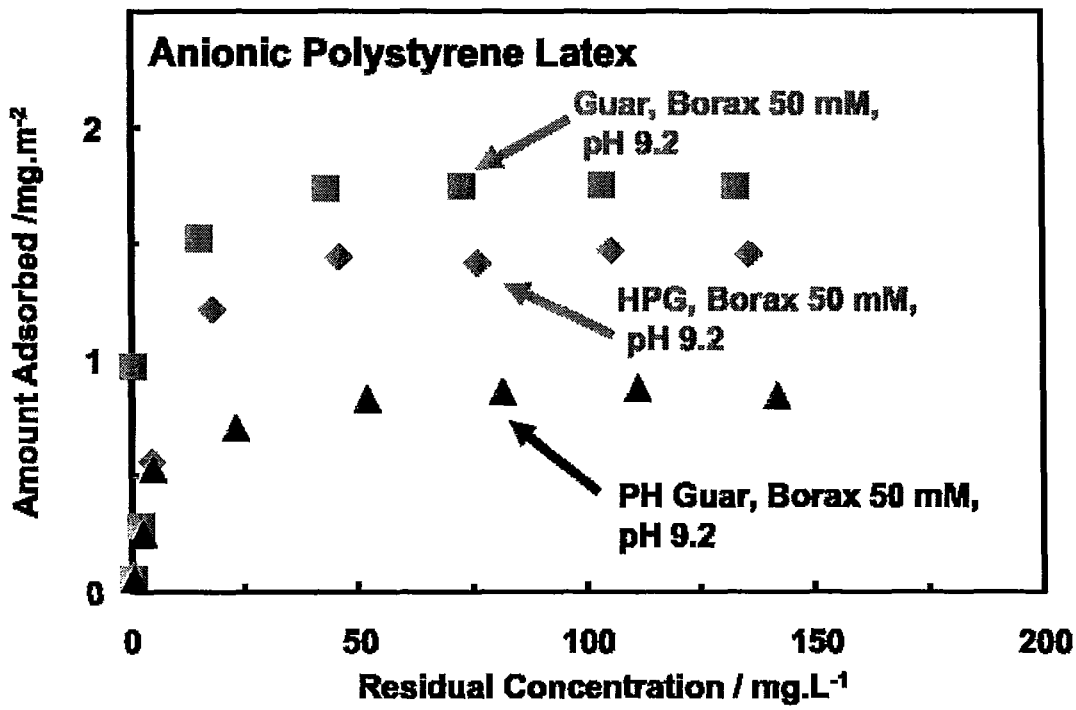

Figure 2. 5. Adsorption isotherms of guar (red squares), HPG (blue diamonds) and partially hydrolyzed

native guar (black triangles) on anionic, surfactant-free polystyrene latex at 25℃, with 50mM borax.

Compared in Figure 2. 5 are the adsorption isotherms for two guars and HPG, all in borax buffer. All three polymers gave high affinity isotherms – again there is no evidence of multilayer adsorption. The adsorption plateau values increased with the polymer molecular weight, which is classical behavior.[19] The hydroxypropyl groups on HPG may contribute to the hydrophobic interactions with polystyrene latex. We do not have data to quantify this effect.

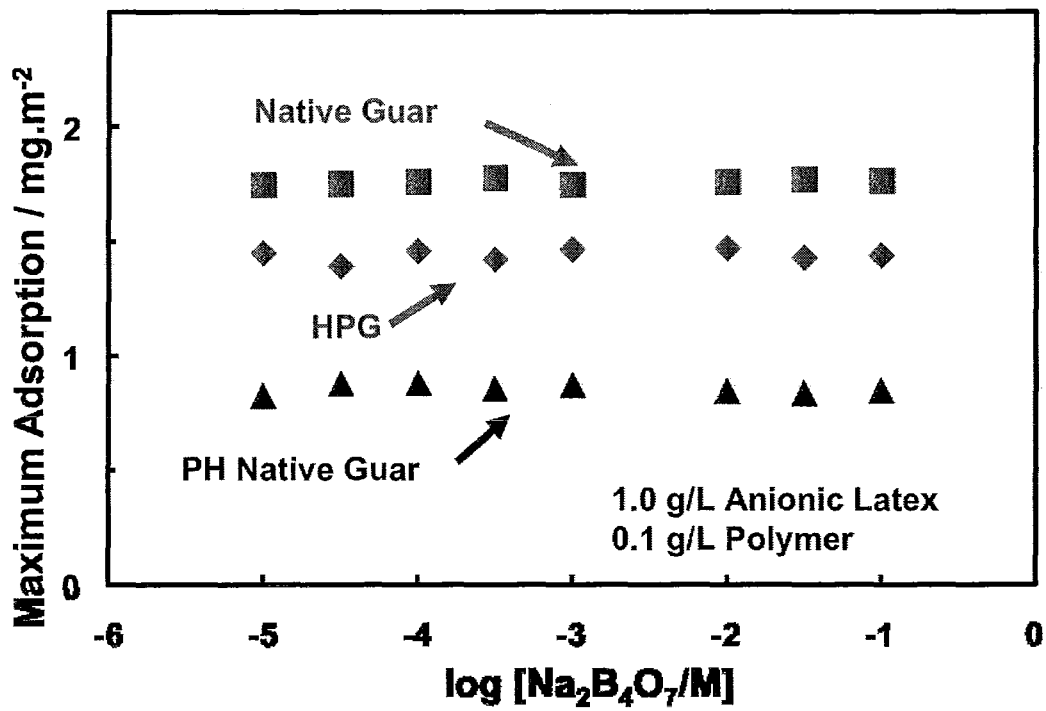

Figure 2. 6 Guar and HPG binding capacity on anionic polystyrene latex as functions of borax concentration. The polymer concentrations during adsorption were 0.1 g/L and the latex was concentration was 1 g/L. Note that the pH varied with borax concentration from 7.2 in 10-5M to 9.2 in 0.1M borax.

The potential impact of borax on guar adsorption was further studied over a broad range of borax concentrations and the results are summarized in Figure 2. 6. The maximum coverage of adsorbed HPG, guar and partially hydrolyzed guar was independent of borax concentration up to 0.1 M. In this series of experiments the pH increased with borax concentration from 7.2 to 9.2. Clearly pH or borax has no effect on guar and HPG adsorption onto hydrophobic polystyrene latex surfaces.

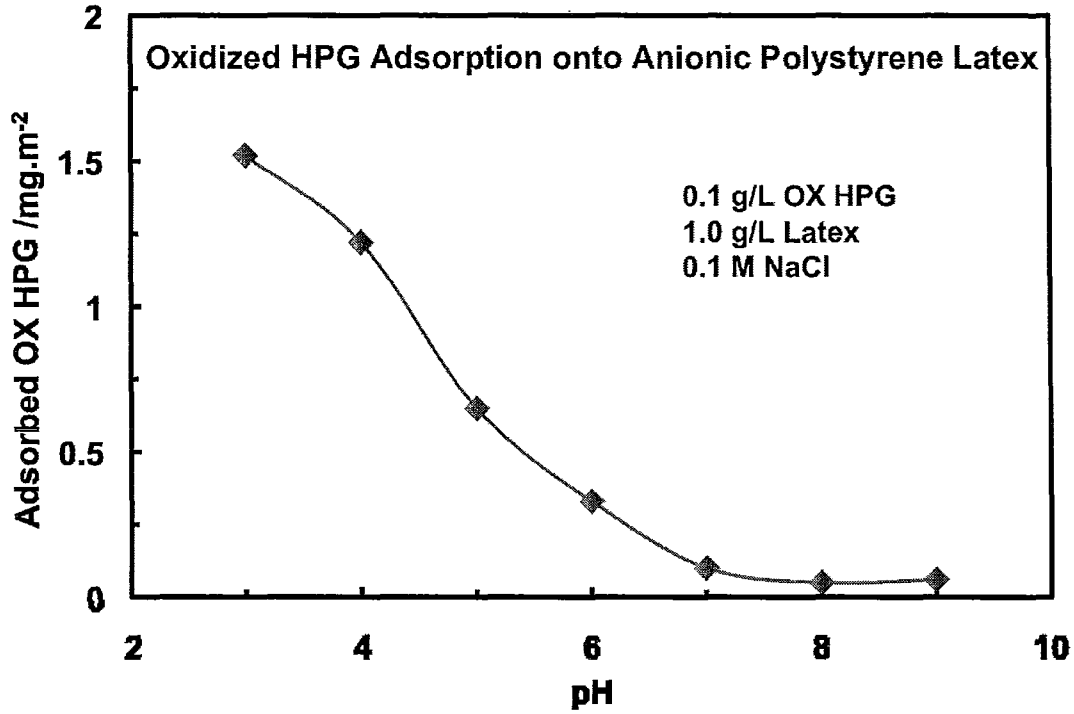

Figure 2. 7. The influence of pH and OX HPG charge density on the maximum adsorption onto anionic polystyrene latex.

Generally we would expect negative charges on a polyelectrolyte to inhibit adsorption onto a negatively charged surface. [19] To illustrate this behavior we oxidized HPG with TEMPO mediated oxidation, a procedure that converts primary alcohols to carboxyl groups with little degradation of carbohydrate chains. [20] Figure 2. 7 shows the saturation adsorption of oxidized hydroxypropyl guar (OX HPG) onto anionic polystyrene latex. At low pH, when OX HPG is essentially uncharged, the latex adsorbed about 1.5 mg/m2. By contrast, above pH 7, where the OX HPG should be completely ionized, very little adsorption occurs. The ionized carboxyl groups are repulsed from the negative latex. The results can be further confirmed by electrophoretic mobility data—see Figure 2. 8

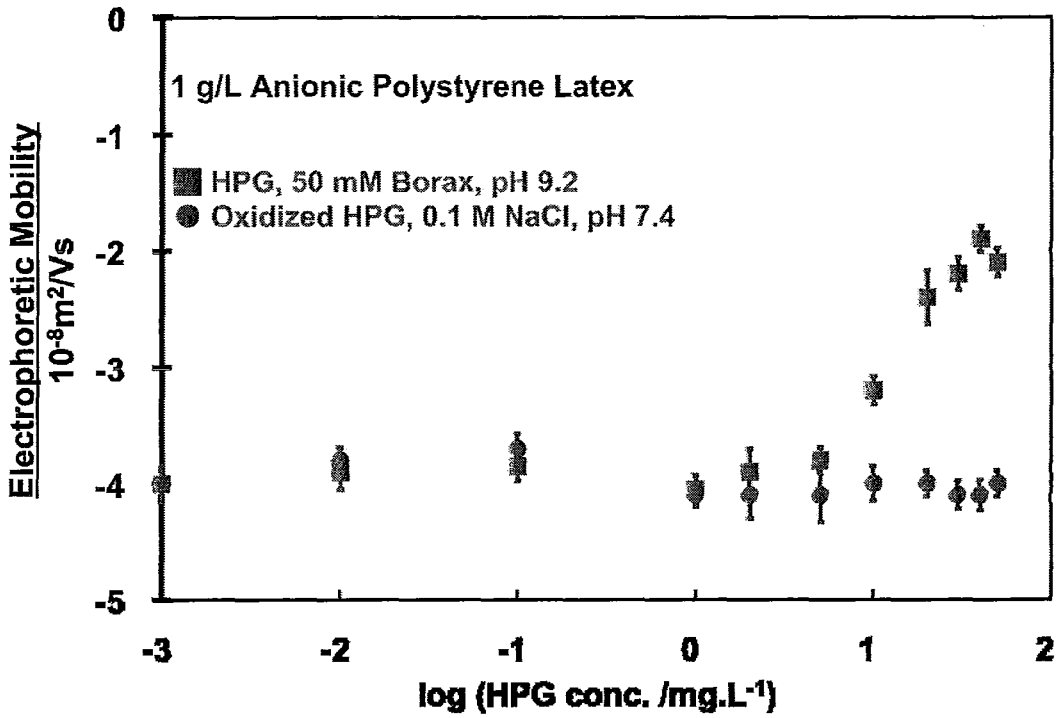

Figure 2. 8. The comparison of the effect of anionic oxidized HPG and anionic HPG-borate on the electrophoretic mobility of anionic surfactant-free polystyrene latex.

The OX HPG had one carboxyl on every five sugar rings (i.e. DS = 0.2) and when fully ionized, OX HPG did not adsorb onto anionic latex (Figure 2. 7). Similarly under the conditions of the experiments in Figure 2. 1 we estimated that HPG was more highly charged (DS = 0.34 vs. 0.2), nevertheless the borate did not influence HPG adsorption onto the anionic latex. Why does the adsorption behavior of HPG-borate differ from that of OX HPG (i.e. charged HPG-borate adsorbs whereas charged OX-HPG does not)? Previously we have shown that the presence of a cationic surface induces more borate to bind to HPG.[7] The extreme sensitivity of the degree of borate binding to the local environment is a reflection of the very low binding constant, 10 to 100 L/mol. The bound borate groups are labile. To explain the results in Figure 2. 4 we propose that borate does not inhibit HPG adsorption on latex because the borate ions desorb as HPG chains approach the anionic latex surface – see Figure 2. 9. The following arguments support this proposal.

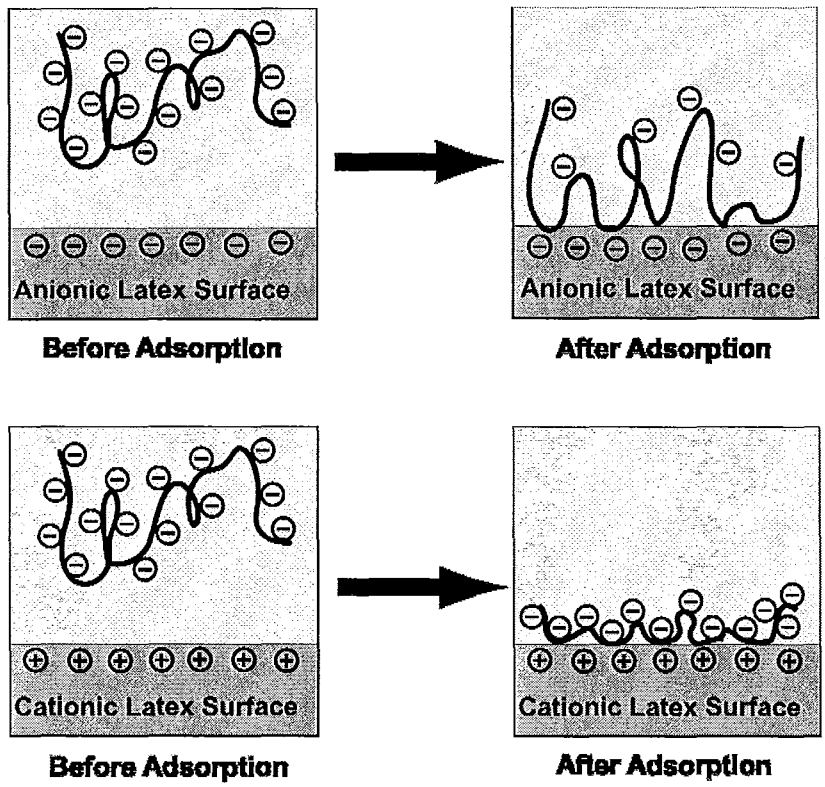

Figure 2. 9. A schematic illustration of the proposed behavior of HPG-borate, a labile polyelectrolyte adsorption onto anionic (upper arrow) and cationic (lower arrow) solid surfaces, respectively.

The concentration of borate ions near the latex surface, [Bs-], will be less than the borate concentration in the bulk solution, [B-], because of the local negative potential. The electrophoretic mobility of the latex was -4, which corresponds to ~-90 mV. According to the Boltzmann equation, the borate concentration near the surface will be only 3% of the concentration away from the surface – see Equation 1 where eo is the charge of an electron, is the electrical potential, k is Boltzmann's constant, and T is temperature. Because the borate binding constant is so low (100 L/mol), the DS of bound borate will be reduced from 0.34 per sugar ring in solution to 0.086 near the surface.

$$\frac{[B_s^-]}{[B^-]} = \exp\left(\frac{e_0 \varsigma}{kT}\right) = 0.03 \qquad (1)$$

With respect to the behavior of HPG-borate in the tear film, our work suggests that HPG will adsorb onto hydrophobic lipid surfaces in the eye, and that bound borate ions will not interfere with adsorption. As pointed out by Audebert many years ago, the borate groups are weakly bound and the equilibrium concentration of ions in solution is high.[5] Under these conditions HPG-borate displays the adsorption characteristics of a nonionic polymer.

2.5 CONCLUSIONS

The main conclusions from this work are:

Guar and hydroxypropyl guar (HPG) show classical high affinity adsorption onto anionic polystyrene latex. The plateau adsorption maximum scaled with the molecular weight.

Although borax addition to HPG converts a nonionic polyelectrolyte into an anionic polyelectrolyte, HPG-borate adsorption onto anionic polystyrene latex was identical to that of HPG alone. We propose that electrostatic repulsion did not prevent HPG adsorption because bound borate ions detached from HPG segments near the anionic latex surface.

Carboxyl groups are easily introduced into HPG by TEMPO mediated oxidation and the resulting polymer does not adsorb onto latex when the carboxyl groups are ionized.

2.6 REFERENCE

1. Ubels, J. L.; Clousing, D. P.; Van Haitsma, T. A.; Hong, B. S.; Stauffer, P.; Asgharian, B.; Meadows, D., Pre-clinical investigation of the efficacy of an artificial tear solution containing hydroxypropyl-guar as a gelling agent. *Curr. Eye Res.* **2004,** 28, (6), 437-444.

2. Christensen, M. T.; Cohen, S.; Rinehart, J.; Akers, F.; Pemberton, B.; Bloomenstein, M.; Lesher, M.; Kaplan, D.; Meadows, D.; Meuse, P.; Hearn, C.; Stein, J. M., Clinical evaluation of an HP-guar gellable lubricant eye drop for the relief of dryness of the eye. *Curr. Eye Res.* **2004,** 28, (1), 55-62.

3. Bron, A. J.; Tiffany, J. M.; Gouveia, S. M.; Yokoi, N.; Voon, L. W., Functional aspects of the tear film lipid layer. *Exp. Eye Res.* **2004,** 78, (3), 347-360.

4. Holly, F., ROLE OF WATER-SOLUBLE POLYMERS IN COLLYRIA. . *Polym. Mater. Sci. Eng.* **1993,** 69, 502-503.

5. Pezron, E.; Ricard, A.; Lafuma, F.; Audebert, R., Reversible Gel Formation Induced by Ion Complexation .1. Borax Galactomannan Interactions. *Macromolecules* **1988,** 21, (4), 1121-1125.

6. Leibler, L.; Pezron, E.; Pincus, P. A., Viscosity Behavior of Polymer-Solutions in the Presence of Complexing Ions. *Polymer* **1988,** 29, (6), 1105-1109.

7. Cui, Y.; Pelton, R.; Ketelson, H., Shapes of Polyelectrolyte Titration Curves 2:The Deviant Behaviour of Labile Polyelectrolytes. *Macromolecules* **2008,** 41, 8198-8203.

8. Horn, D.; Heuck, C. C., Charge determination of proteins with poly-electrolyte titration *J. Biol. Chem.* **1983,** 258, (3), 1665-1670.

9. Goddard, E. D., Polymer Surfactant Interaction .2. Polymer and Surfactant of Opposite Charge. *Colloids Surf.* **1986,** 19, (2-3), 301-329.

10. Cui, Y.; Pelton, R.; Cosgrove, T.; Richardson, R.; Dai, S.; Prescott, S.; Grillo, I.; Ketelson, H.; Meadows, D., Not All Anionic Polyelectrolytes Complex with DTAB. *Langmuir* **2009,** 25, (24), 13712–13717.

11. Pelton, R.; Hu, Z.; Ketelson, H.; Meadows, D., Reversible Flocculation with Hydroxypropyl Guar-Borate, A Labile Anionic Polyelectrolyte. *Langmuir* **2009,** 25, 192-195.

12. Parris, M. D.; MacKay, B. A.; Rathke, J. W.; Klingler, R. J.; Gerald, R. E., Influence of Pressure on Boron Cross-Linked Polymer Gels. *Macromolecules* **2008,** 41, (21), 8181-8186.

13. Laskowski, J. S.; Liu, Q.; O'Connor, C. T., Current understanding of the mechanism of polysaccharide adsorption at the mineral/aqueous solution interface. *International Journal of Mineral Processing* **2007,** 84, (1-4), 59-68.

14. Jenkins, P.; Ralston, J., The adsorption of a polysaccharide at the talc aqueous solution interface. *Colloids Surfaces A* **1998,** 139, (1), 27-40.

15. Wang, J.; Somasundaran, P.; Nagaraj, D. R., Adsorption mechanism of guar gum at solid-liquid interfaces. *Miner. Eng.* **2005,** 18, (1), 77-81.

16. de Nooy, A. E. J.; Besemer, A. C.; vanBekkum, H.; vanDijk, J.; Smit, J. A. M., TEMPO-mediated oxidation of pullulan and influence of ionic strength and linear charge density on the dimensions of the obtained polyelectrolyte chains. *Macromolecules* **1996,** 29, (20), 6541-6547.

17. Stuart, M. A. C.; Scheutjens, J. M. H. M.; Fleer, G. J., Polydispersity Effects and the Interpretation of Polymer Adsorption-Isotherms. *Journal of Polymer Science Part B-Polymer Physics* **1980,** 18, (3), 559-573.

18. Jasinski, R.; Redwine, D.; Rose, G., Boron equilibria with high molecular weight guar: An NMR study. *J. Polym. Sci., Part B: Polym. Phys.* **1996,** 34, (8), 1477-1488.

19. Fleer, G. J.; Cohen Stuart, M. A.; Scheutjens, J. M. H. M.; Cosgrove, T.; Vincent, B., *Polymers at Interfaces*. Chapman & Hall: London, 1993.

20. Anelli, P. L.; Biffi, C.; Montanari, F.; Quici, S., FAST AND SELECTIVE OXIDATION OF PRIMARY ALCOHOLS TO ALDEHYDES OR TO CARBOXYLIC-ACIDS AND OF SECONDARY ALCOHOLS TO KETONES MEDIATED BY OXOAMMONIUM SALTS UNDER 2-PHASE CONDITIONS. *J. Org. Chem.* **1987,** 52, (12), 2559-2562.

21. Bohmer, M. R.; Evers, O. A.; Scheutjens, J. M. H. M., Weak Polyelectrolytes between 2 Surfaces - Adsorption and Stabilization. *Macromolecules* **1990,** 23, (8), 2288-2301.

Chapter 3

Interaction between Hydroxypropyl Guar-borate and Anionic Lipid-stabilized Emulsions

3.1 ABSTRACT

The interactions between hydroxypropyl guar-borate with anionic lipid-stabilized emulsion were studied using dynamic light scattering and electrophoretic mobility. Hydroxypropyl guar and native guar did not adsorb onto anionic emulsion, by contrast, depletion flocculation was observed at high polymer concentration. However, high polymer concentrations inhibited phase separation via increasing viscosity. The presence of borate ions, which converted nonionic polysaccharide into anionic polyelectrolyte, did not affect threshold polymer concentration for depletion-induced macroscopic phase separation. Ionic strength was found to have the biggest influence in tuning stability of lipid stabilized emulsion.

3.2 INTRODUCTION

Chapter 2 described adsorption of HPG-borate onto anionic hydrophobic latex, a model for hydrophobic domains in the tear film such as exposed corneal epithelium and lipid layers[1]. Our research group has systematically studied interaction between HPG-borate and a series of well-defined models under physiological conditions, such as proteins (i.e., lysozyme)[2], cationic polyelectrolyte poly(diallyldimethyl ammonium chloride)[3], cationic lipid (DOTAP), cationic polystyrene latex[4] and cationic surfactants (DTAB)[5], respectively. However, the interactions of anionic lipids with HPG have not been studied. Since ophthalmic lipids are generally anionic, understanding HPG-borate/anionic lipid interaction is importance for designing artificial tears. In this chapter, I describe results using lipid-stabilized emulsion as model system to investigate the interaction between HPG (with or without borate) and anionic lipid. Before describing new work, some background information is required.

As it has been introduced in Chapter 1, the lipid layer is outmost layer of the natural tear film. It is composed by both polar and non-polar lipid molecules and is excreted from meibomian glands. The excreted material follows a complicated delivery process involving transportation through the aqueous phase and spreading on the air interface[1]. McCulley and colleagues suggested that polar lipids spread out in the aqueous phase and then followed by non-polar lipids, which are associated with polar lipids on the hydrophobic "tails"[6]. The creation of lipid layer involves a number of intermolecular interactions with species in aqueous phase, i.e., proteins and mucin. One of the early studies by Holly in 1973[7] suggested mucin lowers surface tension of lipid solution via lipid-mucin interaction (see figure 4 in reference 7)[7]. In addition, complexation between lipid and *lipocalins*, a kind of tear protein previously known as tear-specific prealbumin[1], has been demonstrated to provide low surface tension as well as rheology properties close to that of natural tears[8]. Therefore, administration of HPG-borate into eyes may face issues raised by its interaction with lipid molecules. In current study, we simplify the problem by using lipid-stabilized spherical emulsions. Specifically, the emulsifier is composed by phospholipids, non-polar lipids and fatty acid, which is close to natural composition.

A number of studies have investigated interaction between lipids with natural or synthetic polymers. Millar and co-workers studied lipids interaction with ocular aqueous species using Langmuir-Blodgett trough, a classic technique for probing surface phenomena with high sensitivity[9, 10]. Lipid was distributed evenly on air/water interface. By injecting ocular proteins (i.e., lysozyme) and mucin into aqueous phase, mass uptakes from subphase onto lipid layer has been detected[11-14]. Raised by interests in biomedical areas, some papers have reported liposome-polyelectrolyte interactions[15, 16], which are close to our emulsion system.

Interactions between polysaccharides and emulsions have been extensively studied for the direct application in food, texture and emulsion industry[17]. A large body of

literature has dealt with protein-polysaccharide interactions on the oil-water interface[17, 18]. In the light of previous results, polysaccharide-emulsion interactions may be classified in terms of intermolecular complexation between polysaccharide and surface active agents (i.e., proteins, pectin). If polysaccharide complexes with surface active agents via electrostatic attraction or hydrogen bonding, one may observe bridging flocculation, sterically stabilization or even gelation[19], depending upon the particular chemistry and polysaccharide concentration[17]. If there is no specific complexation between polysaccharide and surface active agent, depletion flocculation is always anticipated. In this case, the emulsion remains stable when polysaccharide is in small dose. However, emulsions will be flocculated with increasing polysaccharide concentration, typically around overlap concentration (c^*) for small volume fraction of emulsion[20]. The threshold polysaccharide concentration for flocculation increases with decreasing emulsion volume fraction and decreasing polysaccharide molecular weight, as predicted by theories[21-23]. In addition, kinetics of macroscopic phase separation of emulsions by adding non-adsorbing polysaccharide (often quoted as creaming), showed non-linear relation with polysaccharide concentration, as interpreted from rheology data. Tuiner and de Kruif[24] found creaming rate strongly increased with polysaccharide concentration at low polysaccharide concentration, while the rate was slowed down at high polysaccharide concentration due to formation of polysaccharide network.

3.3 EXPERIMENTAL

3.3.1 Lipid-stabilized emulsion — The emulsions were prepared by dispersing 150 mg original *Lipoid Nanosolve 5400* (provided by Alcon Laboratories) in 10 ml Millipore water. The emulsifier is composed by phosphatidyl choline (64-79 wt %), Phosphatidyl ethanolamine (12-18 wt %) and small amount of non-polar lipids (smaller than 5 wt %). Detailed parameters of the original sample can be found in appendix. Then the dispersed samples were further diluted 10 times by Millipore water. Using dynamic light scattering (DLS), we determined the emulsions diameter remained 80 nm for at least 3 months

3.3.2 Polymers and emulsion mixture — Polymer and emulsion mixtures were prepared in 20 ml glass bottles. Designed polymer amount was added carefully using pipette. The ionic strength was adjusted using sodium chloride. Samples were capped and then mechanically mixed up for 30 seconds using vortex mixer under 25℃.

3.3.3 Electrophoretic Mobility — It was performed on Brookhaven Zetaplus Zeta Potential Analyzer, which used BIC PALS Zeta Potential Analyzer software (version 2.5). All samples were measured for 10 runs under room temperature (25 ℃).

3.3.4 Dynamic Light Scattering — The hydrodynamic diameters were measured using Brookhaven Dynamic Light Scattering Instrument. The instrument was equipped with BI-9000AT auto-correlator and 35 MV laser. The data was collected

and analyzed by BIC dynamic light scattering software 9kdlsw32 (version 3.34) using the cumulative statistical analysis. All measurements were performed under 25 ℃, maintained by NESLAB water bath.

3.4 RESULTS

Salt Effects — We examined the effect of salt concentration on emulsions size and electrophoretic mobility. All samples were characterized after 48 hours (see Figure 3. 1 and Figure 3. 2). The emulsion is stabilized by mixture of lipids, including phospholipids, non-polar lipids and fatty acid. From dynamic light scattering data, salt concentration higher than 0.05 M NaCl induced emulsions aggregation (see Figure 3. 1).

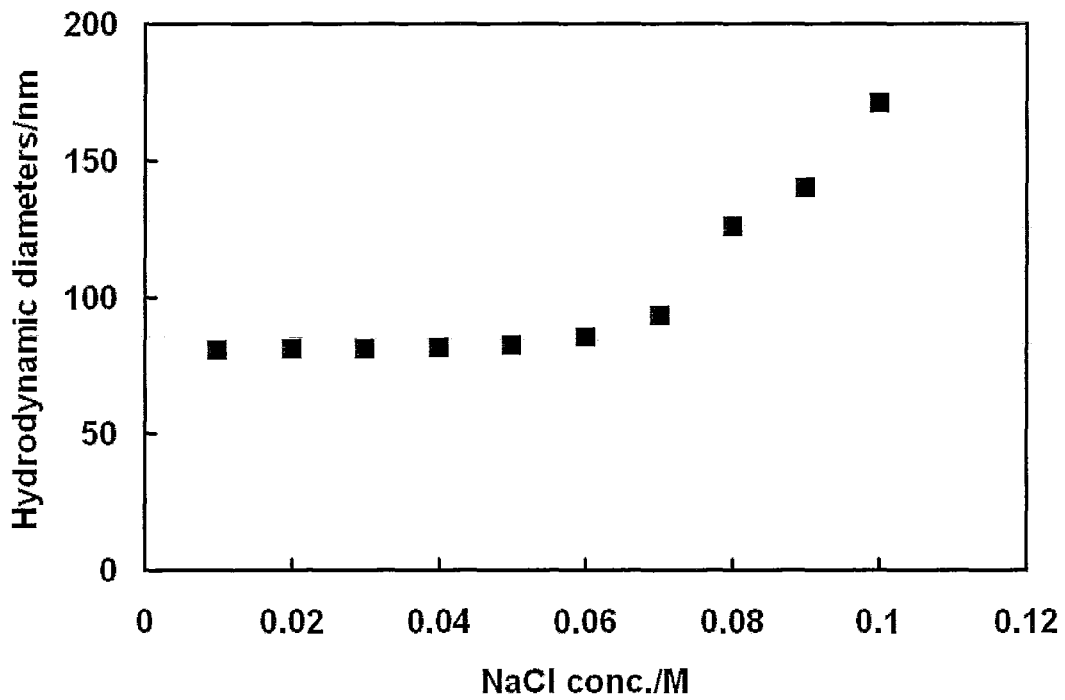

Figure 3. 1. Emulsion droplets sizes under different salt concentrations. Samples were measured after 48 hours.

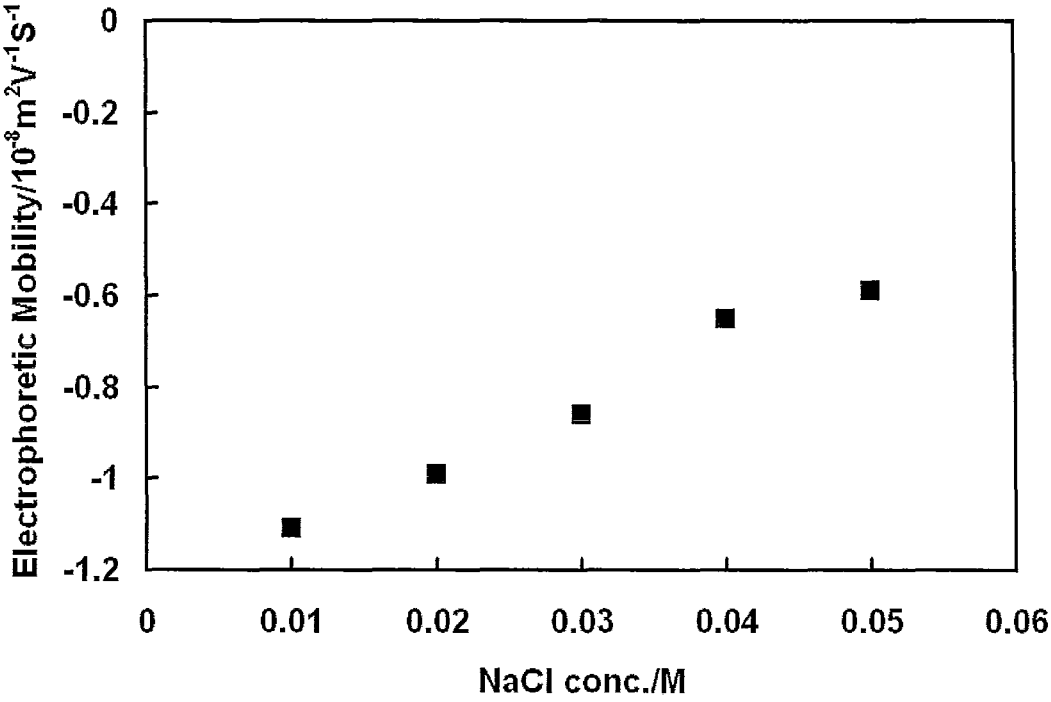

Figure 3. 2 Electrophoretic mobility of emulsion spheres under different salt concentrations. Measurements were performed after 48 hours.

HPG-borate Interaction with Lipid-stabilized Emulsion — From our electrophoretic mobility data (see Figure 3. 3) and dynamic light scattering data (see Figure 3. 4), we found neither HPG nor HPG-borate were adsorbed by the emulsions. The presence of borate ions does not affect HPG interaction with the emulsions.

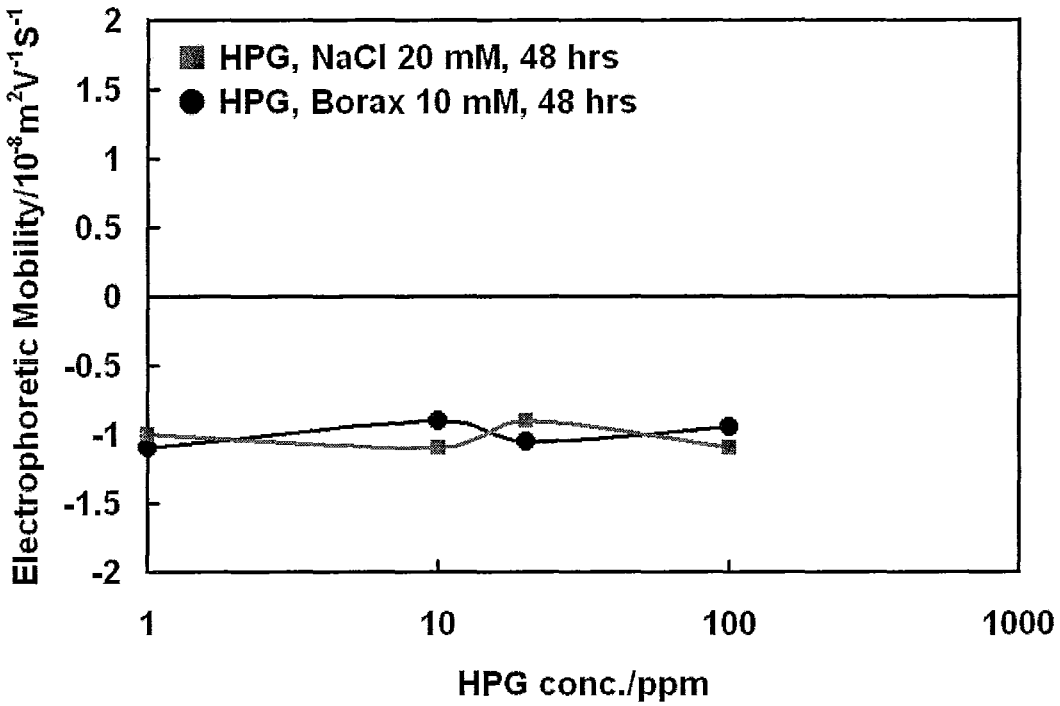

Figure 3. 3 Electrophoretic mobility of emulsion spheres in HPG solutions with (black solid circle) and without (red solid square) borax.

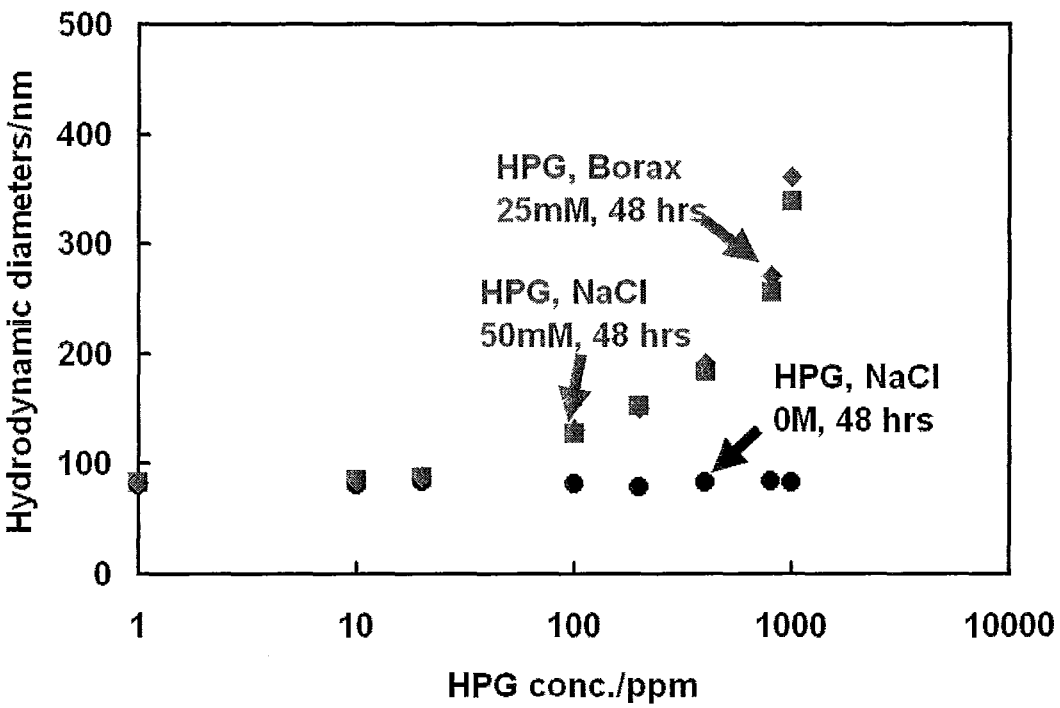

Figure 3. 4 Comparison of emulsion spheres sizes in HPG solutions with different salt concentrations. No salt (black solid circles); 50 mM NaCl (red solid square) and 25 mM borax (blue solid diamond). All samples were measured after 48 hours.

Guar-borate Interaction with Lipid-stabilized Emulsions—HPG is hydroxypropyl substituted guar derivates. The interaction between emulsion spheres and native guar was also monitored by dynamic light scattering (see Figure 3. 5) and electrophoretic mobility (see Figure 3. 6). Again, both sizing and mobility data shows native guar is not adsorbed by emulsion spheres.

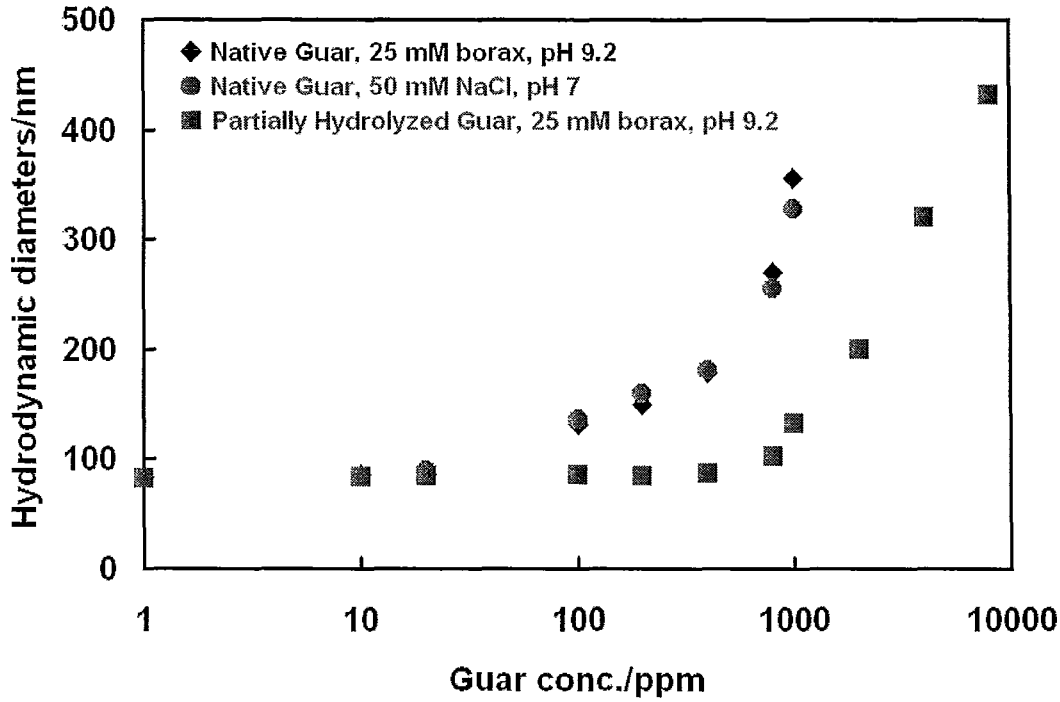

Figure 3. 5 Dynamic light scattering results of emulsion-guar mixtures. Specifically, black solid diamonds represent native guar with 25 mM borax at pH 9.2, red solid circles are native guar with 50 mM at pH 7, blue solid squares are partially hydrolyzed guar with 25 mM borax at pH 9.2.

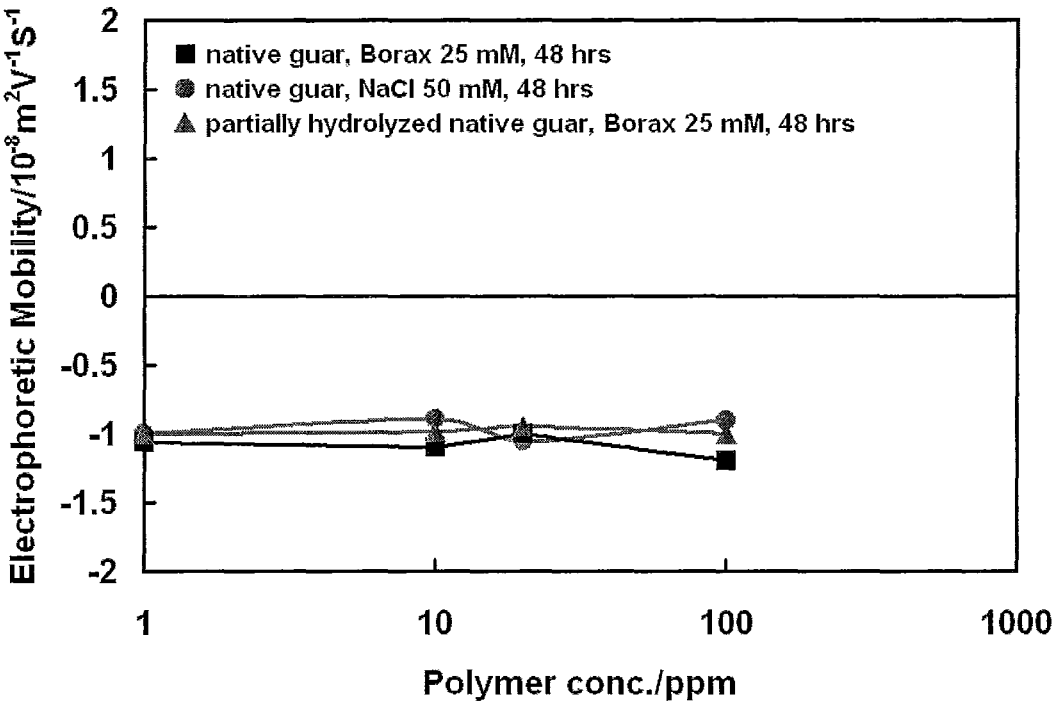

Figure 3. 6 Electrophoretic mobility of native guar/emulsion mixture, specifically, native guar with borax (black solid squares), native guar with sodium chloride (red solid circles) and partially hydrolyzed native guar (blue solid triangle)

Gravitational Stability of the Lipid-stabilized Emulsions by HPG— We also estimated depletion-induced macroscopic phase separation influenced by HPG concentration. Figure 3. 7 shows photographs of flocculated emulsions in 0.1M salt with different HPG concentrations. It was found boundary between phase 1 (the upper phase) and phase 2 (lower phase) went down with increasing HPG concentration.

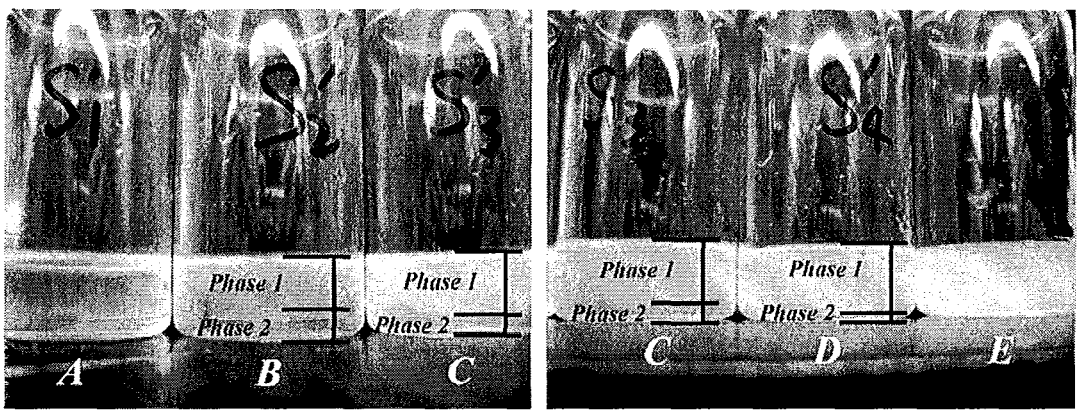

Figure 3. 7. Photographs of depletion flocculated emulsions with increasing HPG concentrations (from A to E: 10, 200, 500, 800, 1000 ppm, respectively). The phase boundaries are highlighted by black solid lines. Thin oil layer was observed in Sample A. Sample E was a cloudy gel-like suspension. The

pictures were taken after one week standing.

3.5 DISCUSSION

Salt Effects — Apparent size increasing was observed above 0.05 M NaCl (see Figure 3. 1). Clearly, salt concentration higher than 0.05 M NaCl induced aggregation. Emulsion particles in our experiments were stabilized by surfactant mixture, which is composed by phospholipids, non-polar lipids and fatty acid. The threshold salt concentration for our emulsion is lower than other type of emulsion such as proteins-stabilized emulsion[25] (in the case of casein, > 0.1 M). The difference might be contributed by rigid nature of the lipid molecules, which cannot provide high flexibility since phospholipids own two hydrophobic tails. At higher salt concentrations, electrostatic repulsions are partially "screened"— see our electrophoretic mobility data in Figure 3. 2. At the same time, the rigid lipid layer limits steric stabilization[26]. This explanation is supported by Gruner[27], Kahlweit[28] and Lindman[29], who emphasized rigidity of phospholipids monolayer, i.e., two orders of magnitude larger than oligo (ethylene oxide) layer[27].

HPG-borate Interaction with Lipid-stabilized Emulsion — In Figure 3. 3 and Figure 3. 4, we found both HPG and HPG-borate were not adsorbed onto the emulsions. The trends can be compared with literature describing interactions between non-adsorbing polymers with emulsions[17, 30-35]. (Note we only carried out mobility measurements less than 100 ppm HPG to reduce viscosity effects). The borate ions did not affect depletion threshold HPG concentration. This result surprised us because HPG-borate and lipids were both negatively charged. We envisioned HPG-borate, as anionic polyelectrolyte, would induce stronger depletion phase separation than that of neutral HPG, as suggested by Prieve and co-workers, who used total internal reflection microscopy to measure total interaction between polylysine and glass beads[36]. However, depletion threshold concentration of HPG and HPG-borate was found to be approximately the same in our experiments.

Salt impairs stability of the emulsions, as it is shown in Figure 3. 4. Emulsion spheres with salt (borax or sodium chloride) were flocculated by HPG within 48 hours, however, no size change was observed in salt-free solution during this period of time. Further observation confirmed cloudy suspensions appeared after 2 weeks standing in all salt-free samples (data not shown).

Depletion-induced phase separation is a dynamic process which normally depends on experimental time scales. Interaction between emulsion spheres is controlled by van der Waals attraction, Columbic repulsion (partially screened) and polymer-induced depletion attraction. The characteristic time of aggregation (τ_a) can be tuned by either salt or polymer concentration[37, 38]. Using dimer formation theory of Brownian flocculation[39], τ_a can be expressed as,

$$\tau_a = \frac{\pi \eta a^3}{\phi k_B T} W \quad (1)$$

$$W = 2a \int_{2a}^{\infty} \frac{\exp(\beta u(r))}{r^2 G(r)} dr \quad (2)$$

Where a is radius of spheres, Φ is volume fraction of spheres, W is the stability ratio, η is solvent viscosity. Total energy $u(r)$ may be expressed using classic DLVO theory via simple summation of van der Waals potential $u_{vdw}(r)$, Coulomb potential $u_{el}(r)$ and depletion potential $u_{dep}(r)$: $u(r) = u_{vdw}(r) + u_{el}(r) + u_{dep}(r)$. $\beta = 1/k_B T$. $G(r)$ is hydrodynamic function describes relative mobility of two spheres along their center-to-center lines[40].

Guar-borate Interaction with Lipid-stabilized Emulsion — It has been reported that HPG has larger chain stiffness than native guar due to intra-chain steric effects between hydroxypropyl groups[41]. The interaction between emulsion spheres and native guar was also monitored by dynamic light scattering (see Figure 3. 5) and electrophoretic mobility (see Figure 3. 6). Both sizing and mobility data shows native guar is not adsorbed by emulsion spheres. The threshold polymer concentration from dynamic light scattering shows classic behavior: it increases with decreasing polymer molecular weight[23, 42].

Gravitational Stability of the Emulsion Spheres by HPG — From dynamic light scattering and electrophoretic mobility, we demonstrated HPG was not adsorbed by the emulsions. Hence, non-adsorbing HPG induces depletion attraction via volume exclusion effects; however, HPG also increased viscosity to slow the phase separation — gravitational stability[34, 43]. This conclusion may be important for artificial tear formulations, i.e., coexistence of hydroxypropyl guar and lipid emulsion for drug delivery. Under physiological conditions, the presence of HPG may retard macroscopic phase separation of the emulsions in eyes, which may impair optical transparency of tear film.

3.6 CONCLUSION

1. Hydroxypropyl guar (HPG) does not adsorb onto 80 nm diameter, negatively charged emulsion droplets stabilized by anionic lipid (*Lipoid Nanosolve 5400).*
2. HPG concentrations above 0.1 g/L induce depletion flocculation of the lipid stabilized emulsion.
3. Although presence of borate ions converts nonionic HPG into anionic polyelectrolyte; borate addition does not affect influence the HPG concentration required to induce depletion flocculation. threshold concentration of HPG under the same ionic strength. (i.e., using sodium chloride as alternative)
4. Ionic strength plays significant role in tuning HPG-lipid stabilized emulsion phase

behavior, especially in the terms of phase separation time. Higher salt concentration accelerated speed of phase separation.

3.7 REFERENCE

1. Bron, A. J.; Tiffany, J. M.; Gouveia, S. M.; Yokoi, N.; Voon, L. W., Functional aspects of the tear film lipid layer. *Exp Eye Res* **2004,** 78, (3), 347-60.
2. Lu, C.; Kostanski, L.; Ketelson, H.; Meadows, D.; Pelton, R., Hydroxypropyl guar-borate interactions with tear film mucin and lysozyme. *Langmuir* **2005,** 21, (22), 10032-10037.
3. Cui, Y. G.; Pelton, R.; Ketelson, H., Shapes of polyelectrolyte titration curves. 2. The deviant behavior of labile polyelectrolytes. *Macromolecules* **2008,** 41, (21), 8198-8203.
4. Pelton, R.; Hu, Z.; Ketelson, H.; Meadows, D., Reversible flocculation with hydroxypropyl guar-borate, a labile anionic polyelectrolyte. *Langmuir* **2009,** 25, (1), 192-195.
5. Cui, Y. G.; Pelton, R.; Cosgrove, T.; Richardson, R.; Dai, S.; Prescott, S.; Grillo, I.; Ketelson, H.; Meadows, D., Not all anionic polyelectrolytes complex with dtab. *Langmuir* **2009,** 25, (24), 13712-13717.
6. McCulley, J. P.; Shine, W. E., Meibomian gland and tear film lipids: Structure, function and control. In *Lacrimal gland, tear film, and dry eye syndromes 3: Basic science and clinical relevance, pts a & b*, Sullivan, D. A.; Stern, M. E.; Tsubota, K.; Dartt, D. A.; Sullivan, R. M.; Bromberg, B. B., Eds. Kluwer Academic/Plenum Publ: New York, 2002; Vol. 506, pp 373-378.
7. Holly, F., Formation and rupture of the tear film. *Experimental Eye Research* **1973,** 15, (5), 515-525.
8. Nagyova, B.; Tiffany, J. M., Components responsible for the surface tension of human tears. *Current Eye Research* **1999,** 19, (1), 4-11.
9. Langmuir, I., The constitution and fundamental properties of solids and liquids. Ii. Liquids.1. *Journal of the American Chemical Society* **1917,** 39, (9), 1848-1906.
10. Blodgett, K. B., Films built by depositing successive monomolecular layers on a solid surface. *Journal of the American Chemical Society* **1935,** 57, (6), 1007-1022.
11. Miano, F.; Calcara, M.; Millar, T. J.; Enea, V., Insertion of tear proteins into a meibomian lipids film. *Colloids and Surfaces B-Biointerfaces* **2005,** 44, (1), 49-55.
12. Millar, T. J.; Mudgil, P., Penetration of tear proteins into a meibomian lipid layer. *Invest. Ophthalmol. Vis. Sci.* **2005,** 46, -.
13. Millar, T. J.; Tragoulias, S. T.; Anderton, P. J.; Ball, M. S.; Miano, F.; Dennis, G. R.; Mudgil, P., The surface activity of purified ocular mucin at the air-liquid interface and interactions with meibomian lipids. *Cornea* **2006,** 25, (1), 91-100.
14. Mudgil, P.; Torres, M.; Millar, T. J., Adsorption of lysozyme to phospholipid and meibomian lipid monolayer films. *Colloids and Surfaces B-Biointerfaces* **2006,** 48, (2), 128-137.
15. Kawakami, K.; Nishihara, Y.; Hirano, K., Effect of hydrophilic polymers on physical stability of liposome dispersions. *Journal of Physical Chemistry B* **2001,** 105, (12), 2374-2385.
16. Bordi, F.; Sennato, S.; Truzzolillo, D., Polyelectrolyte-induced aggregation of liposomes: A new cluster phase with interesting applications. *Journal of Physics-Condensed Matter* **2009,** 21, (20), -.
17. Dickinson, E., Hydrocolloids at interfaces and the influence on the properties of dispersed systems. *Food Hydrocolloids* **2003,** 17, (1), 25-39.
18. de Kruif, C. G.; Tuinier, R., Polysaccharide protein interactions. *Food Hydrocolloids* **2001,** 15, (4-6), 555-563.
19. Dickinson, E.; Pawlowsky, K., Effect of l-carrageenan on flocculation, creaming, and rheology of a protein-stabilized emulsion. *J. Agric. Food Chem.* **1997,** 45, (10), 3799-3806.

20. Tuinier, R.; Rieger, J.; De Kruif, C., Depletion-induced phase separation in colloid–polymer mixtures. *Advances in Colloid and Interface Science* **2003,** 103, (1), 1-31.

21. Fleer G, J.; Scheutjens J. H. M, H.; Vincent, B., The stability of dispersions of hard spherical particles in the presence of nonadsorbing polymer. In *Polymer adsorption and dispersion stability*, American Chemical Society: Washington, D.C., 1984; pp 245-263.

22. Sperry, P. R., A simple quantitative model for the volume restriction flocculation of latex by water-soluble polymers. *Journal of Colloid and Interface Science* **1982,** 87, (2), 375-384.

23. Vrij, A., Polymers at interfaces and interactions in colloidal dispersions. *Pure and Applied Chemistry* **1976,** 48, (4), 471-483.

24. Tuinier, R.; de Kruif, C. G., Phase separation, creaming, and network formation of oil-in-water emulsions induced by an exocellular polysaccharide. *Journal of Colloid and Interface Science* **1999,** 218, (1), 201-210.

25. Dickinson, E.; Semenova, M. G.; Antipova, A. S., Salt stability of casein emulsions. *Food Hydrocolloids* **1998,** 12, (2), 227-235.

26. Kabalnov, A.; Lindman, B.; Olsson, U.; Piculell, L.; Thuresson, K.; Wennerstrom, H., Microemulsions in amphiphilic and polymer-surfactant systems. *Colloid Polym. Sci.* **1996,** 274, (4), 297-308.

27. Gruner, S. M., Stability of lyotropic phases with curved interfaces. *Journal of Physical Chemistry* **1989,** 93, (22), 7562-7570.

28. Kahlweit, M.; Busse, G.; Faulhaber, B., Preparing microemulsions with lecithins. *Langmuir* **1995,** 11, (5), 1576-1583.

29. Shinoda, K.; Araki, M.; Sadaghiani, A.; Khan, A.; Lindman, B., Lecithin-based microemulsions - phase-behavior and microstructure. *Journal of Physical Chemistry* **1991,** 95, (2), 989-993.

30. Dickinson, E.; Goller, M. I.; Wedlock, D. J., Creaming and rheology of emulsions containing polysaccharide and nonionic or anionic surfactants. *Colloids and Surfaces a-Physicochemical and Engineering Aspects* **1993,** 75, 195-201.

31. Dickinson, E.; Goller, M. I.; Wedlock, D. J., Osmotic-pressure, creaming, and rheology of emulsions containing nonionic polysaccharide. *Journal of Colloid and Interface Science* **1995,** 172, (1), 192-202.

32. Manoj, P.; Fillery-Travis, A. J.; Watson, A. D.; Hibberd, D. J.; Robins, M. M., Characterization of a depletion-flocculated polydisperse emulsion i. Creaming behavior. *Journal of Colloid and Interface Science* **1998,** 207, (2), 283-293.

33. Manoj, P.; Watson, A. D.; Hibberd, D. J.; Fillery-Travis, A. J.; Robins, M. M., Characterization of a depletion-flocculated polydisperse emulsion ii. Steady-state rheological investigations. *Journal of Colloid and Interface Science* **1998,** 207, (2), 294-302.

34. Meller, A.; Gisler, T.; Weitz, D. A.; Stavans, J., Viscoelasticity of depletion-induced gels in emulsion-polymer systems. *Langmuir* **1999,** 15, (6), 1918-1922.

35. Meller, A.; Stavans, J., Stability of emulsions with nonadsorbing polymers. *Langmuir* **1996,** 12, (2), 301-304.

36. Pagac, E. S.; Tilton, R. D.; Prieve, D. C., Depletion attraction caused by unadsorbed polyelectrolytes. *Langmuir* **1998,** 14, (18), 5106-5112.

37. Gogelein, C.; Nagele, G.; Buitenhuis, J.; Tuinier, R.; Dhont, J. K. G., Polymer depletion-driven cluster aggregation and initial phase separation in charged nanosized colloids. *J. Chem. Phys.* **2009,** 130, (20), 15.

38. Poon, W. C. K.; Haw, M. D., Mesoscopic structure formation in colloidal aggregation and gelation. *Advances in Colloid and Interface Science* **1997,** 73, 71-126.

39. Russel, W. B.; Saville, D. A.; Schowalter, W. R., *Colloidal dispersions*. Cambridge University Press: Cambridge, 1992.

40. Kim, S.; Karrila, S. J., *Microhydrodynamics: Principles and selected applications* Dover Publications (June 17, 2005): 2005.

41. Cheng, Y.; Prud'homme, R. K.; Chik, J.; Rau, D. C., Measurement of forces between galactomannan polymer chains: Effect of hydrogen bonding. *Macromolecules* **2002,** 35, (27), 10155-10161.

42. De Hek, H.; Vrij, A., Interactions in mixtures of colloidal silica spheres and polystyrene molecules in cyclohexane : I. Phase separations. *Journal of Colloid and Interface Science* **1981,** 84, (2), 409-422.

43. Kim, C.; Liu, Y.; Kuhnle, A.; Hess, S.; Viereck, S.; Danner, T.; Mahadevan, L.; Weitz, D. A., Gravitational stability of suspensions of attractive colloidal particles. *Physical Review Letters* **2007,** 99, (2), 4.

Chapter 4

Colloid Stability Maps for Anionic Labile Polyelectrolytes Interaction with Cationic liposomes

4.1 ABSTRACT

We reported an analytical study on Labile polyelectrolytes (HPG-borate) interaction with cationic 1,2-dioleoyl-3-trimethylammonium-propane (DOTAP) liposomes. Salt-induced adsorption/desorption transition is tested by Muthukumar theory (*J. Chem. Phys.* 1994, 100, (10), 7796-7803.). After electrostatic attraction is screened out, depletion flocculation was observed at high HPG concentration. DLVO-type pair depletion potential shows agreement with our experiments. Finally, we assembled all of our calculation onto a phase diagram, which reflects stability of Labile polyelectrolyte/oppositely charged liposomes mixture in terms of salt and polymer concentration. Influencing factors such as polymer molecular weight, colloid size and colloid volume fraction are presented, respectively.

4.2 INTRODUCTION

The formulation of artificial tear solutions may face stability issues when water soluble polymers and colloid are mixed. For example, we have shown that both anionic lipid-stabilized emulsions (see chapter 3) and cationic liposomes[1] can be flocculated by HPG-borate via bridging or depletion mechanisms. Under physiological conditions, we found electrostatic attraction between anionic HPG-borate and cationic liposomes can be regulated by salt concentration. i.e., the electrostatic attraction can be screened out by excess salt. Namely, a critical salt concentration exists. Figure 4. 1 illustrates different events may happen between HPG-borate and cationic liposomes depending upon the polymer and salt concentrations. Box A and B correspond to interactions above critical salt concentration for adsorption/desorption transition. Box C to F correspond to interactions below the critical salt concentration. When salt screens out electrostatic interactions, liposomes only experience depletion flocculation at high polymer concentration. Below critical salt concentration, Labile polyelectrolyte adsorbs onto the liposomes which results in either flocculation or enhanced stabilization.

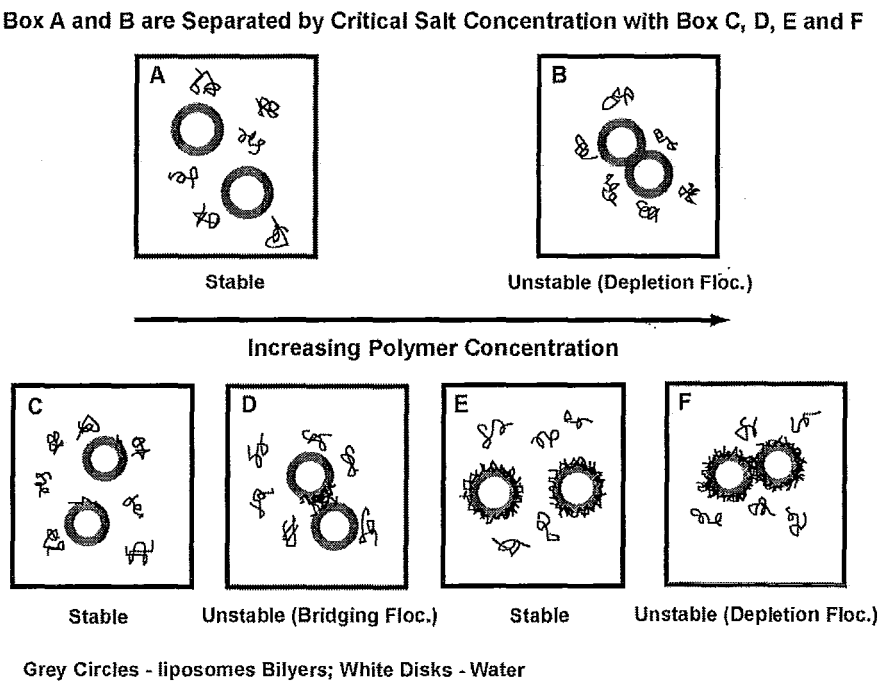

Figure 4. 1 Schematic illustration of the mechanisms by which soluble polymers can interact with dispersed particles. Box A and B are separated by critical salt concentration with box C-F.

The events in Figure 4. 1 can be assembled onto a stability map (see Figure 4. 2 as an example).

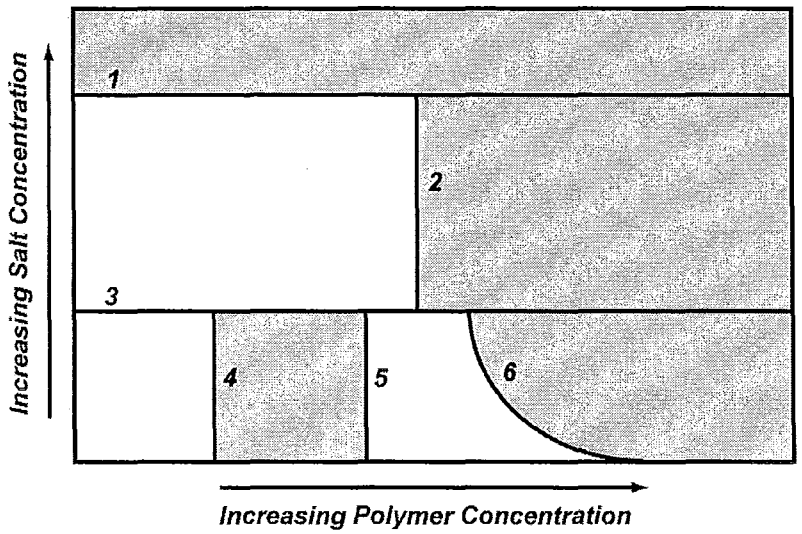

Figure 4. 2 Schematic illustration of HPG-borate interaction with cationic liposomes. Regions shaded by gray color indicate phase separation where liposomes are flocculated.

In Figure 4. 2, unstable regions (where colloids are flocculated by polymer) are grey-shaded. Segments are labeled by numbers. Line 3 is critical salt concentration for electro-adsorption. Polymers are depleted from the colloids surfaces only when salt concentration is above line 3. Generally speaking, region above line 1 represents critical coagulation concentration, where salt screen out electrostatic repulsion between colloids. Region between line 1, 2 and 3 is depletion flocculation region as well as region between line 3 and 6. Region between 3, 4 and 5 is bridging flocculation region. Before we start, some background information about modeling individual segment will be introduced.

Modeling the Critical Salt Concentration for Polymer Adsorption, Line 3 in Figure 4.2

Adsorption of polyelectrolytes with fixed charge onto charged surfaces is a classic problem which has been extensively studied for decades[2-6]. One of the first analytical calculation of polyelectrolyte adsorption onto a charged surface was proposed by Wiegel[7]. Under Gaussian statistics of polyelectrolyte chains, he calculated adsorption amount and thickness as function of salt concentration. Muthukumar and co-workers[8, 9] also considered interaction between charged segments, and derived more general analytical formulas for polyelectrolyte adsorption. In their calculation, polyelectrolyte can adopt any conformation from self-avoiding walk to rod-like structures, depending on ionic strength of the solution. According to their theory[9], critical conditions for adsorption-desorption transition are described by,

$$T_c = \frac{12\pi|\sigma q|}{\varepsilon \kappa^3 b_{eff} b k_b}\left[1-\exp(-2\kappa a)\right] \quad (1)$$

where: T_c is temperature; e_o is the charge of an electron; a is the liposome radius, σ_o is

the liposome charge density, α is the charge per step length of polyelectrolyte, κ is the Debye screening parameter, k_b is Boltzmann's constant, b is the Kuhn step length of the polymer, which we assumed was 0.54 nm corresponding to two mannose units; and, b_{eff} step length that we assumed equaled $13b$, where 13 is the Cheng et al.'s value for the characteristic ratio of HPG[10]. The charge per step length, α, was calculated as a function of pH from the HPG and borate concentrations, assuming that only galactose units bound borate[11] and that the borate binding constant was 100 L/mol[12, 13]. Herein we solved Equation 1 for k which we converted to the equivalent salt concentration.

Modeling the Bridging Flocculation Regions – Line 4 and 5 in Figure 4.2. If polymers have tendency to adsorb onto surfaces of colloids, the colloids may undergo bridging flocculation due to adsorbed polymer "loops" and "tails" attach to other colloids nearby. However, adsorbing polymer can improve stability of a colloid system via steric stabilization[14, 15]. Apart from direct calculation of interaction energy between adsorbed layers using mean field theory or scaling approach[16], kinetic argument has been widely used in practical. The very early framework was proposed by La Mer and colleagues[17-20], who assume the flocculation rate (F) is a product of collision frequency (k), particle number density (N) and collision efficiency factor (E),

$$F = kEN^2 \quad (2)$$

The collision efficiency factor E in equation 2 describes fraction of "successful" collision leading to inter-particles adhesion. It was defined to be the product of fraction of covered surface on one colloid and fraction of un-covered surface on another colloid,

$$E = \theta(1-\theta) \quad (3)$$

Where θ is fraction of surface of colloids covered by polymer. Hogg pointed out a probability of reverse process should also account for collision efficiency factors[21], therefore, E can be rewritten as,

$$E = 2\theta(1-\theta) \quad (4)$$

Modeling the Depletion Flocculation Regions - Line 2 and 6 in Figure 4.2. If non-adsorbing polymer is added into colloidal system, only volume exclusion effect is anticipated[22]. The colloids may be flocculated after polymers occupy the "free space"—depletion flocculation, which maybe understood via pair potential between two colloids. In general, the pair potential can be calculated using superposition approximation, which is composed by Van der Waals potential, electrostatic potential

and depletion potential. The former two can be obtained using classic formulas[23], while depletion potential may be a product of depletion layer thickness and osmotic pressure (see chapter 1). Polymer segmental concentration is zero near the surface and then increases to bulk value over a distance with specific gradient. The distance is known as depletion layer thickness[3], which is considered to be the orders of radius of gyration (R_g)[24] of free polymers. Several theories have been developed to calculate depletion layer thickness[24-26]. As a rule, it decreases with increasing free polymer concentration and increases with increasing polymer molecular weight. Osmotic pressure, on the other hand, can be calculated using either Flory-Huggins expression or Virial expansion[27].

The goal of this work is to calculate individual boundary segments 1 to 6 (as labeled in Figure 4. 2). The rest of the chapter is organized as follows. In theory part, method for individual segment calculation will be presented. Different factors which influence the boundary concentrations, such as HPG molecular weight, colloids volume fraction and colloids size will be modeled. In results and discussion part, we assembled the segments into phase diagrams. Segments shift corresponding to different factors will be discussed

4.3 THE THEORY

4.3.1 Adsorption-Desorption Transition (Line 3). As a starting point, it is crucial to understand the nature of interactions between borate ions and HPG. Linear charge density of HPG-borate can be estimated via standard Langmuir equation,

$$\theta = \frac{K_{eq}' [B]}{1 + K_{eq}' [B]} \quad (5)$$

Where: θ is defined as percent of occupation of all available bonding sizes. K_{eq}' is the effective equilibrium constant. ***[B]*** is concentration of adsorbate.

Leibler et al. emphasized electrostatic repulsion between neighboring bound borate ions decreased probability of borate-*cis* diol formation[28]. As a result, the equilibrium constant can be expressed by,

$$K_{eq}' = K_{eq} \exp(\alpha U / k_b T) \quad (6)$$

Where: numerical factor α is an adjustable parameter represents effect of newly formed charges on existing charges[28]. K_{eq}' approaches K_{eq} if electrostatic repulsion between bound ions is "screened out", i.e., large excess of salt. Typical polyelectrolyte titration experiment from our lab showed borate ions would further bond to HPG when cationic poly(diallyldimethyl ammonium chloride) forms complexation with

HPG-borate[11]. On the other hand, we demonstrated borate had no effects on hydrophobic-driven HPG adsorption onto anionic polystyrene latex. We argued electrical field on latex surface detach the existing charges—a reverse process (see chapter 2).

We found nonionic HPG did not adsorb onto hydrophilic DOTAP liposomes surface. Therefore, adsorption of anionic HPG-borate onto cationic DOTAP is electrostatic driven. Considering $K_{eq}' \approx K_{eq}$ for HPG-borate at DOTAP surface (with 0.1 M NaCl and 50 mM borax), we estimate linear charge density of HPG-borate to be ~ 0.2 by standard Langmuir equation (equilibrium constant 100 L/mole[12, 13], details of the calculation can be found in appendix).

Now we can calculate critical salt concentration as a function of linear charge density using equation 1. The results are shown in Figure 4. 3. The lower point corresponds to HPG-borate without NaCl. The upper point corresponds to HPG-borate with 0.1 M NaCl. Two curves are plotted corresponding to two values of DOTAP liposome surface charge density. The higher one is 0.23 C/m^2, assuming 0.7 nm^2 per head group. This value may be overestimated because it does not consider salt condensation[29, 30]. The other curve corresponds to 0.08 C/m^2 fits well with our experiments—the lower and upper points fall into adsorption and desorption regions, respectively.

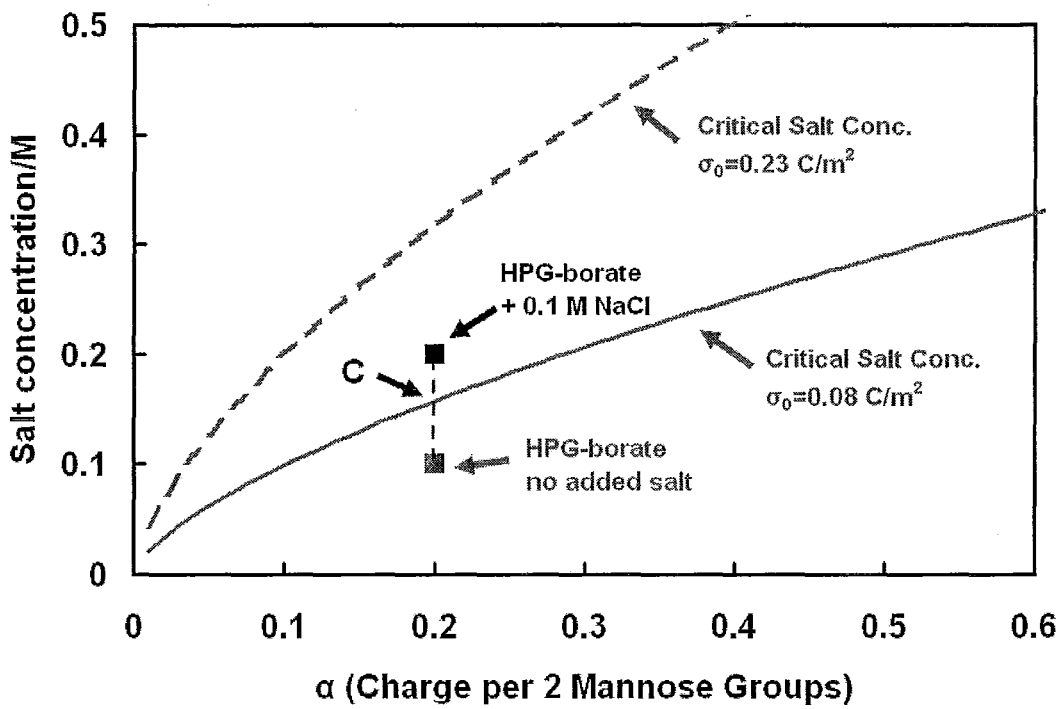

Figure 4. 3 Critical salt concentration versus linear charge density for electrostatic-driven polyelectrolyte adsorption onto oppositely charged curved surfaces, calculation is performed using Muthukumar model[9].

The height of line 3 can be picked from intersecting point (see point C labeled in Figure 4. 3)

4.3.2 Depletion Flocculation (line 2 and 6) Pair potential of two approaching liposomes can be expressed using superposition approximation. Add depletion potential into total pair potential between two liposome spheres V_{total} reads,

$$V_{total} = V_{elect} + V_{vdw} + V_{dep} \quad (7)$$

V_{elect} represents electrostatic potential between two liposome spheres. V_{vdw} is the attractive potential from van der Waals interactions. V_{dep} is the depletion potential contributed by non-adsorbing polymer. (Note, all potential energies are normalized by k_bT)

We used well-documented expressions for electrostatic and Van der Waals potentials,

$$V_{elect} = (2\pi\varepsilon\varphi^2 a \ln(1+\exp(-\kappa h)))\frac{1}{k_bT} \quad (8)$$

$$\kappa = \sqrt{\frac{e_0^2 N_{av}}{\varepsilon_r \varepsilon_0 k_b T}\sum_i c_i z_i^2} \quad (9)$$

$$V_{vdw} = -\frac{A}{12}\left(\frac{4a^2}{h^2+4ah} + \frac{4a^2}{h^2+4ah+4a^2} + 2\ln\left(\frac{h^2+4ah}{h^2+4ah+4a^2}\right)\right)\frac{1}{k_bT} \quad (10)$$

φ is effective surface potential. κ is inverse Debye screening length, ε_r denotes the relative permittivity (ε_r =78 for water). ε_0 denotes permittivity of free space (ε_0 =8.854×10^{-12} F/m). k_b is the Boltzmann constant, N_{av} is Avogadro's constant, c_i is concentration of ion type i (mol/L), Z_i is valence of ion type i (1, 2 or 3), T is the absolute temperature; e_0 is the charge of electron (1.6×10^{-19} coul). a is radius of liposome sphere. h is inter-sphere distance.

In this model, we use an old analytical formula derived from SCF[25]. It didn't treat polymers as penetrable hard spheres and more generally, the depletion layer thickness is subjected to change with polymers addition.

$$V_{dep} = -\frac{2}{3}\pi\Pi\left(\Delta - \frac{h}{2}\right)^2\left(3a + 2\Delta + \frac{h}{2}\right)\frac{1}{k_bT} \quad (11)$$

$$\Pi = RT\rho\phi\left(\frac{1}{M_w} + B_2\rho\phi\right) \quad (12)$$

Π is osmotic pressure. B_2 is the second viral coefficient of the solution. M_w and Φ is molecular weight and volume fraction of non-adsorbing polymer. z is charge number of the polyelectrolyte. c_s is total salt concentration. Δ is depletion layer thickness, which is decreased along with non-adsorbing polymer addition.[10] We used analytical formula developed by Vincent [26] for calculation of Δ.

$$\frac{\Delta}{\Delta_0^2} - \frac{1}{\Delta} = -\frac{N_{av}\rho}{2}\left(\frac{v}{\phi}\right)^{2/3}\Pi \quad (13)$$

Δ_0 is the range of the depletion effect in the limit that bulk polymer concentration goes to zero. Using calculated results from Fleer and colleagues [25], Δ_0 is equal with $1.4R_g$. R_g is radius of gyration. v is molecular volume of a single chain. ($v=M_w/N_{av}\rho$)

It is critical to incorporate volume fraction of the colloids (Φ^c) into our model. Here we use linear approximation reported by Fleer, Vincent and co-workers[25, 31]—see equation 14. In very dilute colloid suspension (say, $\Phi^c = 10^{-6}$), we may expect phase boundary located at polymer overlap volume fraction (c^*). The threshold polymer concentration for phase separation decreases with increasing Φ^c.

$$\frac{V_{critical}}{k_b T} = C + \beta \log \phi^c \quad (14)$$

Where: $V_{critical}$ is critical pair potential at secondary minimum for phase separation. C is critical pair potential at secondary minimum under $\Phi^c = 10^{-6}$ colloid volume fraction. β value is adopted from reference 1[25]. We estimate C by inserting secondary minimum value at polymer volume fraction $\Phi = c^*$ into equation 8. (Specifically, we use $V_{critical} = 4.49\ k_bT$ at $\Phi^c = 10^{-6}$ and $V_{critical} = 1\ k_bT$ at $\Phi^c = 0.2\%$)

We show effects of HPG molecular weight, colloids size and colloids volume fraction on C_{dep} (g/L). General features are summarized in Figure 4.3 to 4.5. Assuming liposome radius a 45 nm, surface potential φ 38 MV and colloid volume fraction Φ^c 0.2 %, figure 2 shows the influence of HPG molecular weight on C_{dep} (g/L).We find larger mass is required for lower MW HPG to induce depletion flocculation. Modeling results can be compared with our experimental data. We found larger amount low molecular weight guar is required to flocculate liposomes than high molecular weight guar. On the contrary, smaller mass is required to flocculate larger particles at a given MW—see figure 3. Larger liposomes volume fraction (Φ^c) requires smaller amount of polymer to induce depletion flocculation—see figure 4.

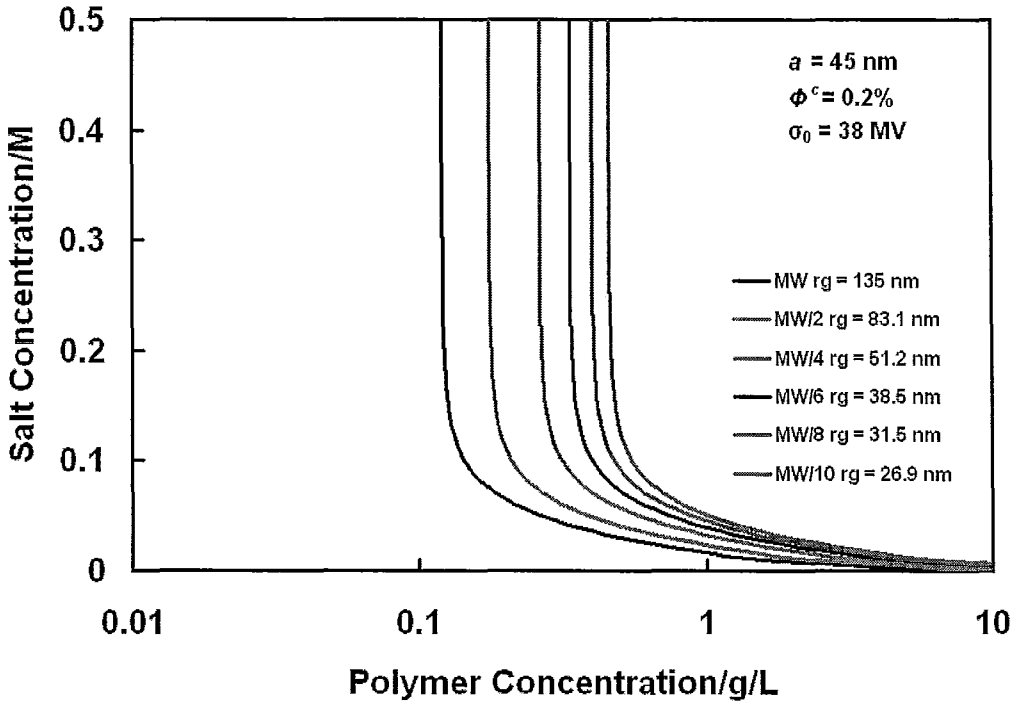

Figure 4. 4 Patterns of the depletion flocculation boundary polymer concentration C_{dep} (g/L) against salt concentration under various of HPG molecular weight (1, 500, 000 g/mole as the initial value, 2, 4, 6, 8 and 10 times lower, from the right side to the left, respectively). Corresponding values of radius of gyration (r_g) are also listed in the figure. The radius of gyration for each molecule weight are calculated using proportional relation $r_g \sim MW^{0.7}$

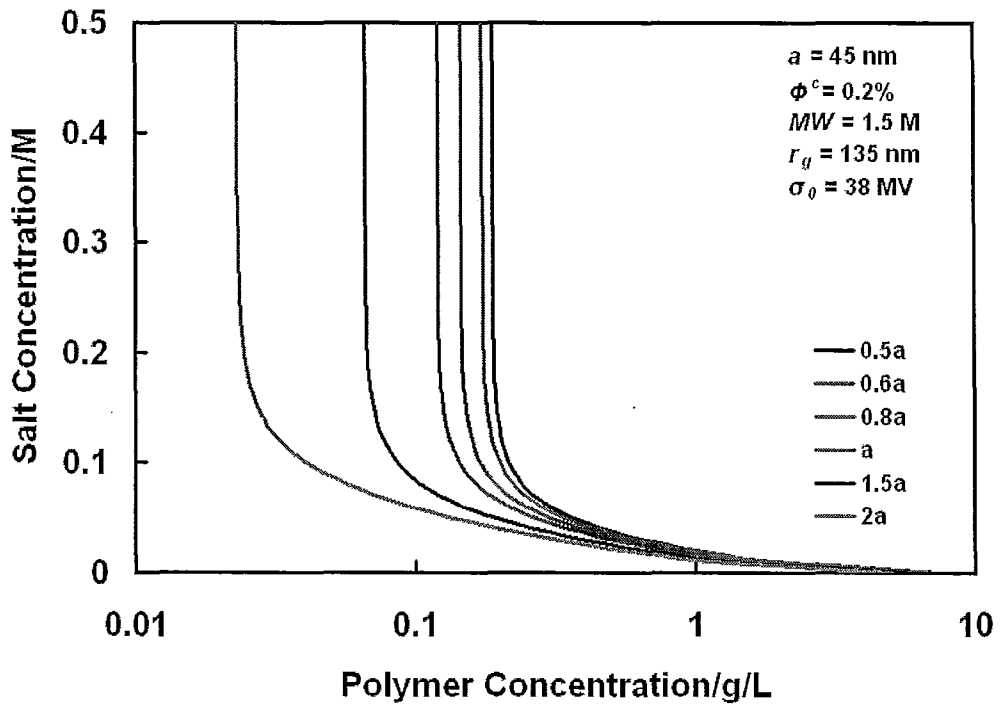

Figure 4. 5 Changing patterns of depletion flocculation boundary concentration C_{dep} (g/L) against salt concentration under a number of liposomes radius (the initial value is 45 nm, from left to the right, 0.5, 0.6, 0.8, 1, 1.5 and 2 times initial liposome radius a, respectively).

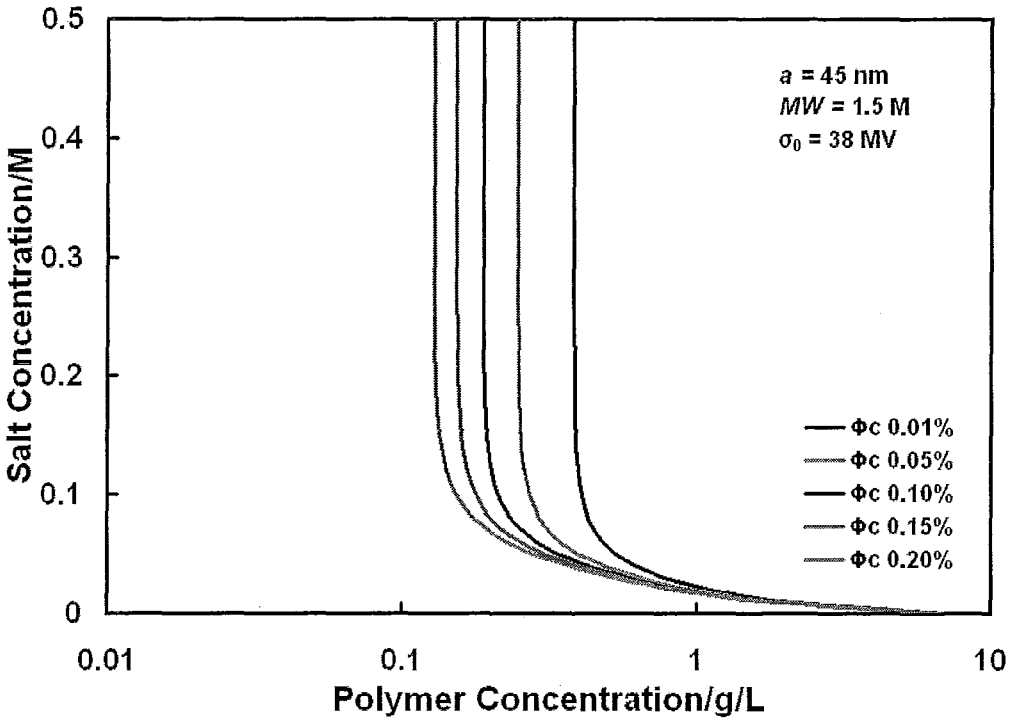

Figure 4. 6 Influence of liposomes volume fraction on threshold polymer concentration for depletion flocculation. Increasing liposomes volume fraction leads to decreasing threshold polymer concentration.

Note depletion flocculation below critical salt concentration occurs after colloids are saturated. Therefore, adsorbed amount should be added in to total polymer concentration when line 6 is plotted on the phase diagram.

4.3.3 Bridging flocculation boundary concentrations (line 4 and 5) Bridging flocculation usually starts from a few ppm flocculant and stops when saturation is reached. The optimum polymer dose for bridging flocculation is around half coverage (~0.5 mg/m^2) of liposome spheres. Here, saturation value of polymer adsorption onto liposome is assumed to be around 1 mg/m^2—see equation 9. In our experiments, DOTAP concentration is 1mM. Calculated spheres concentration is 6.7×10^{15} per Liter, indicates a maximum value of 170 mg polymer is adsorbed by 1 liter liposome suspension—the upper boundary. On the other hand, lower boundary of bridging flocculation may be determined by considering at least one polymer chain to link every two colloids—see equation 10. Therefore, lower boundary is equal to 1/2 colloid concentration, which is 11 mg per 1 Liter liposome suspension.

$$C_{upper} = \frac{3\Gamma\phi^c}{a} \quad (15)$$

$$C_{lower} = \frac{3\phi^c M_w}{8\pi a^3 N_{av}} \quad (16)$$

Where: Φ^c is number density of liposomes particles (i.e., 0.2 % in our experiment). Γ is saturation amount of HPG onto liposomes surfaces (i.e., 1 mg/m^2). a is radius of the liposomes. It is clear that C_{upper} and C_{lower} are *linearly* against liposomes volume fraction. Figure 4. 7 shows calculated results compared with experimental data. Mathcad file of one calculation example can be found in appendix 3.

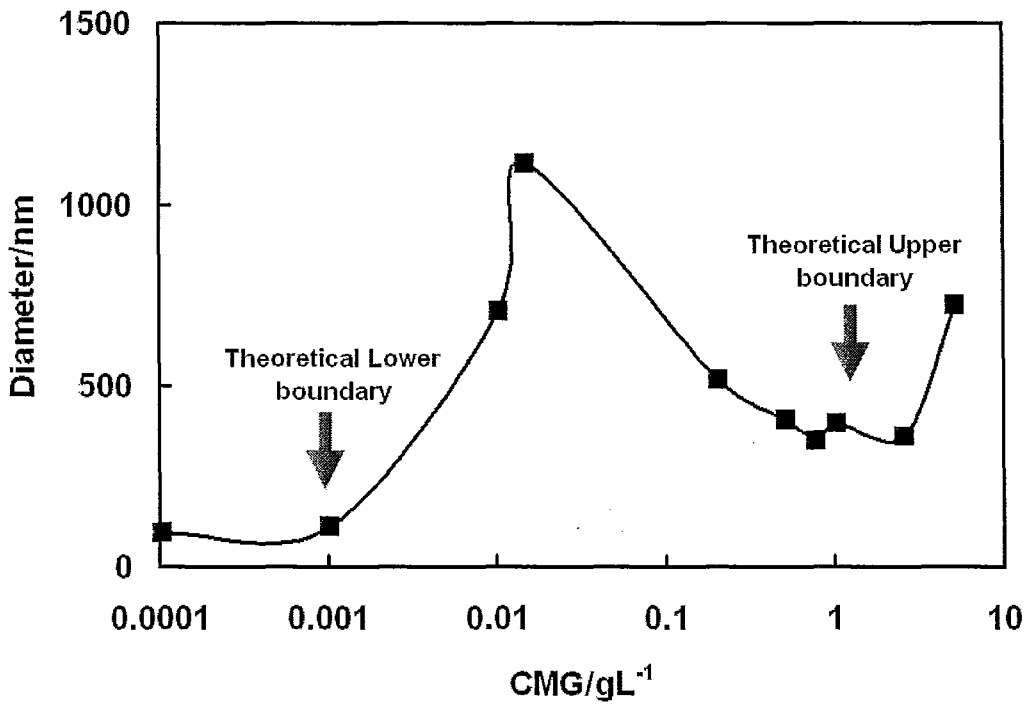

Figure 4. 7 Comparison between experimental results (black square) with calculated boundary position. Experimental data was adapted from reference. Specifically, experimental results shows dynamic light scattering results of DOTAP lipsomes mixed with carboxymethyl guar.

4.4 RESULTS AND DISCUSSION

Figure 4.8 to 4.10 show molecular weight, colloid size and colloid volume fraction effects on the phase separation boundaries, respectively. Original phase boundaries are plotted in black solid lines (by assuming MW 1.5 M, r_g 135 nm, a 45 nm, σ_0 38 MV and Φ^c = 0.2 %). Shifted boundaries are plotted in dotted blue lines. After the colloids are saturated with adsorbed polymer, the size is assumed to be 1.5 times larger than original one and surface charge potential is assumed to be the same value (38 MV).

The blue lines in Figure 4. 8 show boundaries when molecular weight lower 2 times. In *depletion* flocculation regions, larger polymer mass is required to induce depletion flocculation at lower molecular weight. However, larger colloid size requires smaller amount of polymer to induce depletion flocculation. Therefore, both dotted blue lines move to the right hand side with a different magnitude. The lower boundary for *bridging* flocculation, smaller molecular weight polymer has higher number of density under same mass, hence, lower boundary of bridging region moves towards left hand side.

The blue lines in Figure 4. 9 show boundaries when colloid radius lower 2 times. Under same volume fraction, smaller colloids have larger surface-to-volume ratio, leading to higher number density and larger surface area. Therefore, more polymers are needed to bridging the colloids as well as saturating the colloids (see *bridging* zone is moved to the right hand side).

The blue lines in Figure 4. 10 show boundaries when colloid volume fraction lower 2 times. It requires smaller amount of polymer to induce *bridging* flocculation. Smaller amount of colloids needs more polymers to induce *depletion* flocculation because only volume exclusion exists in depletion zones. Therefore, critical pair potential becomes larger in the case of smaller volume fraction of colloids.

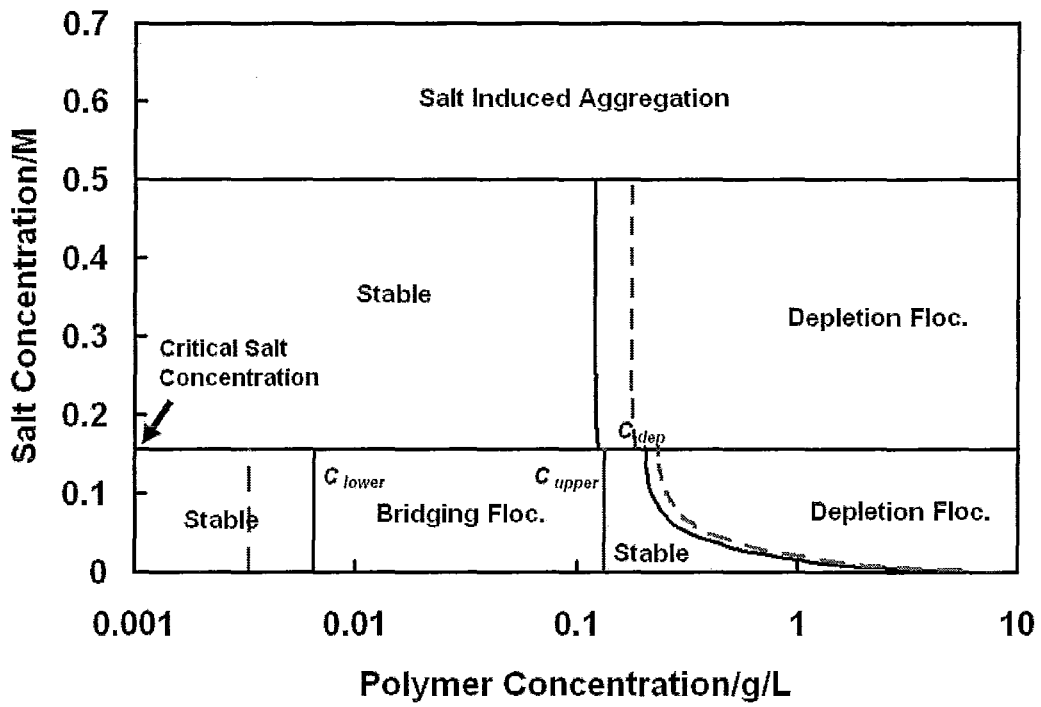

Figure 4. 8 Analytical phase diagram for Labile polyelectrolyte interaction with oppositely charged liposomes. Specifically, MW = 1.5 M, r_g = 135 nm, a = 45 nm, Φ^c = 0.2 %, σ_0 = 38 MV, borax concentration 50 mM; for black solid lines. Blue lines are for MW = 0.75 M, r_g = 83.1 nm, a = 45 nm, Φ^c = 0.2 %, σ_0 = 38 MV

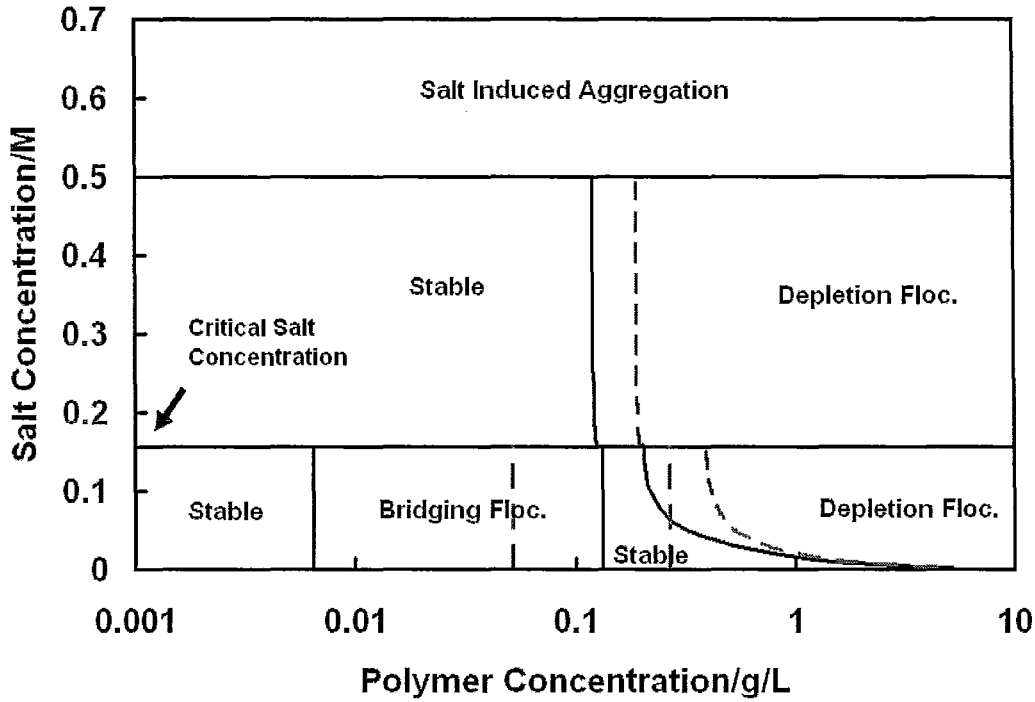

Figure 4. 9 Analytical phase diagram for Labile polyelectrolyte interaction with oppositely charged liposomes. Specifically, MW = 1.5 M, r_g = 135 nm, a = 45 nm, Φ^c = 0.2 %, σ_0 = 38 MV, borax concentration 50 mM for black solid lines. Blue lines are for MW = 1.5 M, r_g = 135 nm, a = 22.5 nm, Φ^c = 0.2 %, σ_0 = 38 MV

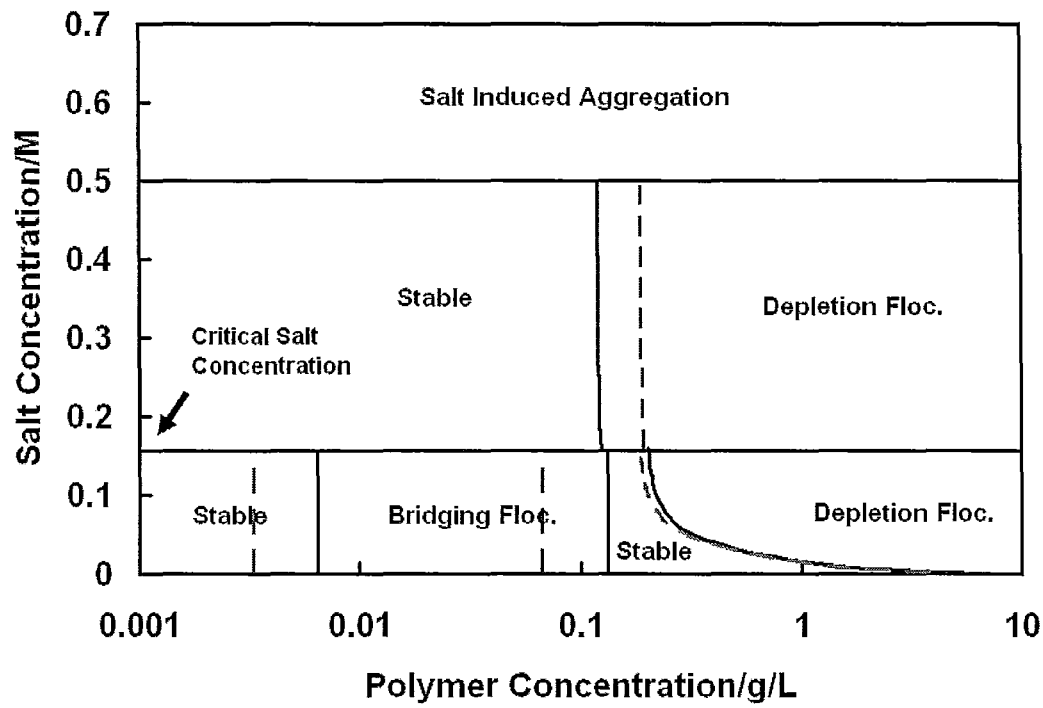

Figure 4. 10 Analytical phase diagram for Labile polyelectrolyte interaction with oppositely charged

liposomes. Specifically, MW = 1.5 M, r_g = 135 nm, a = 45 nm, Φ^c = 0.2 %, σ_0 = 38 MV, borax concentration 50 mM for black solid lines. Blue lines are for MW = 1.5 M, r_g = 135 nm, a = 45 nm, Φ^c = 0.1 %, σ_0 = 38 MV

4.5 CONCLUSIONS

1. Novel colloid stability maps provide formulators a clear picture of the interplay between electrolyte concentration and HPG-borate concentration.
2. The effects of critical parameters including polymer molecular weight, colloid volume fraction and colloid size are clearly illustrated on the stability maps.

4.6 REFERENCE

1. Khanal, A.; Cui, Y.; Zhang, L.; Pelton, R.; Ren, Y.; Ketelson, H.; James, D., Cationic liposome colloidal stability in the presence of guar derivatives suggests depletion interactions may be operative in artificial tears. *Biomacromolecules.*
2. Dobrynin, A. V.; Rubinstein, M., Theory of polyelectrolytes in solutions and at surfaces. *Prog. Polym. Sci.* **2005,** 30, (11), 1049-1118.
3. Fleer, G. J.; Cohen Stuart, M. A.; Scheutjens, J. M. H. M.; Cosgrove, T.; Vincent, B., *Polymers at interfaces*. Springer: 1993.
4. Grosberg, A. Y.; Nguyen, T. T.; Shklovskii, B. I., Colloquium: The physics of charge inversion in chemical and biological systems. *Rev. Mod. Phys.* **2002,** 74, (2), 329-345.
5. Kawaguchi, M.; Takahashi, A., Polymer adsorption at solid liquid interfaces. *Advances in Colloid and Interface Science* **1992,** 37, (3-4), 219-317.
6. Netz, R. R.; Andelman, D., Neutral and charged polymers at interfaces. *Phys. Rep.-Rev. Sec. Phys. Lett.* **2003,** 380, (1-2), 1-95.
7. Wiegel, F. W., Adsorption of a macromolecule to a charged surface. *Journal of Physics a-Mathematical and General* **1977,** 10, (2), 299-303.
8. Muthukumar, M., Adsorption of a polyelectrolyte chain to a charged surface. *J. Chem. Phys.* **1987,** 86, (12), 7230-7235.
9. Vongoeler, F.; Muthukumar, M., Adsorption of polyelectrolytes onto curved surfaces. *J. Chem. Phys.* **1994,** 100, (10), 7796-7803.
10. Cheng, Y.; Brown, K. M.; Prud'homme, R. K., Characterization and intermolecular interactions of hydroxypropyl guar solutions. *Biomacromolecules* **2002,** 3, (3), 456-461.
11. Cui, Y. G.; Pelton, R.; Ketelson, H., Shapes of polyelectrolyte titration curves. 2. The deviant behavior of labile polyelectrolytes. *Macromolecules* **2008,** 41, (21), 8198-8203.
12. Jasinski, R.; Redwine, D.; Rose, G., Boron equilibria with high molecular weight guar: An nmr study. *Journal of Polymer Science Part B-Polymer Physics* **1996,** 34, (8), 1477-1488.
13. Lu, C.; Kostanski, L.; Ketelson, H.; Meadows, D.; Pelton, R., Hydroxypropyl guar-borate interactions with tear film mucin and lysozyme. *Langmuir* **2005,** 21, (22), 10032-10037.
14. Klein, J.; Luckham, P. F., Variation of effective adsorbed polymer layer thickness with molecular-weight in good and poor solvents. *Macromolecules* **1986,** 19, (7), 2007-2010.
15. Klein, J.; Luckham, P. F., Forces between 2 adsorbed poly(ethylene oxide) layers in a good aqueous solvent in the range 0-150 nm. *Macromolecules* **1984,** 17, (5), 1041-1048.
16. Dickinson, E.; Eriksson, L., Particle flocculation by adsorbing polymers. *Advances in Colloid and Interface Science* **1991,** 34, 1-29.
17. Smellie, R. H.; La Mer, V. K., Flocculation, subsidence and filtration of phosphate slimes : Vi. A quantitative theory of filtration of flocculated suspensions. *Journal of Colloid Science* **1958,** 13, (6), 589-599.
18. Healy, T. W.; Mer, V. K. L., The adsorption-flocculation reactions of a polymer with an aqueous colloidal dispersion. *The Journal of Physical Chemistry* **1962,** 66, (10), 1835-1838.
19. La Mer, V. K.; Healy, T. W., Adsorption-flocculation reactions of macromolecules at solid-liquid interface. In *Reviews of pure and applied chemistry*, 1963; Vol. 13, pp 112-133.
20. La Mer, V. K., Filtration of colloidal dispersions flocculated by anionic and cationic polyelectrolytes. In *Discussions of the Faraday Society* 1966; Vol. 42, pp 248-254.

21. Hogg, R., Collision efficiency factors for polymer flocculation. *Journal of Colloid and Interface Science* **1984,** 102, (1), 232-236.

22. de Kruif, C. G.; Tuinier, R., Polysaccharide protein interactions. *Food Hydrocolloids* **2001,** 15, (4-6), 555-563.

23. Israelachvili, J., *Intermolecular and surface forces*. Academic press London: 1991.

24. Degennes, P. G., Polymers at an interface - a simplified view. *Advances in Colloid and Interface Science* **1987,** 27, (3-4), 189-209.

25. Fleer G, J.; Scheutjens J. H. M, H.; Vincent, B., The stability of dispersions of hard spherical particles in the presence of nonadsorbing polymer. In *Polymer adsorption and dispersion stability*, American Chemical Society: Washington, D.C., 1984; pp 245-263.

26. Vincent, B., The calculation of depletion layer thickness as a function of bulk polymer concentration. *Colloids and Surfaces* **1990,** 50, 241-249.

27. Flory, P. J., *Principles of polymer chemistry*. Cornell University Press: 1953.

28. Leibler, L.; Pezron, E.; Pincus, P. A., Viscosity behavior of polymer-solutions in the presence of complexing ions. *Polymer* **1988,** 29, (6), 1105-1109.

29. Virden, J. W.; Berg, J. C., Nacl-induced aggregation of dipalmitoylphosphatidylglycerol small unilamellar vesicles with varying amounts of incorporated cholesterol. *Langmuir* **1992,** 8, (6), 1532-1537.

30. Dimitrova, M. N.; Tsekov, R.; Matsumura, H.; Furusawa, K., Size dependence of protein-induced flocculation of phosphatidylcholine liposomes. *Journal of Colloid and Interface Science* **2000,** 226, (1), 44-50.

31. Long, J. A.; Osmond, D. W. J.; Vincent, B., The equilibrium aspects of weak flocculation. *Journal of Colloid and Interface Science* **1973,** 42, (3), 545-553.

Appendix 1

LIPOID E 80 S

Description

Fatfree egg lecithin with 64 – 79 % phosphatidyl choline

Art.-No.	120
EINECS - No.	297-639-2
CAS - No.	93685-90-6

Chemical Composition

Phospholipids [g/100 g]	
Phosphatidyl choline	64.0 – 79.0
Phosphatidyl ethanolamine	12.0 – 18.0
Lysophosphatidyl choline	n.m.t. 3.0
Sphingomyelin	n.m.t. 3.0
Other natural components	n.m.t. 1.5
Non-polar lipids [g/100 g]	n.m.t. 5.0
Triglycerides	n.m.t. 3.0
Cholesterol	n.m.t. 1.0
Free fatty acids	n.m.t. 1.0
DL-α-Tocopherol	0.05 – 0.1
Typical fatty acid composition in % to total fatty acids)	
Palmitic acid	28 – 34
Stearic acid	12 – 15
Oleic acid	26 – 30
Linoleic acid	13 – 18
Linolenic acid	n.m.t. 1.0
Polyunsaturated fatty acids C 20 and higher	6 – 10

Analytical Data

Phosphorus	[g/100 g]	3.5 – 4.1
Water	[g/100 g]	n.m.t. 2.0
Ethanol	[g/100 g]	n.m.t. 0.2
Peroxide value	[meq O_2/kg]	n.m.t. 3
Iodine value		64 – 69
Heavy metals	[ppm]	n.m.t. 10

Physical Properties

Consistency	coarse agglomerates
Colour	light yellow
Solublity (5 % solution)	
Water	dispersible 20°C
Fat	soluble 60°C
Chlorinated hydrocarbons	soluble 20°C
Ethanol	soluble 20°C

Document D-120 of 01.02.2006
Supersedes 07.02.2003

Bacteriological Data

C.F.U.	[/g]	n.m.t. 100
Yeasts	[/g]	n.m.t. 10
Moulds	[/g]	n.m.t. 10
Escherichia coli	[/10 g]	negative
Salmonellae	[/10 g]	negative
Staphylococcus aureus	[/10 g]	negative
Pseudomonas aeruginosa	[/10 g]	negative

Endotoxins

Endotoxins	[EU/g]	n.m.t. 6

Aflatoxins

Aflatoxin B1	[ppb]	n.m.t. 2
Aflatoxins B1, B2, G1, G2	[ppb]	n.m.t. 4

Particle Test

Particle test	complies with method PM 1

Packaging

Standard packaging 5 kg in double PE-bag

Storage Conditions

Recommended storage: in closed containers at – 20 ± 5 °C.
Close opened containers immediately.

n.m.t. = not more than

All data and recommendations as well as formulations made herein are based on our present state of knowledge. We disclaim all liability on risks or formulae that may result from the use of our products, including improper and illicit use.

Appendix 2

TEMPO Oxidation of Guar and its Derivatives

Selective oxidation of polysaccharides using 2,2,6,6-tetramethylpiperidine-1-oxyl (TEMPO).

Polymer 0.5 g was dissolved in 0.5 Liter distilled water. TEMPO 0.01 g and NaBr 0.05 g were added. The solution was stirred and cooled in an ice bath (3±1℃).

15% sodium hypochlorite (3 ml) was cooled (3±1℃) and pH was adjusted to 9.4 with 2M HCl.

The solutions were mixed and pH was maintained at 9.4 by 0.5M NaOH. The reaction was quenched by adding 3 ml methanol and neutralized to pH 6 by adding 4 M HCl. Then excess sodium borohydride (0.25 g) was added and the solution was stirred over night.

Appendix 3: The goal is to generate phase diagram for liable polyelectrolyte (HPG-borate) interaction with oppositely charged colloids

Constants in this calculation

$T := 298K$ temperature $a := 45nm$ Radius of liposomes $\rho := \frac{gm}{cm^3}$ Density of HPG

$\varepsilon_r := 78$ $\varepsilon := \varepsilon_o \cdot \varepsilon_r$ $r_g := 135nm$ radius of gyration

$NaCl := 0.25 \frac{mole}{L}$ $R := 8.314 \frac{joule}{K \cdot mole}$ Gas constant $\phi := 0.01$ HPG volume fraction, numerically same with mass fraction

$\varphi := 38mV$ $M_W := 1500000 \frac{gm}{mole}$ HPG molecular weight

$A := 4 \cdot 10^{-21} joule$ $B_2 := 0.0000325 \frac{cm^3 \cdot mole}{gm^2}$ second virial coefficient of HPG

$\kappa(NaCl) := \left(\frac{e_o^2 \cdot N_{av}}{\varepsilon_o \cdot \varepsilon_r \cdot k_b \cdot T} \cdot 2 \cdot NaCl \right)^{0.5}$ calculate kappa $h := nm$ surface-surface distance

Theoretical Framework (Note: all potentials are normalized by k_bT)

Electrostatic Potential

$$V_{elect}(r, NaCl, h, \varphi) := \left(2 \cdot \pi \cdot \varepsilon \cdot \varphi^2 \cdot a \cdot \ln(1 + \exp(-\kappa(NaCl) \cdot h))\right) \cdot \frac{1}{k_b \cdot T}$$

Van der Waals interaction potential

$$V_{vdw}(h, A, a) := \frac{-A}{12} \cdot \left(\frac{4 \cdot a^2}{h^2 + 4 \cdot a \cdot h} + \frac{4 \cdot a^2}{h^2 + 4 \cdot a \cdot h + 4 \cdot a^2} + 2 \ln\left(\frac{h^2 + 4 \cdot a \cdot h}{h^2 + 4 \cdot a \cdot h + 4 \cdot a^2} \right) \right) \cdot \frac{1}{k_b \cdot T}$$

Depletion potential

1. Calculate depletion layer thickness Δ using Vincent's analytical approach
(*Colloids and Surfaces*, 50 (1990) 241-249)

$$\frac{\Delta}{\Delta_o^2} - \frac{1}{\Delta} = \frac{-N_{av}\cdot\rho}{2}\left(\frac{v_2}{\phi}\right)^{\frac{2}{3}}\cdot\left(\frac{\phi}{M_w} + B_2\cdot\rho\cdot\phi^2\right)$$

Governing equation modified by Seebergh and Berg
(*Langmuir, Vol. 10, No. 2, 1994*)

$$v_2 = \frac{M_w}{N_{av}\cdot\rho}$$

molecular volume of a polymer chain

$\phi := 0.001$

$\Delta := 40nm$

use "root function" to solve Δ

$$\Delta_t := root\left[\frac{N_{av}\cdot\rho}{2}\cdot\left(\frac{\frac{M_w}{N_{av}\cdot\rho}}{\phi}\right)^{\frac{2}{3}}\cdot\left[\frac{\phi}{M_w} + B_2\cdot\rho\cdot\phi^2 + \frac{3000^2\cdot\left(\frac{\rho\cdot\phi^2}{M_w^2}\right)}{4NaCl}\right] + \left[\frac{\Delta}{(1.4\cdot r_g)^2} - \frac{1}{\Delta}\right], \Delta\right]$$

2. Depletion potential calculation using Fleer & Scheutjens & Vincent's approach
(*ACS Symp. Ser.* 1984, NO. 240, page 245)

$$V_{dep}(\phi, a, h) := \frac{-2}{3}\cdot\pi\cdot R\cdot T\cdot\rho\cdot\phi\cdot\left[\frac{1}{M_w} + B_2\cdot\rho\cdot\phi + \frac{10000^2\cdot\left(\frac{\rho\cdot\phi}{M_w^2}\right)}{4\cdot NaCl}\right]\cdot\left(\Delta_t - \frac{h}{2}\right)^2\cdot\left(3\cdot a + 2\cdot\Delta_t + \frac{h}{2}\right)\cdot\frac{1}{k_b\cdot T}$$

$V_{dep}(0.001, a, h) = -15.8795$

Imput viables to plot DLVO-type pair potential

$h := 0.01nm, 0.02nm .. 100nm$ $rg := 135.1nm$ $M_W := 1500000 \frac{gm}{mole}$

$org(h) := 0$ $\phi := 0.001$ $\varphi := 38mV$ $NaCl := 0.2 \frac{mol}{L}$

$$\Delta_t := root\left[\frac{N_{av}\cdot\rho}{2}\cdot\left(\frac{\frac{M_W}{N_{av}\cdot\rho}}{\phi}\right)^{\frac{2}{3}}\cdot\left(\frac{\phi}{M_W}+B_2\cdot\rho\cdot\phi^2\right)+\left[\frac{\Delta}{(1.4\cdot r_g)^2}-\frac{1}{\Delta}\right],\Delta\right]$$

$\Delta_t = 132.2058\cdot nm$

$$V_{dep}(\phi,a,h,M_W) := \frac{-2}{3}\cdot\pi\cdot R\cdot T\cdot\rho\cdot\phi\cdot\left(\frac{1}{M_W}+B_2\cdot\rho\cdot\phi\right)\cdot\left(\Delta_t-\frac{h}{2}\right)^2\cdot\left(3\cdot a+2\Delta_t+\frac{h}{2}\right)\cdot\frac{1}{k_b\cdot T}$$

$V_{dep}(\phi,a,2nm,M_W) = -6.0782$

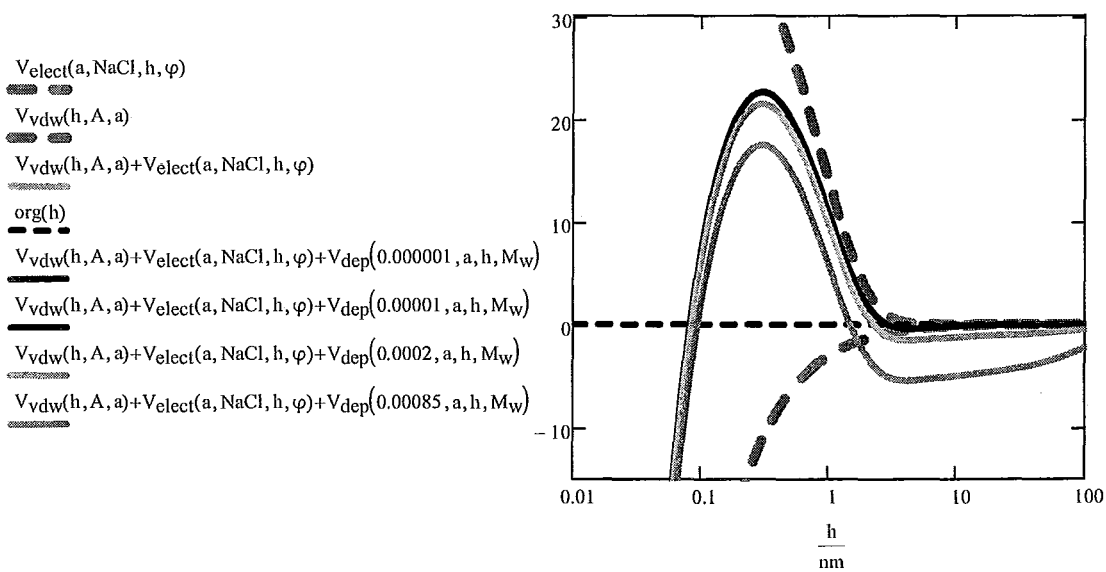

Solve required polymer concentration for depletion flocculation at a given salt concentration

$h := 6nm \qquad a := 45nm$

Given

$V_{vdw}(h, A, a) + V_{elect}(a, NaCl, h, \varphi) + V_{dep}(\phi, a, h, M_W) = -1$

$1nm \le h \le 10nm$

$dep(h, a, NaCl, M_W) := Find(\phi)$

$dep\left(6nm, 45nm, 0.1\frac{mole}{L}, M_W\right) = 1.4309 \times 10^{-4}$

Plot Salt concentration against threshold HPG concentration for depletion flocculaion

$NaCl := 0\frac{mole}{L}, 0.01\frac{mole}{L} .. 0.5\frac{mole}{L}$

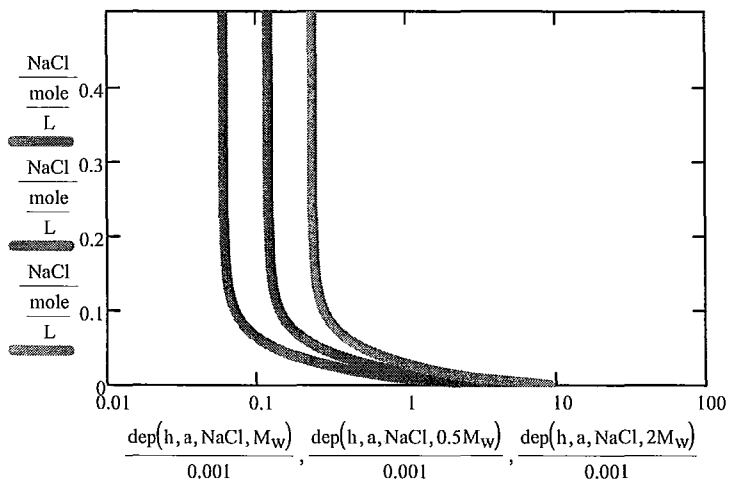

Ionic strength versus threshold HPG (different MW) concentration for depletion floc.

We find smaller mass is required for lower MW of HPG to induce depletion flocculation

Modeling Bridging Flocculation

$TOL := 10^{-10}$

$\Gamma_{max} := \frac{mg}{m^2}$ Assumed monolayer coverage of HPG on DOTAP

$c_{lip} := 6.7 \cdot 10^{15} \cdot \frac{1}{L}$ Number density for 1 mM DOTAP

$d_{lip} := 45nm$ Liposome radius

Lower boundary for Bridging flocculation

Assumption: To form a macroscopic floc needs at least one polymer chain to link every two particles

$Mw := 10^6 Da$

$FBL2 := \frac{c_{lip} \cdot Mw}{N_{av}}$

$FBL2 = 11.1256 \cdot \frac{mg}{L}$

Summary - upper boundary choose floc conc. giving saturated coverage
- lower boundary choose floc conc. equal to 1/2 particle conc.